PB87-129250

Reactivity Study of SO2 Control with Atmospheric and Pressure Hydrated Sorbents

Energy and Environmental Research Corp.
Irvine, CA

Prepared for

Environmental Protection Agency
Research Triangle Park, NC

Nov 86

U.S. Department of Commerce
National Technical Information Service
NTIS

EPA/600/7-86/040
November 1986

PB87-129250

Reactivity Study of SO_2 Control with Atmospheric and Pressure Hydrated Sorbents

by:

B. J. Overmoe, J. M. McCarthy, S. L. Chen,
W. R. Seeker, and D. W. Pershing

ENERGY AND ENVIRONMENTAL RESEARCH CORPORATION
18 MASON
IRVINE, CALIFORNIA 92718-2798

EPA Contract 68-02-3995, Work Assignments No. 17 & 19

EPA Project Officer: B. K. Gullett
Air and Energy Engineering Research Laboratory
U.S. Environmental Protection Agency
Research Triangle Park, NC 27711

AIR AND ENERGY ENGINEERING RESEARCH LABORATORY
OFFICE OF RESEARCH AND DEVELOPMENT
U.S. ENVIRONMENTAL PROTECTION AGENCY
RESEARCH TRIANGLE PARK, NC 27711

REPRODUCED BY
U.S. DEPARTMENT OF COMMERCE
NATIONAL TECHNICAL
INFORMATION SERVICE
SPRINGFIELD, VA. 22161

TECHNICAL REPORT DATA
(Please read Instructions on the reverse before completing)

1. REPORT NO. EPA/600/7-86/040	2.
3. RECIPIENT'S ACCESSION NO. PB87 129250/AS	
4. TITLE AND SUBTITLE Reactivity Study of SO_2 Control with Atmospheric and Pressure Hydrated Sorbents	5. REPORT DATE November 1986
	6. PERFORMING ORGANIZATION CODE
7. AUTHOR(S) B. J. Overmoe, J. M. McCarthy, S. L. Chen, W. R. Seeker, and D. W. Pershing	8. PERFORMING ORGANIZATION REPORT NO.
9. PERFORMING ORGANIZATION NAME AND ADDRESS Energy and Environmental Research Corporation 18 Mason Irvine, California 92718-2798	10. PROGRAM ELEMENT NO.
	11. CONTRACT/GRANT NO. 68-02-3995, Tasks 17 and 19
12. SPONSORING AGENCY NAME AND ADDRESS EPA, Office of Research and Development Air and Energy Engineering Research Laboratory Research Triangle Park, NC 27711	13. TYPE OF REPORT AND PERIOD COVERED Task Final; 5-10/85
	14. SPONSORING AGENCY CODE EPA/600/13

15. SUPPLEMENTARY NOTES AEERL project officer is Brian K. Gullett, Mail Drop 4, 919/541-1534.

16. ABSTRACT

The report gives results of a study to develop an understanding of the factors that control the reactivity of hydrated sorbents toward SO2 in coal fired furnaces. It focused on the impacts of hydrate properties (e.g., particle size, surface area, and chemical composition) and the furnace temperature of the injection location. A bench scale hydrator was used to produce atmospheric and pressure hydrated sorbents, with parameters pertinent to the hydration process varied. The chemical and physical properties were characterized for these and several commercially available hydrates, and they were tested for SO2 sorption reactivity on bench (17.6 kW) and pilot scale (300 kW) furnaces. Study results indicate that pressure hydrates generated under well controlled conditions are more reactive than commercially produced atmospheric hydrates. The important production and operating parameters for the pressure hydration process included the size and composition of the quicklime, the hydration temperature and pressure, the rate of water addition, and the pressure progression during discharge. Comparison of commercial atmospheric hydrates showed significant differences in reactivity, from 40 to 58% at a molar Ca/S of 2. All hydrates, atmospheric and pressure, exhibited a strong dependence on injection temperature.

17. KEY WORDS AND DOCUMENT ANALYSIS

a. DESCRIPTORS		b. IDENTIFIERS/OPEN ENDED TERMS	c. COSATI Field/Group
Pollution	Hydration	Pollution Control	13B 07D
Sulfur Dioxide	Reactivity	Stationary Sources	07B
Furnaces	Calcium Oxides	Hydrated Sorbents	13A
Coal			21D
Combustion			21B
Sorbents			11G

18. DISTRIBUTION STATEMENT Release to Public	19. SECURITY CLASS (This Report) Unclassified	21. NO. OF PAGES 126
	20. SECURITY CLASS (This page) Unclassified	22. PRICE

EPA Form 2220-1 (9-73)

NOTICE

This document has been reviewed in accordance with U.S. Environmental Protection Agency policy and approved for publication. Mention of trade names or commercial products does not constitute endorsement or recommendation for use.

ABSTRACT

The purpose of this study was to develop an understanding of the factors that control the reactivity of hydrated sorbents toward SO_2 in coal fired furnaces. The study focused on the impacts of hydrate properties such as particle size, surface area, and chemical composition, and the furnace temperature of the injection location. A bench scale hydrator was used for production of atmospheric and pressure hydrated sorbents, with parameters pertinent to the hydration process varied. The chemical and physical properties were characterized for these hydrates and several commercially available hydrates, and they were tested for SO_2 sorption reactivity on bench scale (17.6 kW) and pilot scale (300 kW) furnaces.

The results of this study indicated that pressure hydrates generated under well controlled conditions were more reactive than commercially produced atmospheric hydrates. The important production and operating parameters for the pressure hydration process included the size and composition of the quicklime, the hydration temperature and pressure, the rate of water addition, and the pressure progression during discharge. Comparison of commercial atmospheric hydrates showed significant differences in reactivity, ranging from 40 to 58 percent at a calcium to sulfur molar ratio of 2. All hydrates, atmospheric and pressure, exhibited a strong dependence on injection temperature.

ACKNOWLEDGEMENTS

This work was performed under Subcontract No. 588-84 with PEI Associates, Inc. Bernie Laseke was the PEI project manager. The authors are grateful to their colleagues, Eric Moller and Loi Ho, for conducting the experiments.

TABLE OF CONTENTS

Section		Page
ABSTRACT		iii
LIST OF FIGURES		vi
LIST OF TABLES		viii
1.0	INTRODUCTION	1-1
	1.1 Background	1-1
	1.2 Purpose and Scope	1-2
2.0	EXPERIMENTAL FACILITIES	2-1
	2.1 Pressure Hydrator	2-1
	2.2 Control Temperature Tower (CTT)	2-2
	2.3 Boiler Simulator Furnace (BSF)	2-6
	2.4 Measurement Systems and Analytical Methods	2-8
3.0	SORBENTS AND FUELS	3-1
	3.1 Sorbent Physical and Chemical Properties	3-1
	3.2 Fuel Analyses	3-7
4.0	RESULTS AND DISCUSSION	4-1
	4.1 Linwood and Longview Sorbents	4-1
	4.2 Pressure Hydration	4-9
	4.3 Comparison of Commercial Hydrates	4-21
	4.4 Performance of Demo Sorbents	4-25
5.0	CONCLUSIONS	5-1
6.0	REFERENCES	6-1
	APPENDIX A: Design of a Bench Scale Hydrator	A-1
	APPENDIX B: Quality Assurance	B-1

Preceding page blank

LIST OF FIGURES

Section		Page
2-1	EER's bench scale pressure hydrator.	2-4
2-2	Cross sectional views of the control temperature tower	2-5
2-3	Boiler simulator furnace (BSF)	2-7
2-4	Continuous monitoring sampling system.	2-9
2-5	SO_2 continuous monitoring system	2-10
3-1	Commercial hydrate particle size distributions	3-4
3-2	Commercial hydrate pore size distributions	3-5
3-3	Comparison of atmospheric and pressure hydrate particle size distribution.	3-6
3-4	Particle size distribution of several pressure hydrates.	3-8
3-5	Pore size distributions of pressure and atmospheric hydrate.	3-9
3-6	Demo sorbents particle size distributions.	3-11
4-1	CTT temperature profile from injection point	4-2
4-2	BSF temperature profile	4-3
4-3	Linwood sorbents with gas and coal	4-5
4-4	Longview sorbents with gas and coal.	4-6
4-5	Estimation of quicklime reactivity	4-7
4-6	Degree of hydration effects.	4-8
4-7	Linwood vs. Longview sorbents with gas	4-10
4-8	Linwood vs. Longview sorbents with coal	4-11
4-9	Comparison of PH and AH - natural gas.	4-12
4-10	Comparison of PH and AH - coal	4-13
4-11	Comparison of UNDERC and EER PH.	4-14
4-12	Effect of pressurization process on partially hydrted sorbent	4-16
4-13	Variations in pressure hydrate generation.	4-17

LIST OF FIGURES (CONTINUED)

Section		Page
4-14	Effect of H_2O addition time	4-19
4-15	Comparison of Linwood AH and PH on BSF	4-20
4-16	Comparison of commercial hydrates on CTT	4-22
4-17	Influence of injection temperature	4-23
4-18	Facility comparison.	4-24
4-19	Commercial hydrate performance summary	4-26
4-20	Demo sorbent performance summary	4-27
4-21	Performance with different fuels	4-28
4-22	Large scale performance - BSF.	4-30

LIST OF TABLES

Section		Page
2-1	Pressure Hydrator Comparison	2-33
3-1	Linwood and Longview Sorbent Physical and Chemical Data. . .	3-2
3-2	Commercial Hydrate Physical and Chemical Data.	3-33
3-3	Physical and Chemical Data for Demo Sorbents	3-10
3-4	Fuel Analyses.	3-12

1.0 INTRODUCTION

1.1 Background

Limestone Injection Multi-Staged Burners (LIMB) was originally conceived as an SO_2 control process that would use untreated, pulverized limestone injected through a distributed mixing low NO_x burner. Despite a concentrated research effort by a wide variety of research organizations, the level of limestone utilization which can be expected today is still relatively low. Experiments in facilities ranging from EER's laboratory reactor (Cole, 1985), bench scale reactor (Greene, 1985) and pilot scale furnace (Overmoe, 1985) to the TVA Shawnee Boiler (Gartrell, 1973) all show limestone utilizations less than 25 percent, regardless of the thermal and other combustion conditions. While it is still unclear what limits ultimate sorbent utilization, the fundamental processes are now reasonably well identified.

The overall process can be viewed as a sequential coupling of an activation step in which the limestone or hydrate calcines to produce CaO and a sulfation step where the CaO reacts to form calcium sulfate. The activation step controls the reactivity of the material and both steps clearly influence the ultimate utilization of the sorbent. Sulfation can be viewed as a set of serial resistances: diffusion of SO_2 to the particle surface, diffusion through the macropores of the particle, diffusion through any previously deposited calcium sulfate product layer, and heterogeneous chemical reaction at the CaO interface. Although the rates of these individual steps have not been individually determined, the overall process has been well characterized by Borgwardt (1970). His results show a strong sensitivity to reaction temperature indicating an activated process; below 1600°F the rate is too slow to be of commercial interest in conventional boilers. Above 2250°F the process is limited by equilibrium considerations; the favored product, calcium sulfate, is unstable.

The process parameters which control the SO_2 removal efficiency with calcium-based sorbents have been studied extensively. Recent LIMB investigations (Overmoe, 1985; Slaughter, 1985; Beittle, 1985) have indicated

that capture efficiency depends strongly on the injection location (temperature) and the sorbent type. In general, hydrates perform better than carbonates and dolomitic sorbents are superior to calcitic sorbents (on an equivalent calcium basis) at the same injection temperatures. Captures in excess of 50 percent at a Ca/S ratio of 2.0 have been achieved with pressure hydrated dolomitic sorbents. In addition, a DOE supported study (Weber, 1985) has reported that calcium utilizations approaching 40 percent were obtained with laboratory prepared calcitic pressure hydrates at the University of North Dakota Energy Research Center (UNDERC). Thus, there is significant evidence available that indicates the superiority of hydrated lime (both pressure and atmospheric, calcitic and dolomitic) over limestone.

There are two apparent advantages of using hydrates as sorbents for SO_2 control: (1) the hydrates calcine (dehydrate) significantly quicker than the carbonates so the residence time available for sulfation is greatly increased. This effect is likely to be particularly important with rapid quench conditions and low temperature injections, and (2) the hydration process, pressure hydration particularly, generally results in decreased particle sizes; hence, pore diffusion effects are reduced. However, it is not clear whether their potential reactivity is due to some physical alteration through hydration or simply through the reduction in particle size. The importance of the original parent limestone is another unknown factor in predicting subsequent hydrate performance.

1.2 Purpose and Scope

The purpose of this study was to develop an understanding concerning the factors controlling the reactivity of hydrates to capture SO_2 when injected into a coal fired furnace. The approach taken was to generate hydrates, both atmospheric and pressure, under well controlled conditions and compare their reactivity with that of the corresponding quicklimes and parent limestones. Under the consultation of UNDERC, a bench scale hydrator was designed and constructed to produce batches (approximately 20 pounds each) of atmospheric and pressure hydrated limes. Parameters pertinent to the hydration process were varied and the hydrates were characterized in terms of surface area,

particle size and pore size distributions. These prepared hydrated limes together with commercially available hydrates were tested for SO_2 absorption reactivity on both the bench scale (60×10^3 Btu/hr) Control Temperature Tower (CTT) and the pilot scale (1.0×10^6 Btu/hr) Boiler Simulator Furnace (BSF).

A description of the hydrator and the two furnaces is given in Chapter 2.0 and details of the sorbent properties and composition are presented in Chapter 3.0. The results of the program are given in Chapter 4.0 in four subsections. The first deals specifically with the Linwood and Longview series sorbents ($CaCO_3$, CaO, and atmospheric and pressure $Ca(OH)_2$), the second with the effect of pressure hydration, the third compares the reactivity of different atmospheric hydrates, and the last subsection discusses the performance of the commercial sorbents proposed for the LIMB demonstration project.

2.0 EXPERIMENTAL FACILITIES

Three facilities were used in these experimental investigations: a 20-lb pressure hydrator for generation of both atmospheric and pressure hydrates, a bench scale reactor (CTT) for sorbent reactivity screening and a pilot scale furnace (BSF) for performance evaluation under simulated field conditions.

2.1 Pressure Hydrator

When hydrate is processed at high pressure in an excess of water, the formation of small particles is promoted by a controlled, explosive discharge of the hydrate. The discharge of the hydrate from high pressure (usually in excess of 80 psig) to atmospheric pressure results in flash vaporization of water within the pores of the particles.

This rapid expansion effectively explodes the particle into smaller particles with a surface area considerably larger than that of the parent quicklime. The process of hydration at high pressure was originally developed for masonry applications, in order to promote complete hydration of "hard-burned" or dolomitic (CaO·MgO) limes, which do not hydrate completely at atmospheric pressure.

The bench scale pressure hydrator was designed under the consultation of UNDERC. Appendix A gives the detailed descriptions of the design approach, calculations, features and operating procedures of the hydrator. Only a brief summary will be presented here.

Major design criteria for the bench scale hydrator included:

- A production capacity of 20 lbs of hydrate per batch. A batch of this size will supply a sufficient amount of sorbent for testing on the 1 MMBtu/hr Boiler Simulator Furnace.

- A pressure and temperature capability of 200 psig and 450°F, respectively. These are within the range of values commonly employed for the pressure hydration process.

- A controlled and explosive discharge. This causes the fragmentation of the product particles, promoting the formation of small particles with a large surface area.

- The ability to electrically heat the reactor. Since significant heat losses occur from the reactor d???to the large surface area to volume ratio which is characteristic of small systems, it is necessary to have an external heat source.

The bench scale pressure hydrator is a second-generation version of the UNDERC system with several modifications incorporated to improve the operation. The bench scale hydrator was 10 inches in diameter and 2 feet in length whereas the UNDERC hydrator was 8 inches in diameter and 1 foot in length. Table 2-1 list the critical operational parameters for both systems. The two systems are quite similar except for size and capacity, where the EER reactor is larger. Figure 2-1 illustrates EER's pressure hydrator with its major components. A more detailed description of the pressure hydrator design and operation can be found in Appendix A.

2.2 Control Temperature Tower

An overall diagram of the 60 x 10^3 Btu/hr Control Temperature Tower furnace (CTT) is presented in Figure 2-2. The reactor entry (top section) included a 45.7 cm long quarl that diverged from 5.1 cm to 20.3 cm. The long quarl provided flame stabilization as well as established a one-dimensional flow pattern. Numerous ports located along the axis of the reactor enabled supplementary equipment; i.e., zone separation chokes, fuel and air injectors, and cooling coils, to be placed in the reactor.

The CTT had the capability of manipulating the time/temperature profile by firing one or both of the back-fired heating sections (second and fourth

TABLE 2-1. PRESSURE HYDRATOR COMPARISON

	EER	UNDERC
Mode of Operation	Batch	Batch
Capacity (lb/run)	20	5
Reactor Size	10"D x 24"	8"D x 12"
Pressure (psig)	to 200	to 150
Temperature (^{o}F)	300-400	380 - 420
Residence Time (min)	10 - 30	20
$(H_2O/CaO)_{molar}$	1.3 - 2.0	1.4
Explosive Discharge Method	Pressure Controlled	Approximately Isobaric @ 100 psig
Material of Construction	Stainless Steel	Carbon Steel

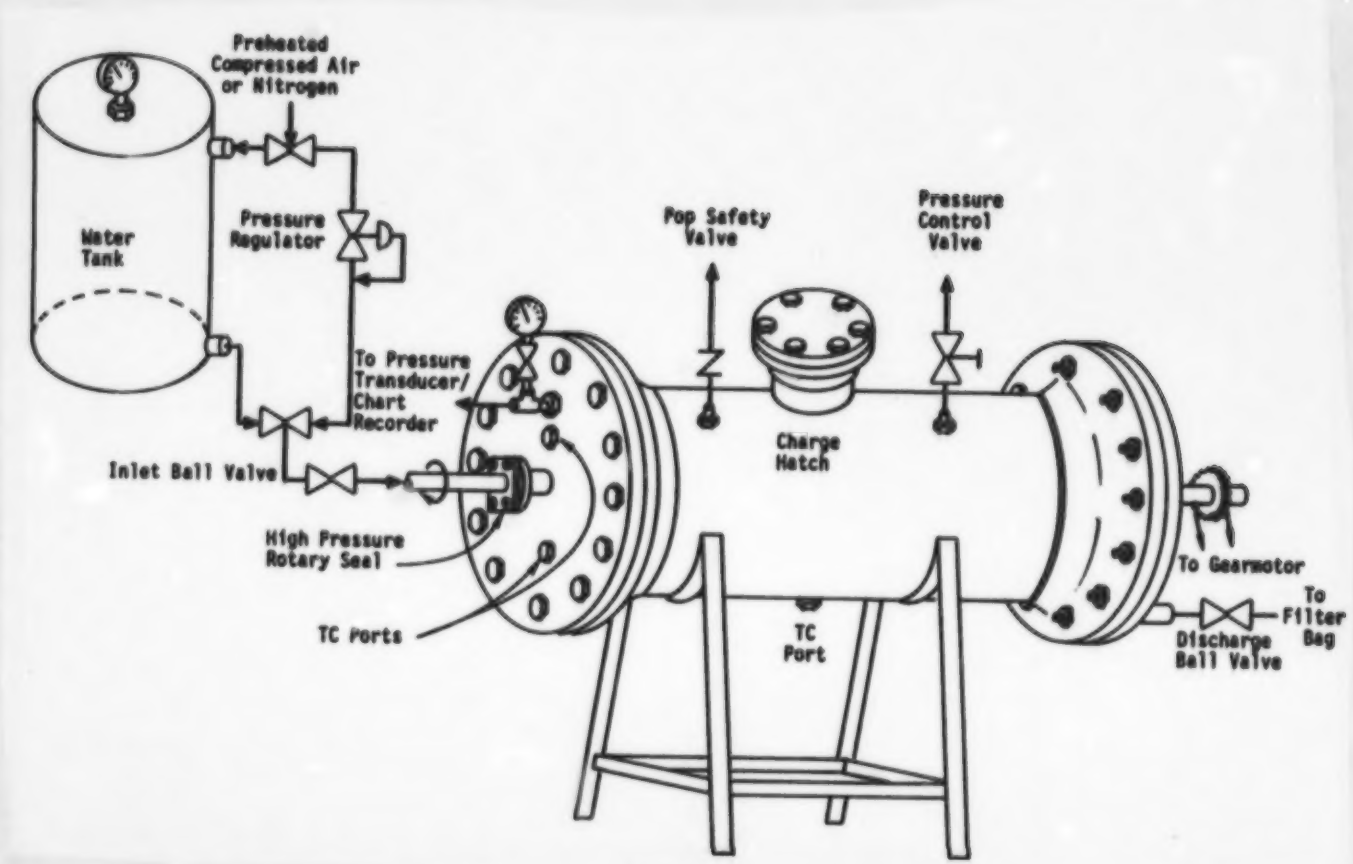

Figure 2-1. EER's bench scale pressure hydrator.

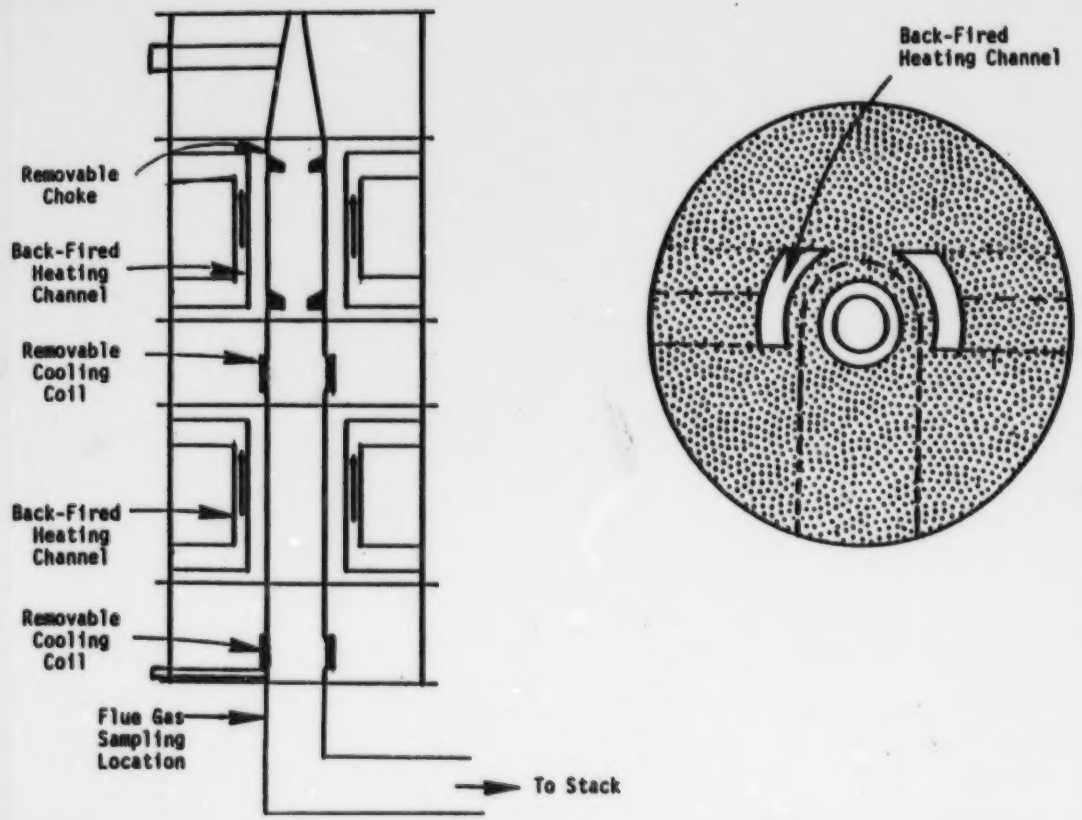

Figure 2-2. Cross-sectional views of the control temperature tower.

sections from the top). The back-fired sections employed natural gas burners which fired in the direction opposite to the main combustion gas. The back-fired effluent passed through channels in the refractory walls surrounding the main combustion zone (see the radial cross-sectional view in Figure 2-2). Backfiring in this manner minimized the temperature decay of the combustion products in the main combustion zone. Additional alteration of the temperature profile could be accomplished by inserting cooling coils in the main combustion chamber.

Additional information on the CTT can be found in a report by Greene (1985).

2.3 Boiler Simulator Furnace

Some of the data presented in this report were obtained with the 1.0 MBtu/hr Boiler Simulator Furnace which is illustrated in Figure 2-3. The facility consisted of two main sections; a refractory-lined vertical radiant tower and a horizontal convective section containing air-cooled heat exchangers. The radiant tower had an ID of 1.8 ft. and an OD of 3.2 ft. and consisted of eight modular sections with multiple access ports. The BSF can be used to simulate a wide range of time/temperature profiles by positioning water-cooled panels or rods appropriately in the furnace. The horizontal convective section contained air-cooled tube bundles that simulated the superheaters, economizers and air heaters in a boiler. Cooling air was supplied by an FD fan with a damper to control flow.

The furnace was equipped with a versatile DMB (Distributed Mixing Burner) modeled after the EPA prototoype burner. Two secondary air streams supplied the burner and the air swirl could be controlled by modifying the swirl and axial air flow rates. The burner had four external staging air ports supplied with separately metered tertiary air. The burner was designed to fire coal or natural gas. NO_x levels were minimized with the DMB due to the fuel-rich core that was produced in the flame zone.

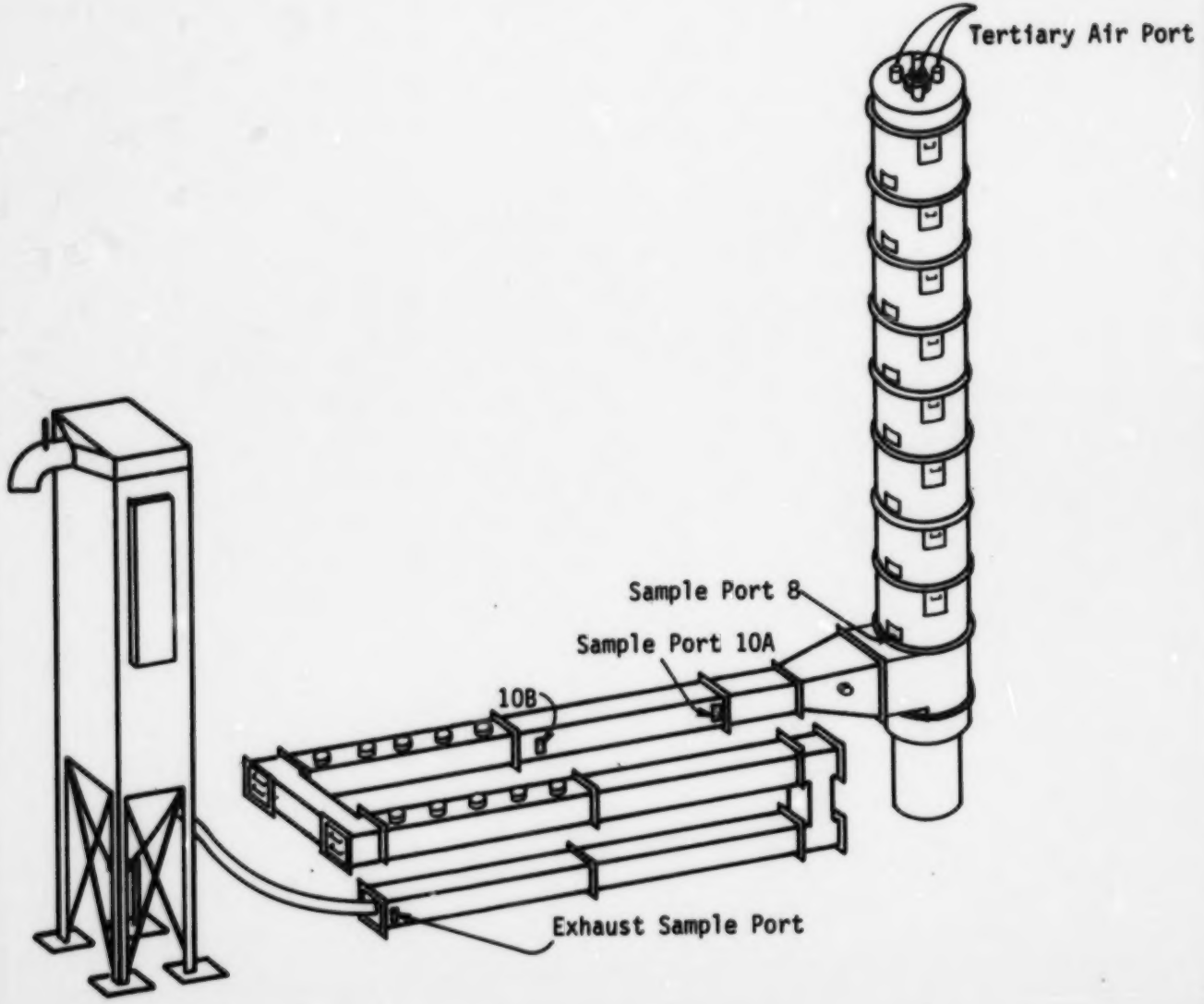

Figure 2-3. Boiler simulator furnace (BSF).

Complete documentation on the BSF facility and fundamental sorbent injection work can be found in an earlier report (Overmoe, 1984).

2.4 Measurement Systems and Analytical Methods

Exhaust gas samples were taken in both the CTT and BSF with a stainless-steel, water-jacket probe and analyzed using standard continuous instrumentation for O_2, CO and CO_2. The schematic of the sampling system is shown in Figure 2-4. SO_2 samples were pulled through the phase discrimination portion of the probe which separated any sorbent particles from the gas stream. The SO_2 samples were then carried via a heated sample line to a permeation dryer and on to a DuPont non-dispersive ultraviolet SO_2 analyzer. Figure 2-5 shows the schematic of the SO_2 sampling system. Furnace temperature profiles were characterized with a suction pyrameter.

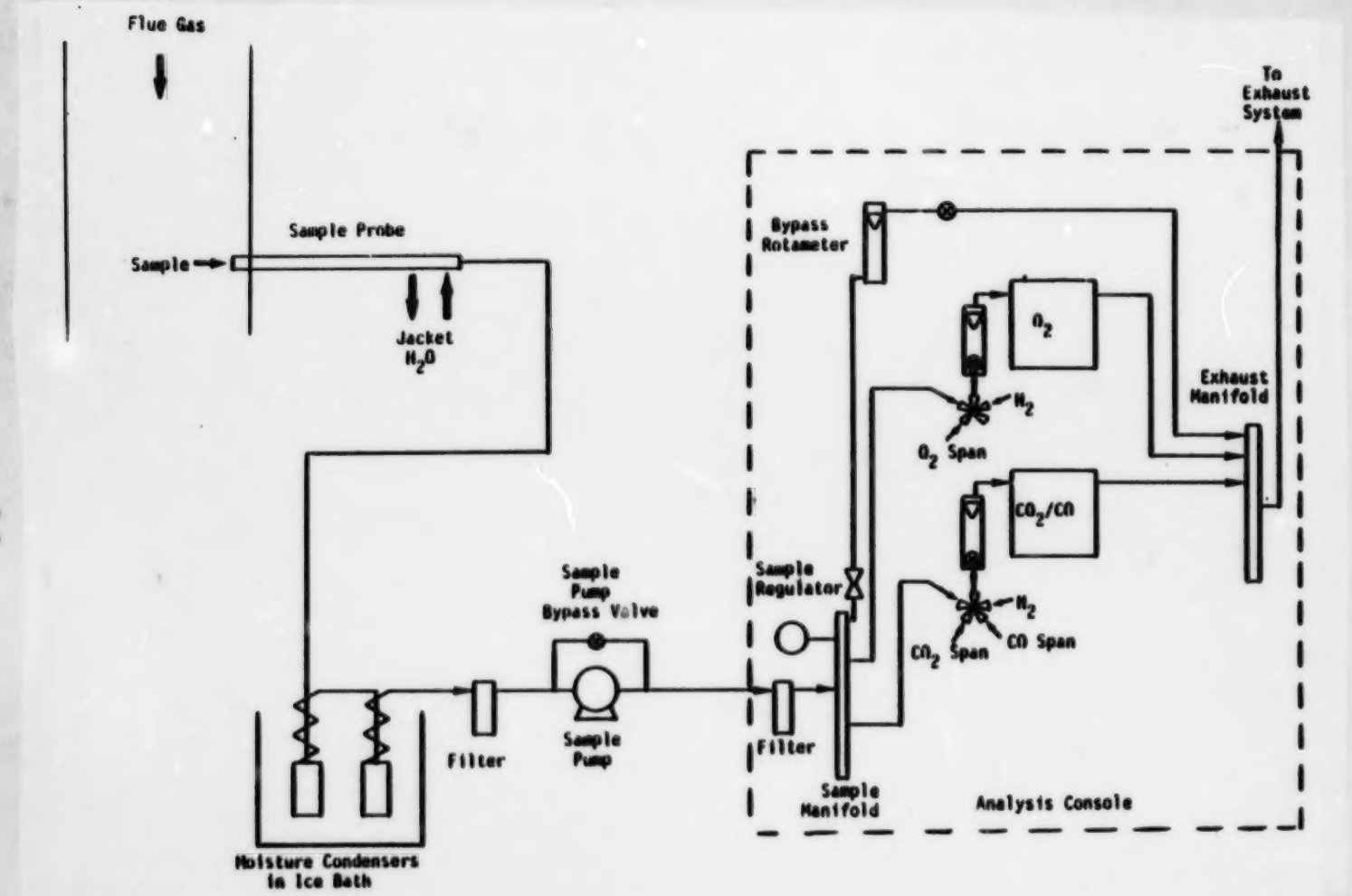

Figure 2-4. Continuous monitoring sampling system.

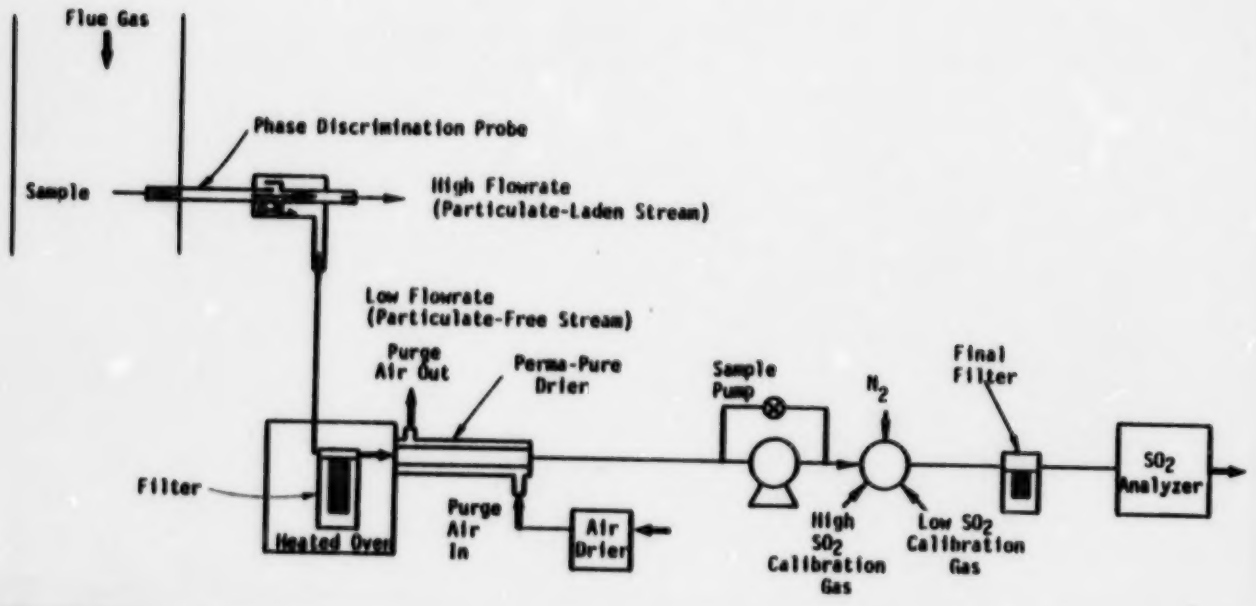

Figure 2-5. SO_2 continuous monitoring system.

3.0 SORBENTS AND FUELS

3.1 Sorbent Physical and Chemical Properties

All of the physical and chemical data for any of the sorbents discussed in Chapter 4.0 are included in this section and reference will be made to specific tables to support the capture data. Table 3-1 is a comparison of the Linwood and Longview sorbent series physical and chemical data. In each box, the upper figure corresponds to the Linwood series and the lower number to the Longview series. Much of the data is similar for the two parent sorbents but a few differences exist. For the atmospheric hydrates, the median particle size for the Longview is nearly twice that of the Linwood and in terms of the trace elements such as magnesium, the Linwood has a higher concentration. These parameters may have an effect on sorbent reactivity. Table 3-2 shows data for three commercial hydrates including the Colton AH which appears to be similar to the Longview in all respects except percent Ca and silica content. The presence of silica is thought to decrease sorbent reactivity due to the formation of calcium silicates, thus preventing the reaction between calcium and SO_2. The particle size distributions for the three commercial hydrates are shown in Figure 3-1 on an equivalent spherical diameter versus cumulative mass percent basis. The Linwood clearly has a smaller mean diameter than the Colton or Longview, but the Colton has a higher percentage of particles that are less than one micron in diameter. Figure 3-2 gives similar information about the pore size distribution for the three hydrates. The sharp peaks in the center of the graph indicate interstitial volume and do not reflect particle pores. Below about 0.10 microns the curves represent incremental pore volume and, as in the previous plot, the Colton is above the other sorbents.

The effect of pressure hydration on particle size distribution is shown in Figure 3-3 for Linwood atmospheric hydrate and one of EER's more reactive pressure hydrates (#8-1). The data indicates that the pressure hydrate was finer than the atmospheric hydrate for all particle sizes which supports the fact that the capture was higher with the pressure hydrate (see Chapter 4.0). Several other pressure hydrate batches were analyzed for particle size

TABLE 3-1. LINWOOD AND LONGVIEW SERIES PHYSICAL AND CHEMICAL DATA

	LIMESTONE	QUICKLIME	ATMOSPHERIC HYDRATE	PRESSURE HYDRATE
DENSITY, g/cm^3	2.71 2.68	2.24	2.30 2.27	2.26
SURFACE AREA M^2/g	1.1 0.9	2.2 3.4	14.0 16.1	6.8 7.2
MEDIAN PARTICLE SIZE μM	13.3 11.1	3.2	2.2 3.8	2.1
SOURCE	LINWOOD/EER DRAVO/EER	LINWOOD/EER DRAVO/EER	LINWOOD DRAVO	EER
CA (WT %)	38.6 39.0	67.9 64.8	51.6 48.8	51.6 51.0
MG	0.60	0.72	0.97 0.48	0.57
NA	0.01	0.00	0.00 0.02	0.01
K	0.03	0.02	0.04 0.01	0.03
FE	0.17	0.30	0.27 0.15	0.24
SI	0.38	0.56	0.66 0.35	0.18
AL	0.12	0.21	0.18 0.10	0.19

UPPER = LINWOOD
LOWER = LONGVIEW

TABLE 3-2. COMMERCIAL HYDRATE PHYSICAL AND CHEMICAL DATA

SORBENT	COLTON	LONGVIEW	LINWOOD
DENSITY, G/CM^3	2.28	2.27	2.30
SURFACE AREA, M^2/G	15.2	16.1	14.0
MEDIAN PARTICLE SIZE, μM	4.0	3.9	2.2
CA, %	51.4	48.8	51.6
MG	0.25	0.48	0.97
NA	0.01	0.02	0.00
K	0.05	0.01	0.04
FE	0.10	0.15	0.27
SI	3.30	0.35	0.66
AL	0.21	0.10	0.18

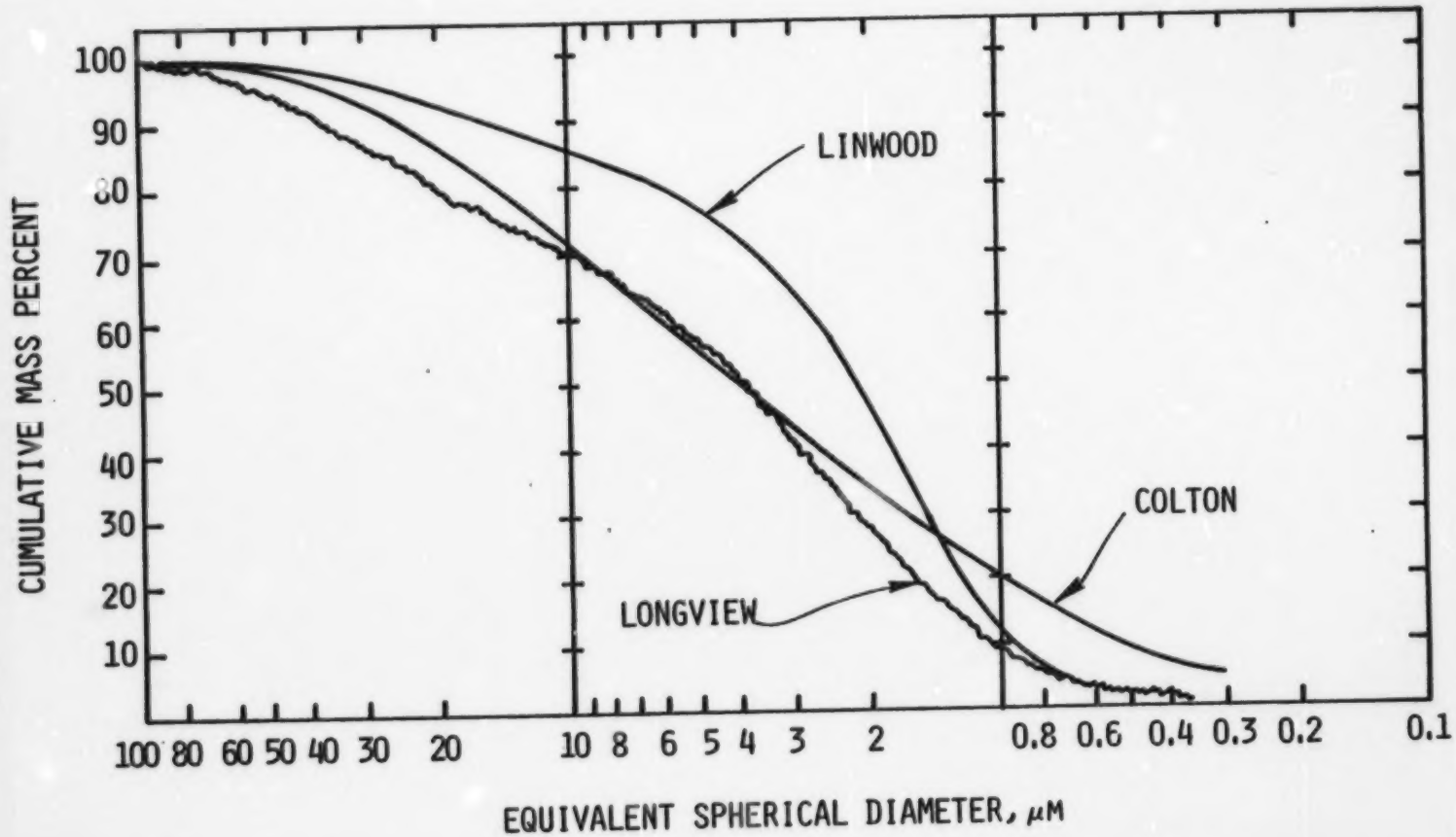

Figure 3-1. Commercial hydrate particle size distributions.

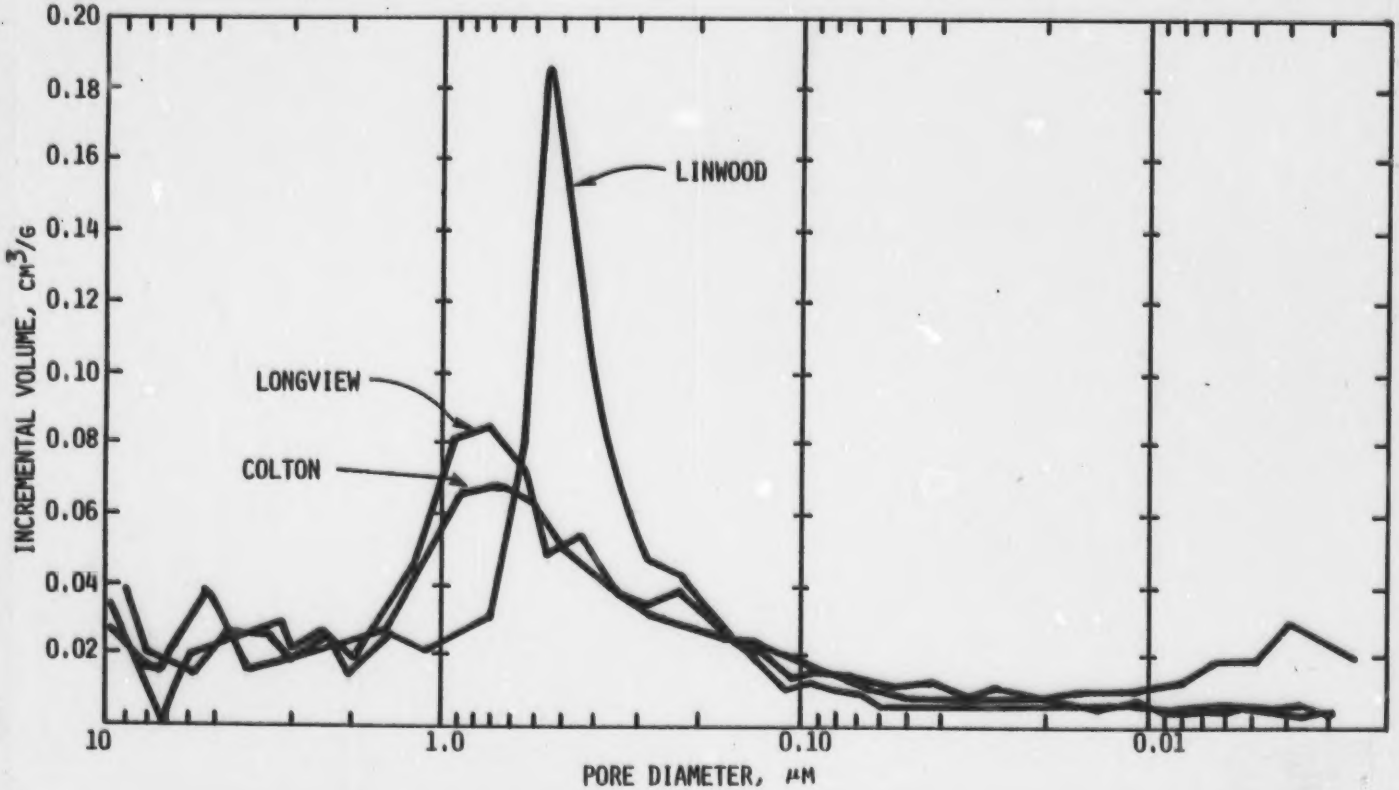

Figure 3-2. Commercial hydrate pore size distributions.

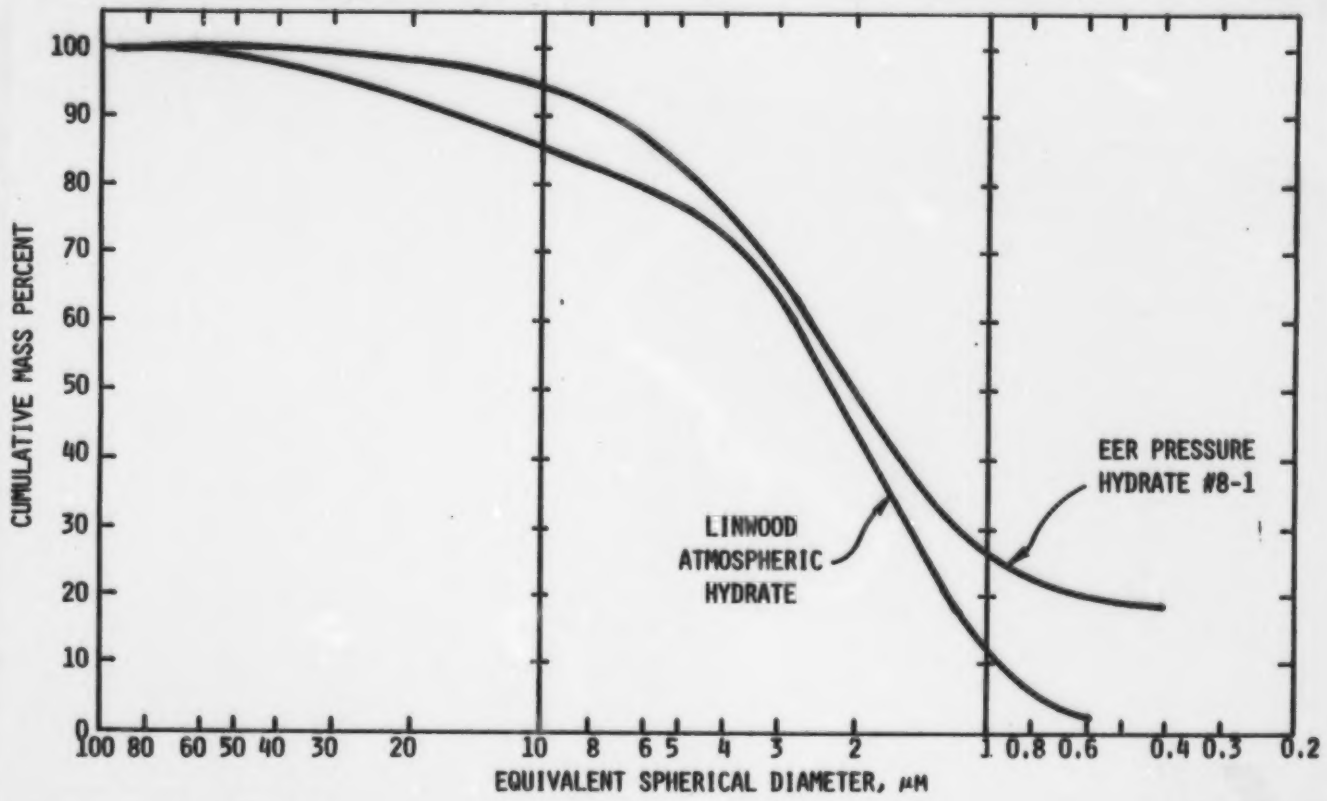

Figure 3-3. Comparison of atmospheric and pressure hydrate particle size distribution.

distribution and the results are shown in Figure 3-4. Both batches were coarser than run 8-1 and subsequent testing on the CTT suggested that these sorbents were not as reactive as the 8-1 batch (see Section 4.2).

Pore size distributions for Linwood atmospheric and the UNDERC pressure hydrate (produced with the same CaO in UNDERC hydrator) are shown in Figure 3-5. The interstitial peaks are quite similar on this plot and below 0.10 microns. It appears that pressure hydration did not alter the pore size distribution of the hydrate.

The chemical and physical data for the six demonstration sorbents are given in Table 3-3. The first four sorbents listed are high-calcium atmospherically hydrated limes (AH), Kemidol is an atmospherically hydrated dolomitic lime (AHD), and the Ivory is a pressure hydrated dolomitic lime (PHD). The Linwood AH is shown for comparison. Figure 3-6 is a composite plot of particle size distributions for the demo sorbents with the Linwood again shown for comparison. All of the sorbents appear to be grouped tightly except for the Kemidol which was coarser than any of the others. Also, the Linwood was finer than all of the demo sorbents.

3.2 Fuel Analyses

Table 3-4 shows the proximate and ultimate analyses of the fuels used for this program. The Illinois and the Demonstration coal were both relatively high sulfur fuels with uncontrolled SO_2 emissions of more than 2500 ppm (0 percent O_2). The ultimate analyses of the two fuels were quite similar and the only major differences in the proximate analyses were the moisture content where the Illinois was much wetter, and the fixed carbon content for which the demo coal was higher. Both coals were ground to approximately 70 percent through 200 mesh.

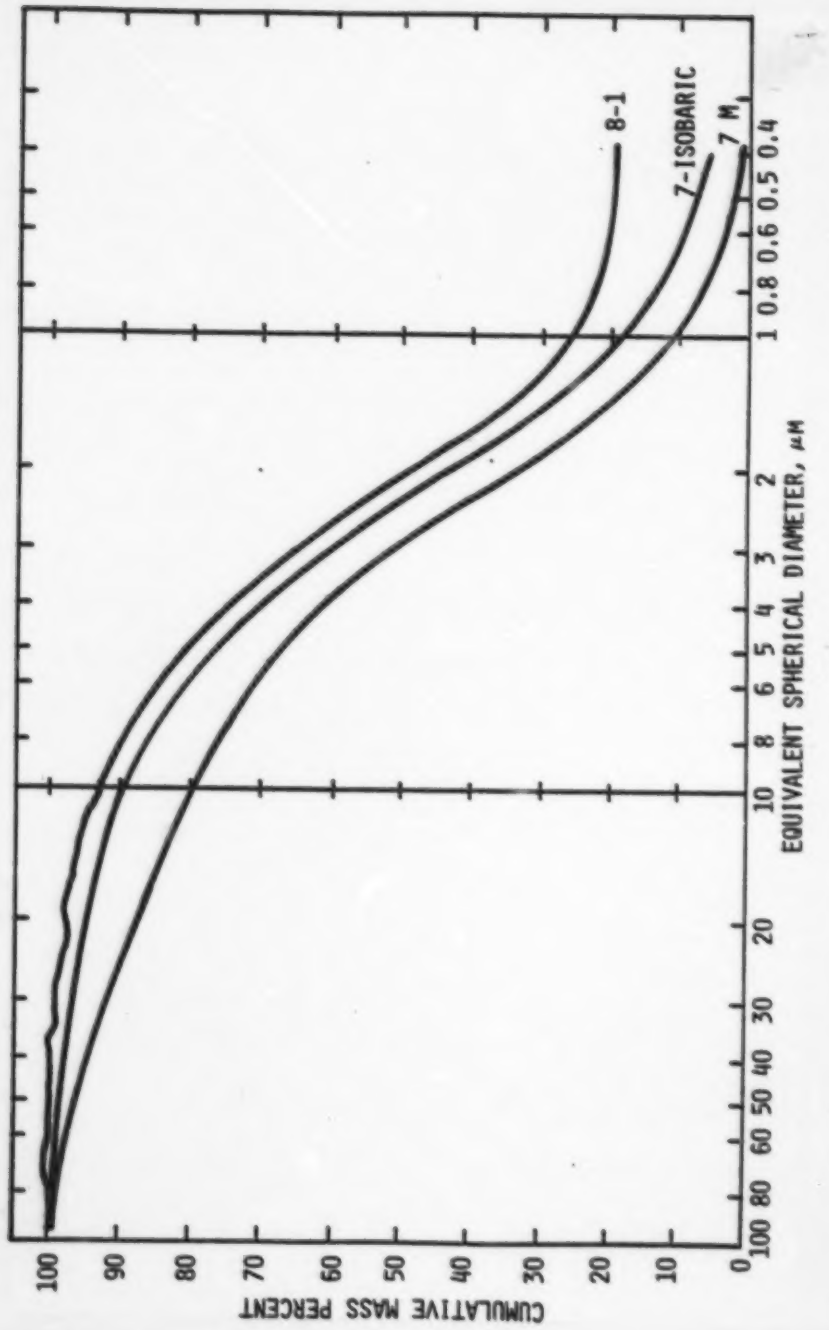

Figure 3-4. Particle size distribution of several pressure hydrates.

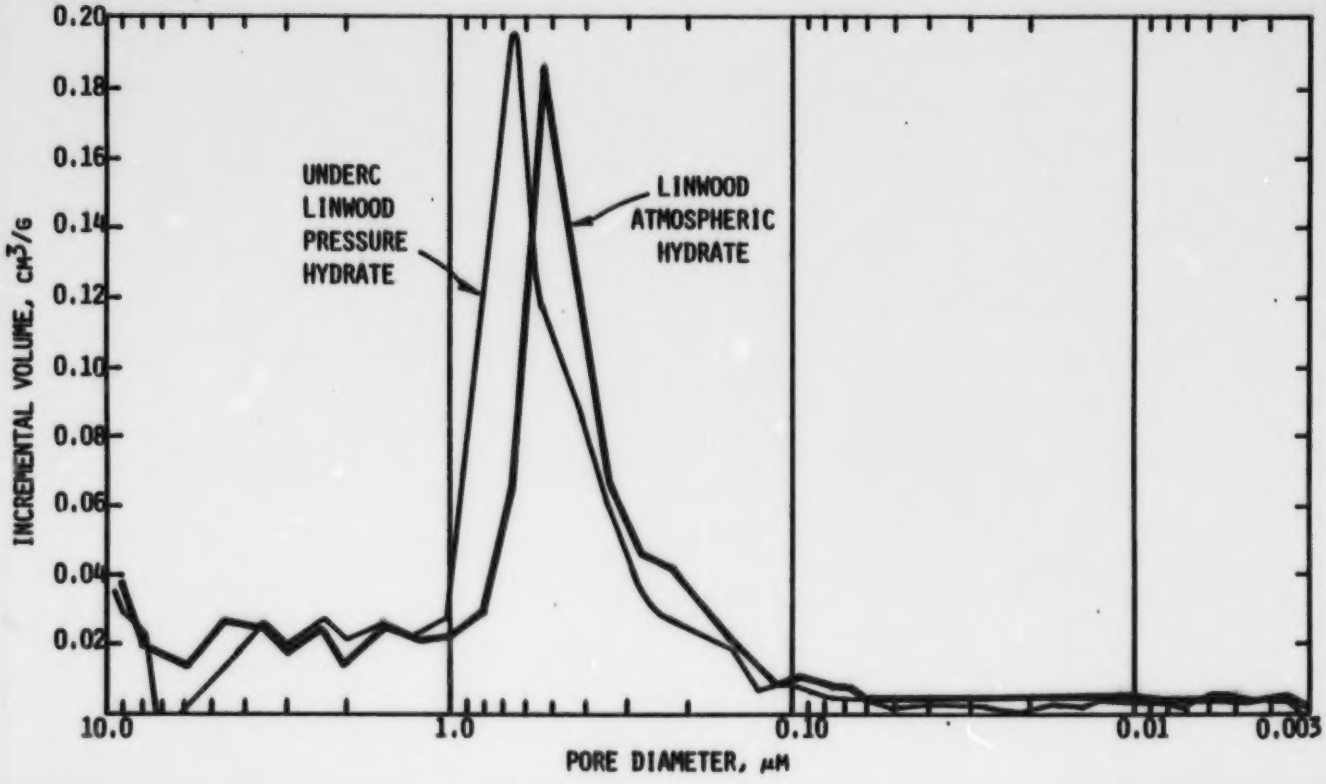

Figure 3-5. Pore size distributions of pressure and atmospheric hydrate.

TABLE 3-3. PHYSICAL AND CHEMICAL DATA FOR DEMO SORBENTS

SORBENT	KEMIKAL	DETROIT	MARBLEHEAD	MERCER	KEMIDOL AHD	IVORY PHD	LINWOOD AH
DENSITY (G/CM^3)	2.24	2.25	2.26	2.24	2.40	2.33	2.30
SURFACE AREA (M^2/G)	12.50	16.14	13.13	15.41	15.36	16.23	16.0
MEDIAN PARTICLE SIZE (μM)	3.5	3.9	4.1	4.1	6.0	4.0	2.2
CHEMICAL COMPOSITION (WT%)							
CA	48.3	51.9	52.2	51.3	28.9	29.5	51.6
MG	1.06	0.48	0.64	0.42	18.7	17.9	0.97
NA	0.02	0.02	0.01	0.02	0.02	0.02	0.00
K	0.05	0.01	0.01	0.02	0.01	0.01	0.04
FE	0.22	0.15	0.38	0.40	0.10	0.10	0.27
SI	0.59	0.26	0.47	0.43	0.10	0.10	0.66
AL	0.23	0.10	0.15	0.15	0.05	0.05	0.18

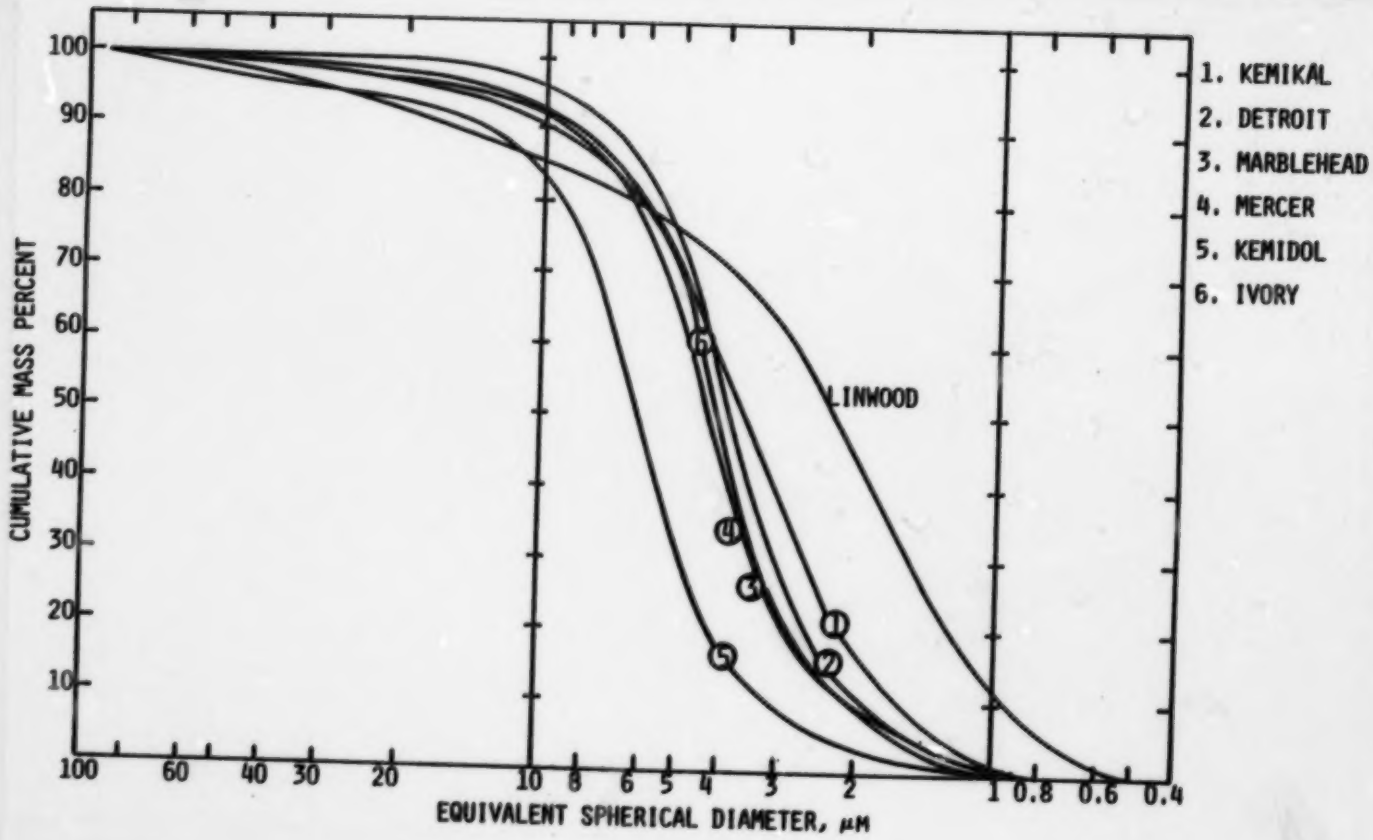

Figure 3-6. Demo sorbents particle size distributions.

TABLE 3-4. FUEL ANALYSES

Property \ Fuel	Illinois	Demo Coal
Proximate (wt%, as received)		
Moisture	15.79	2.28
Volatile Matter	35.44	35.66
Fixed Carbon	40.39	51.98
Ash	8.38	10.08
Ultimate (wt%, dry)		
C	70.71	73.41
H	4.86	4.85
N	1.12	1.32
S	3.94	3.18
O	9.30	6.92
Ash	9.95	10.32
HHV (Btu/lb, dry)	14114	13173
Ash Analysis (wt%, dry)		
SiO_2	46.74	45.31
Al_2O_3	16.85	20.23
TiO_2	0.85	0.79
Fe_2O_3	18.33	28.88
CaO	6.21	1.13
MgO	0.85	0.63
Na_2O	1.55	0.23
K_2O	2.12	1.39
P_2O_5	0.18	0.29
SO_3	5.75	1.06

4.0 RESULTS AND DISCUSSION

This chapter describes the capture results obtained on the CTT and BSF facilities with the sorbents that were received from the lime companies or generated on the pressure hydrator. The chapter has been divided into four subsections; each of which addresses a different aspect of the program. The first subsection presents data from the Linwood and Longview sorbents and makes a comparison between the relative reactivity of each group. Subsection 4.2 looks at the effect of pressure hydration on sorbent reactivity and Subsection 4.3 is devoted to the relative performance of commercially available atmospheric hydrates. The last subsection in this chapter addresses the performance of the six commercial sorbents that were proposed for the LIMB demonstration project.

All of the sorbents tested in the CTT were injected downstream at 2250°F with a radial injector positioned at the centerline of the furnace. Either natural gas or the Illinois coal was used as the fuel and the upper back-fired channels were fired up while the lower ones were turned off (see Figure 2-2). Figure 4-1 shows the time/temperature histories between the injection point (2250°F) and the gas sampling location for both fuels. The majority of the testing in the BSF was conducted with natural gas. In some cases the sorbents were injected at different locations in the furnace. Figure 4-2 presents the thermal profile from the burner to the sampling location (Port 10B in Figure 2-3).

4.1 Linwood and Longview Sorbents

The Linwood and Longview sorbent series were chosen since commercial limestones, quicklimes, and atmospheric hydrates are available and because pressure hydrates are available from UNDERC. The availability of the entire sorbent series allowed for testing the reactivity variation in the calcination and hydration processes. The availability of the pressure hydrate provided an opportunity to see if the high reactivity of the UNDERC sorbent could be duplicated in the bench scale hydrator.

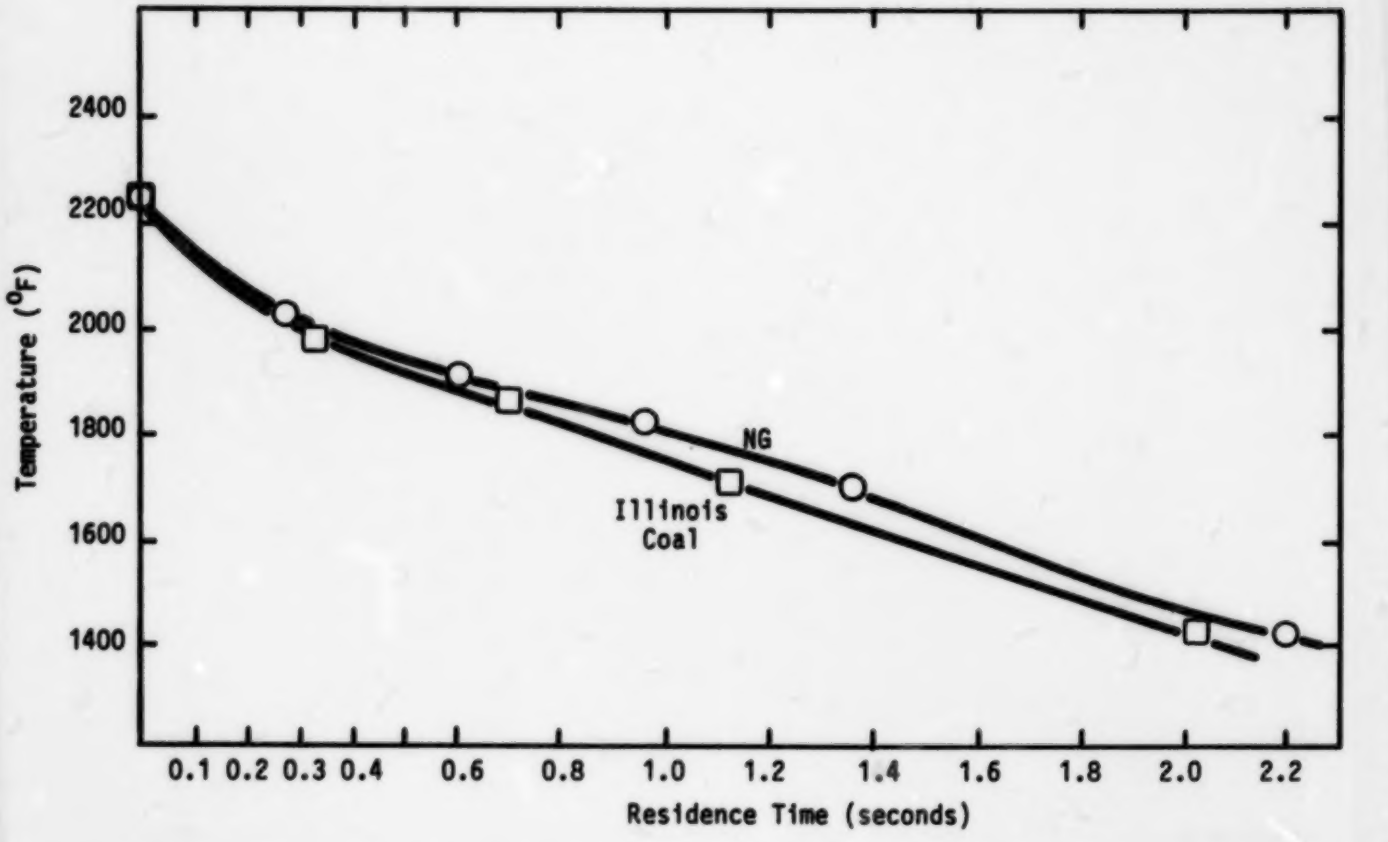

Figure 4-1. CTT temperature profile from injection point.

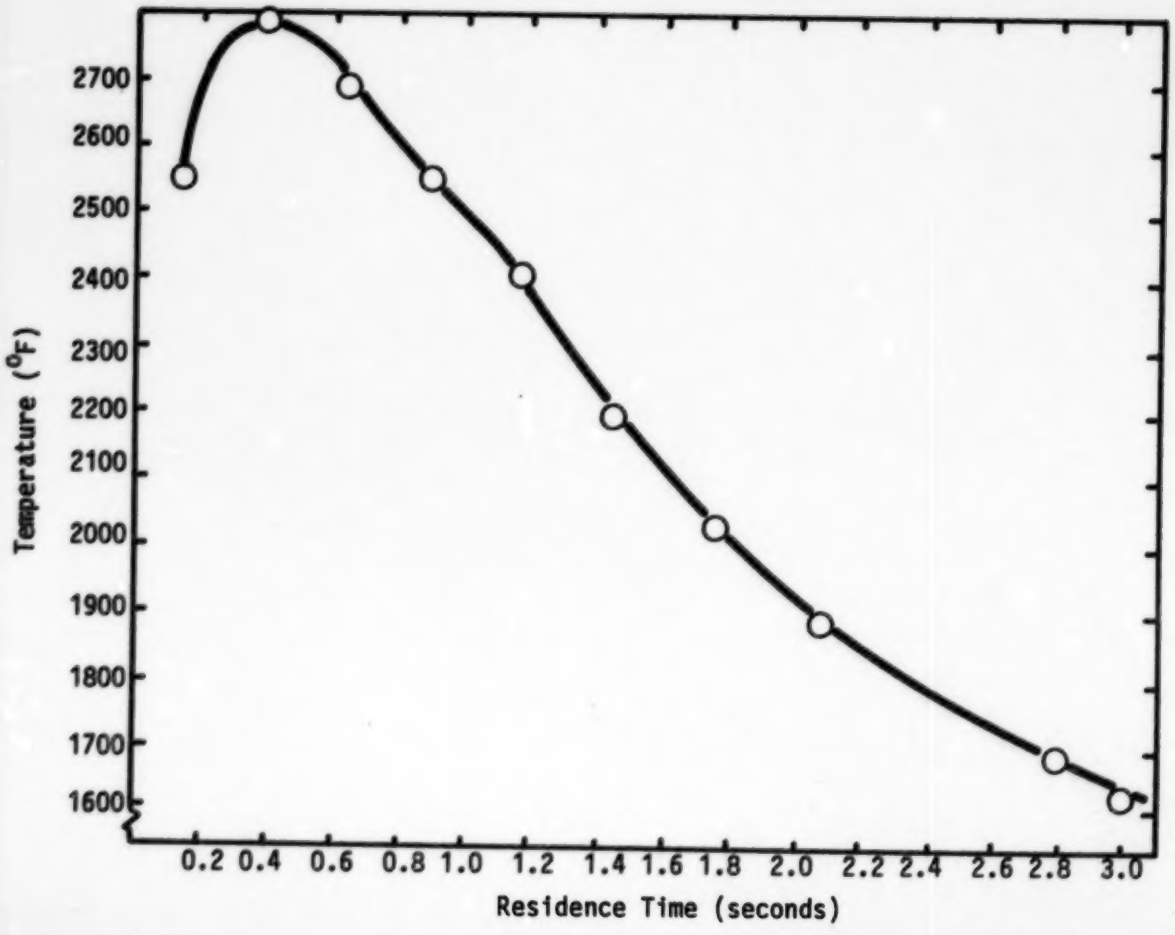

Figure 4-2. BSF temperature profile.

After contacting the lime companies, the materials were received in their raw form. The Linwood carbonate had the consistency of sand and the quicklime was received as pebbles of about 1/2 inch diameter. The Longview carbonate came as rocks, some of which were larger than 1-1/2 inch in diameter, and the quicklime resembled small flakes that were easily broken apart. Each of these materials were pulverized at EER in order to put them through the sorbent feed system. Properties of these sorbents are shown in Table 3-1. Initially, each sorbent was tested on the CTT with both natural gas and Illinois coal. Figure 4-3 shows the results of the Linwood sorbents injected downstream at 2250°F. For both fuels, the atmospheric hydrate gave quite high capture while the quicklime and carbonate performed about the same at a much lower level. For the atmospheric hydrate (AH) and the carbonate, the results were about as expected but the capture for the quicklime was somewhat above the expected value. Figure 4-4 shows an analogous plot for the Longview sorbents and again, the AH produced the highest capture followed by the quicklime and carbonate which were similar in capture. For the coal case especially, the Longview quicklime gave higher results than were expected.

After re-analyzing the chemical composition of the two quicklimes, it was noticed that the hydrogen content of both materials had increased and apparently, the materials had both partially hydrated. Given this information, the high capture results of the quicklimes could be explained since a fraction of the material was essentially an atmospheric hydrate. An estimate of the true CaO capture was calculated based on the information shown in Figures 4-3 and 4-4. By knowing the composition of the "quicklime" and the reactivity of the AH, the results could be corrected downward to give the dashed lines shown in Figure 4-5. The estimates give a more accurate value for the pure quicklime capture which implies that the carbonates are actually more reactive than the quicklimes. The data shown in Figure 4-6 supports the argument from the hydrate point of view. Here the Longview atmospheric hydrate is compared against a batch of atmospheric hydrate produced at EER beginning with the Longview quicklime. Subsequent analysis of the EER batch indicated that the material was only 80 percent hydrated compared to 94 percent for the commercial sorbent. The remainder of the EER

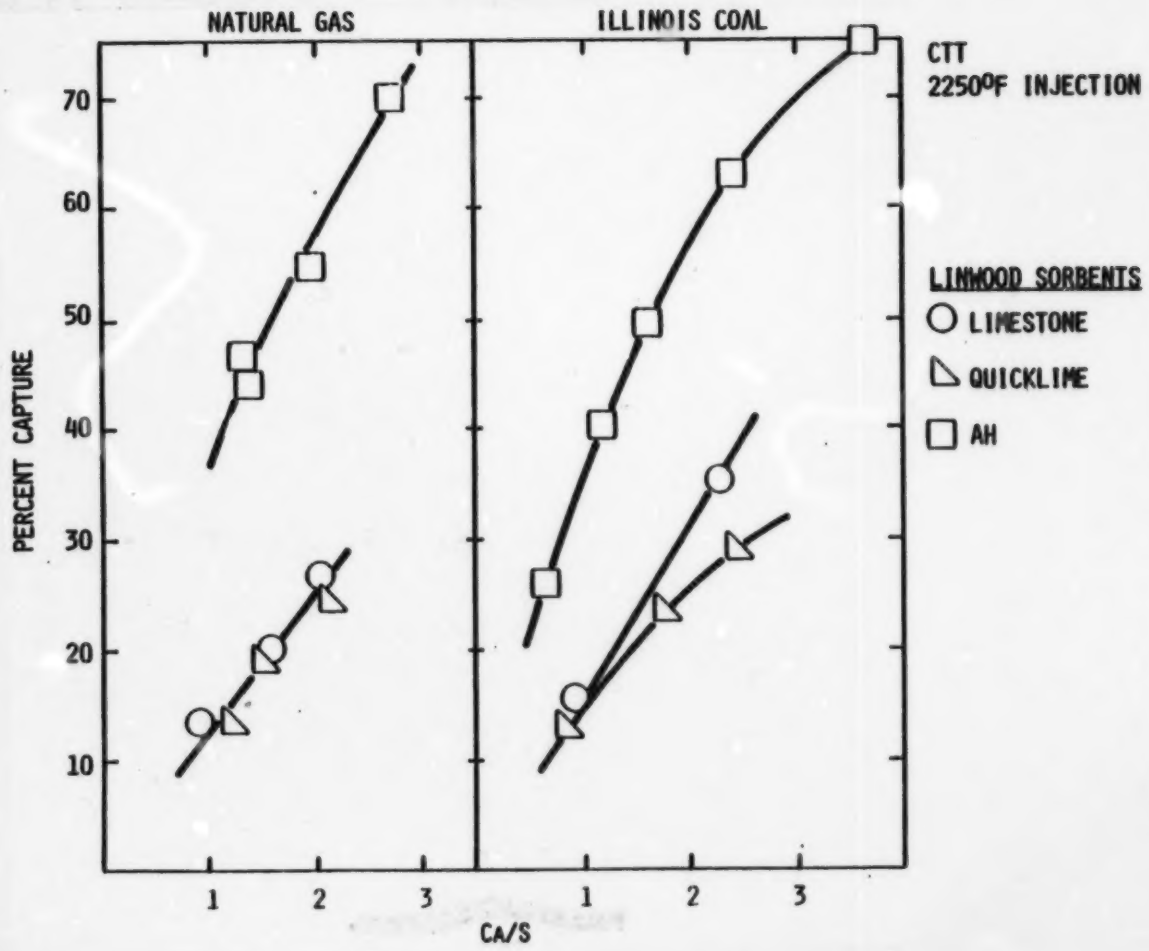

Figure 4-3. Linwood sorbents with gas and coal.

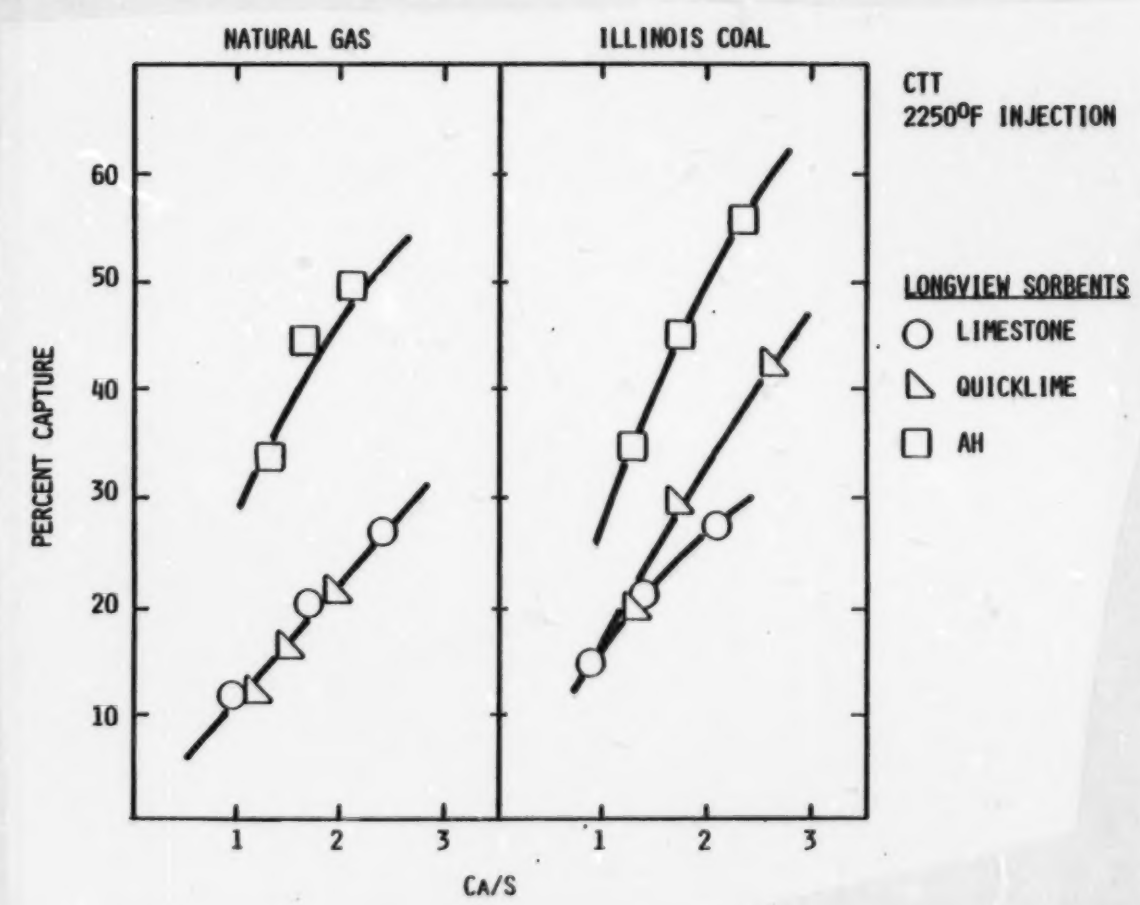

Figure 4-4. Longview sorbents with gas and coal.

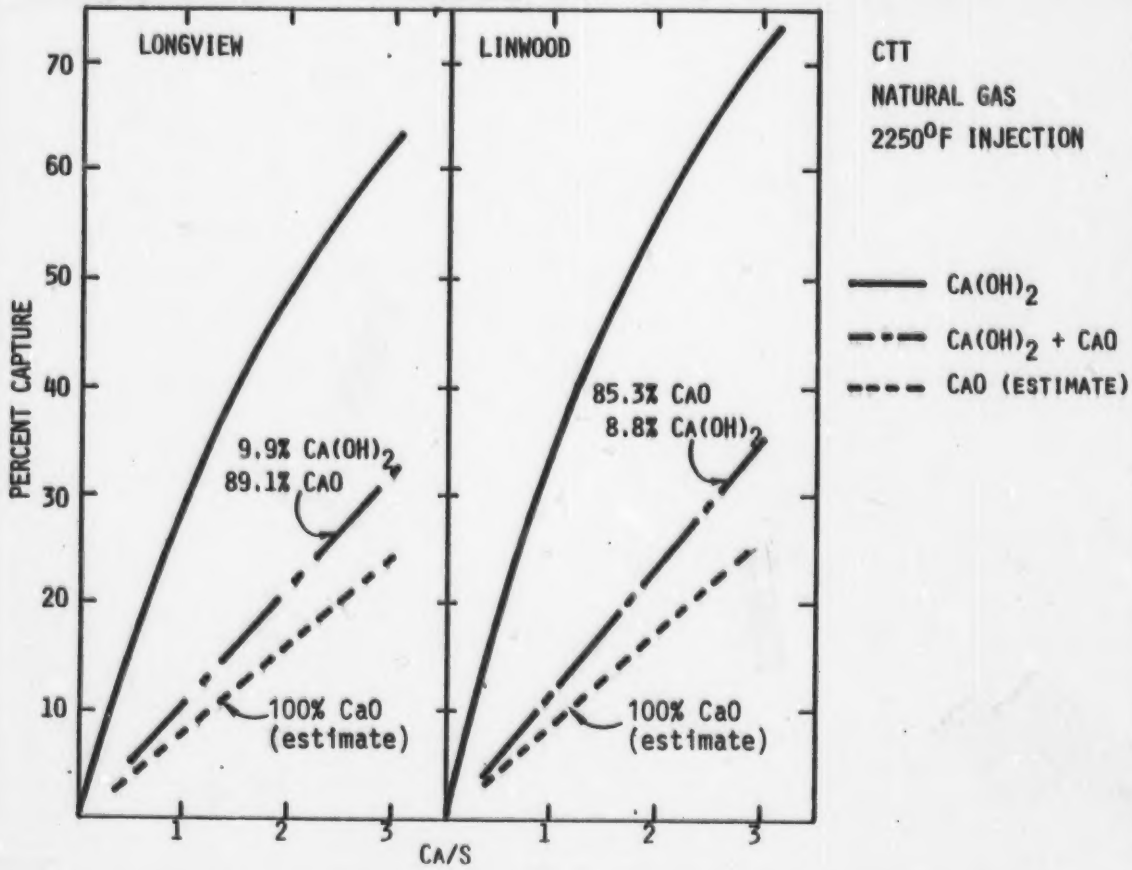

Figure 4-5. Estimation of quicklime reactivity.

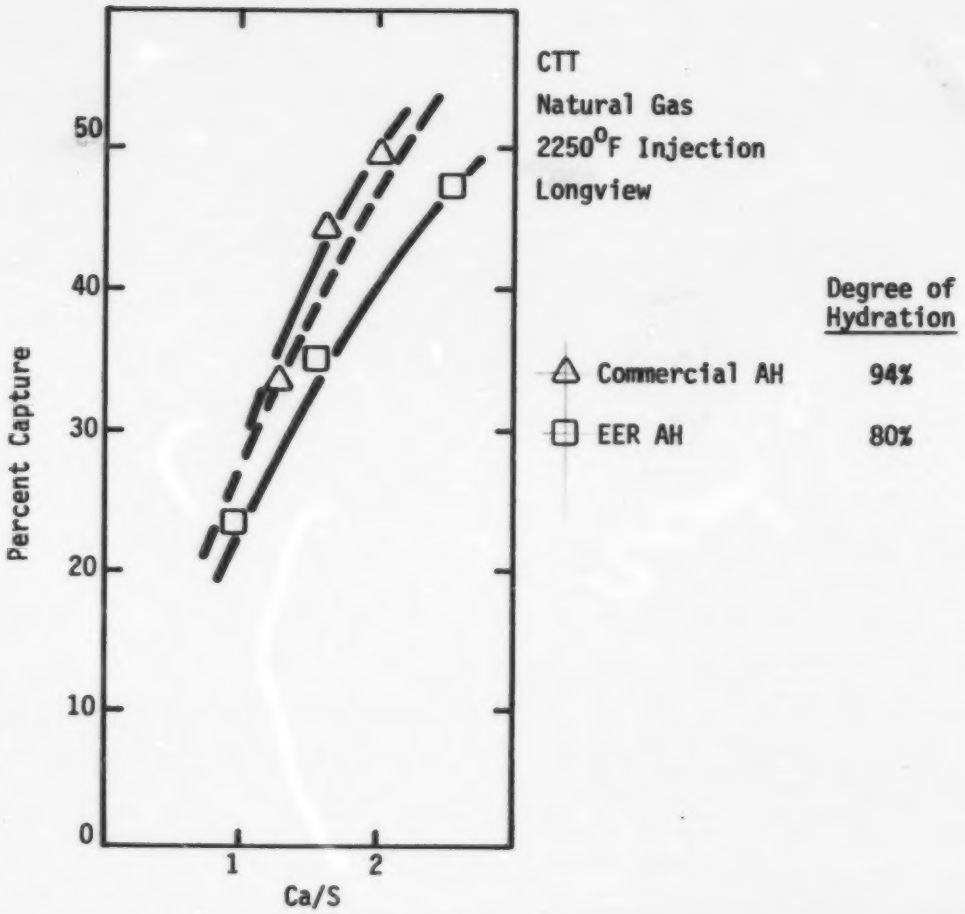

Figure 4-6. Degree of hydration effects.

hydrate was primarily calcium oxide which was much less efficient in terms of sulfur removal. The dashed line on the plot represents the estimated capture of material that is 100 percent hydrated. These results fall much closer to the commercial hydrate which was almost completely hydrated.

Figures 4-7 and 4-8 show a direct comparison of the Linwood and Longview sorbent families for natural gas and Illinois coal, respectively. For gas, the Linwood was a better sorbent than the Longview in every category except for the quicklime. For coal, the Linwood produced better capture for the atmospheric and pressure hydrates. The limestone results were about the same for both sorbents and only for the quicklime was the Longview sorbent better although this effect was attributed to partial hydration as discussed above. In general, the Linwood sorbent series were more effective than the Longview sorbent series for all of the firing conditions tested.

4.2 Pressure Hydration

One of the central issues of this program was to define the effect, if any, of the pressure hydration process on sorbent reactivity. Initially, the Linwood atmospheric hydrate and the EER pressure hydrate were run with natural gas at two different injection temperatures. Figure 4-9 shows that at an injection temperature of 2150°F, the pressure hydrate gave about 10 percent better capture at all Ca/S ratios. At an injection temperature of about 2250°F however, the difference between pressure and atmospheric was nonexistent which was somewhat surprising. The same sorbents were then run with coal at an injection temperature of 2250°F as illustrated by Figure 4-10. For both Illinois and the demo coal, pressure hydration enhanced sulfur capture to some extent.

One of the initial objectives of this study was to match the results produced by UNDERC's pressure hydrate. The data in Figure 4-11 compares the capture from UNDERC's sorbent versus two of EER's more reactive batches and indicates that indeed, it was possible to reproduce the data. Both pressure hydrates were better than the atmospheric hydrate which is included for comparison. Not every batch produced on the pressure hydrator gave the same

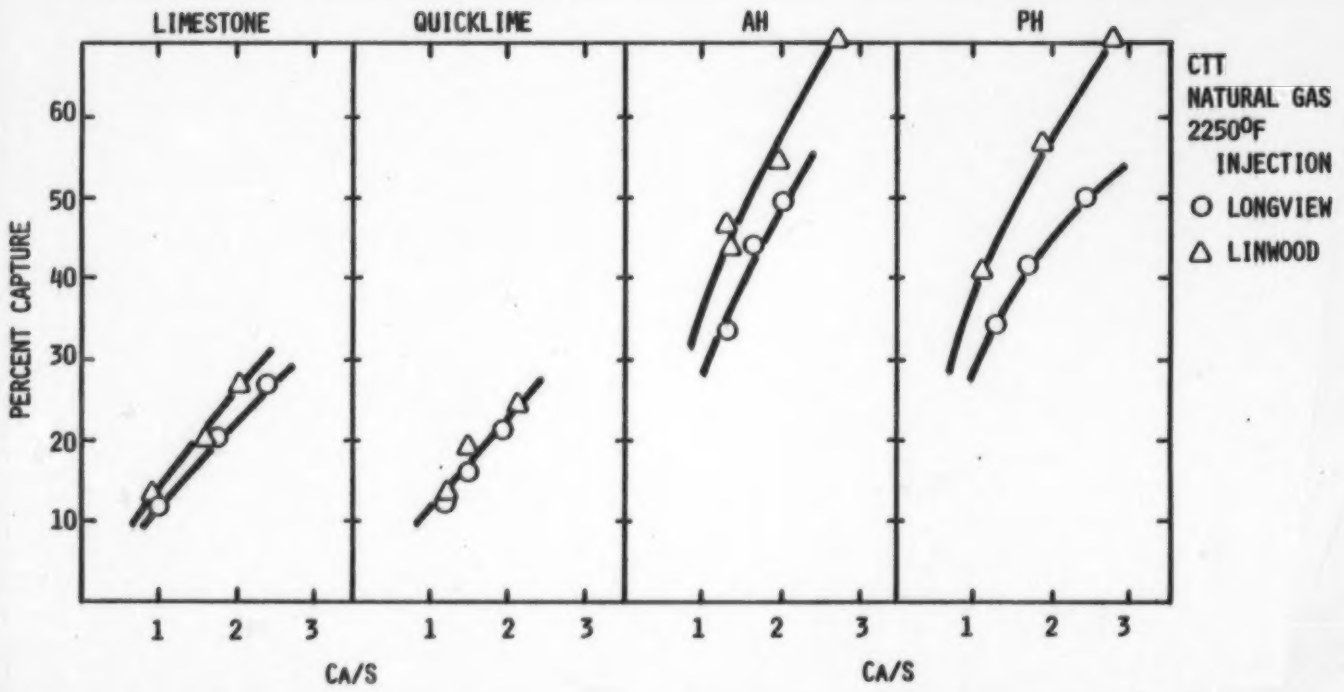

Figure 4-7. Linwood vs. Longview sorbents with gas.

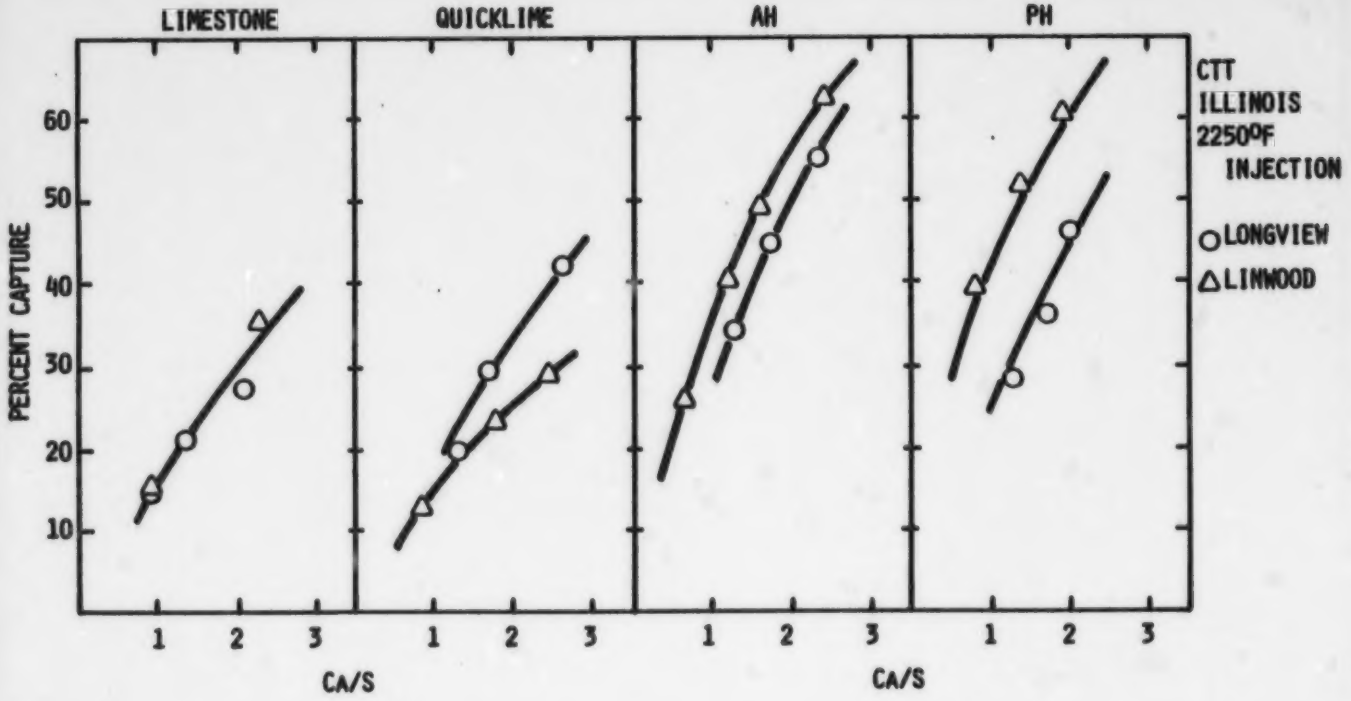

Figure 4-8. Linwood vs. Longview sorbents with coal.

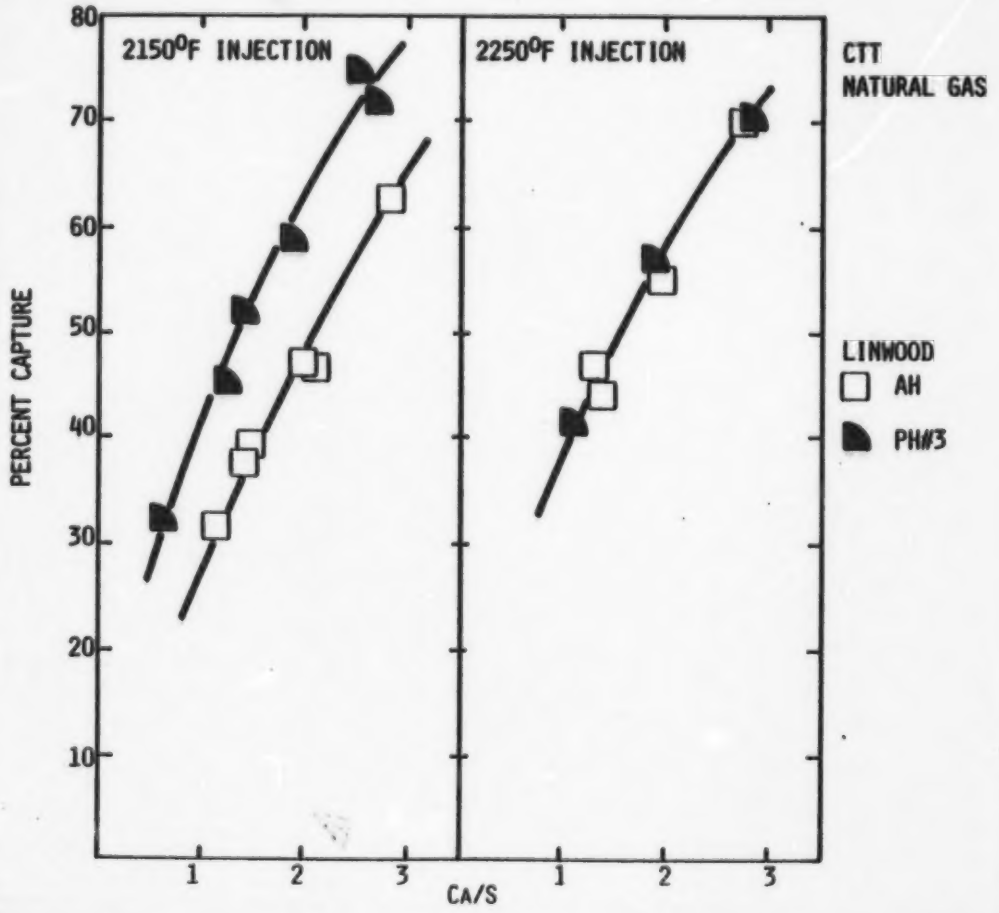

Figure 4-9. Comparison of PH and AH - Natural gas

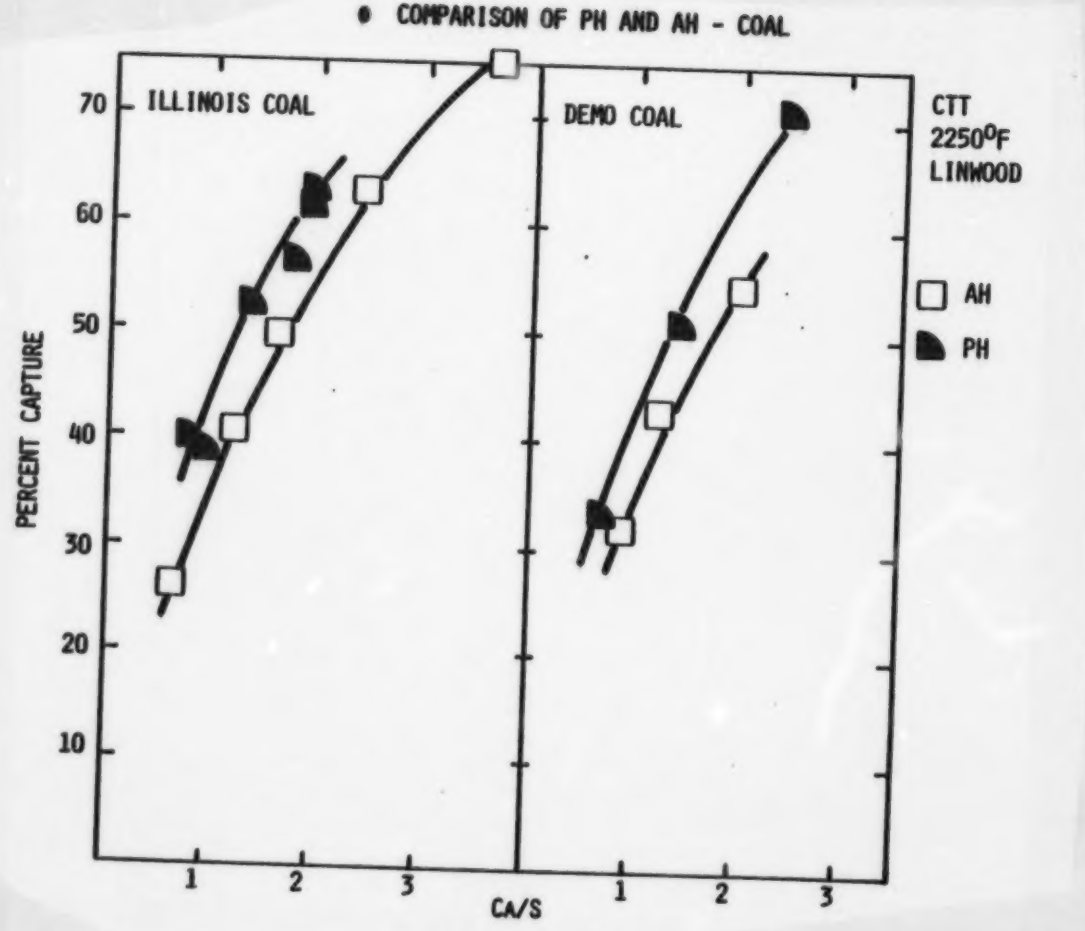

Figure 4-10. Comparison of PH and AH - coal.

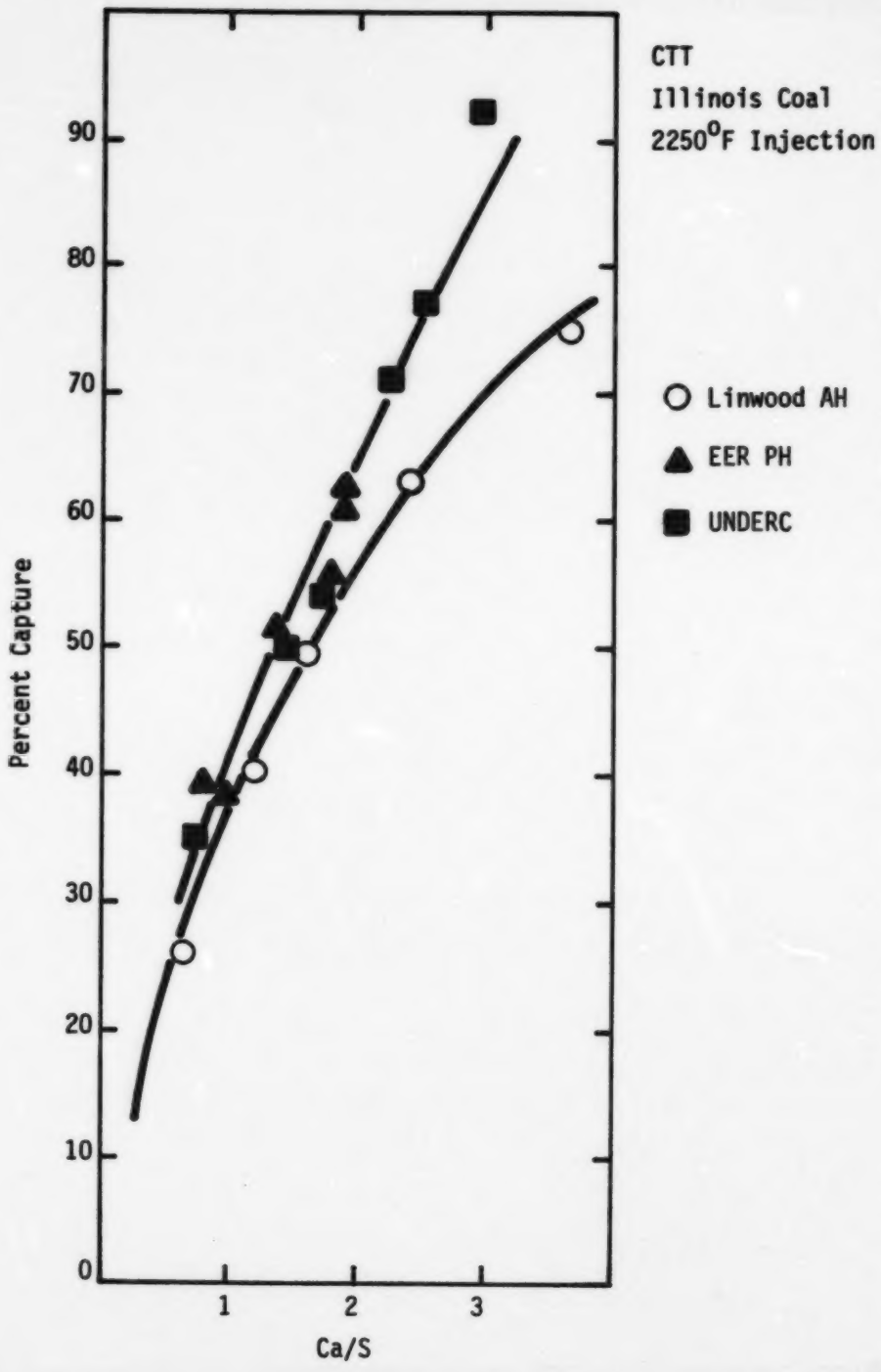

Figure 4-11. Comparison of UNDERC and EER PH.

high capture results as those already shown. After analyzing the strip charts for each batch, it was apparent that there were some differences in the conditions under which each batch was generated. Although the purpose of this task was not designed to optimize the hydration process, some advancements were made in this direction as part of the research effort. This information will be discussed in the following figures in this section.

One apparent advantage of the pressurization process is that the quicklime hydrates more readily than under atmospheric pressure. The left half of Figure 4-12 shows that beginning with the same quicklime, the pressure hydration process was able to achieve a higher degree of $Ca(OH)_2$ (93 percent versus 80 percent) as compared with the atmospheric process. This difference in hydrated vs. unhydrated lime could certainly account for the difference in reactivity observed as was pointed out earlier in this chapter. The right half of Figure 4-12 is a comparison of the commercial Longview AH and the same EER PH results. Under these circumstances, the pressure hydrate did not fare as well which may be attributable to the fact that more than 1/4 of the material was hydrated before experiencing the temperature and pressure produced in the hydrator during the run. The absorption of atmospheric moisture during handling by the highly reactive quicklime accounted for the high degree of preliminary hydration observed. It is possible that the reactivity of a hydrated lime may be diminished if exposed to the conditions of the pressure hydration process.

Figure 4-13 illustrates the approximate range of capture produced from all of the runs made on the hydrator. A similar percent hydration was observed for all of the pressure hydrates (92 to 95 percent). Over the course of this study, several different batches of the raw quicklime were obtained from the lime company and after pulverization a sieve analysis was run for each batch. Deviations in particle size were observed between batches and pressure hydrates formed from the finer quicklimes exhibiting higher reactivity. The surface area of each batch is also shown next to the particle size data and aside from batch #3 which had the highest surface area and was one of the most reactive batches, the others did not appear to be affected significantly by this parameter. Comparing the reactivity of the

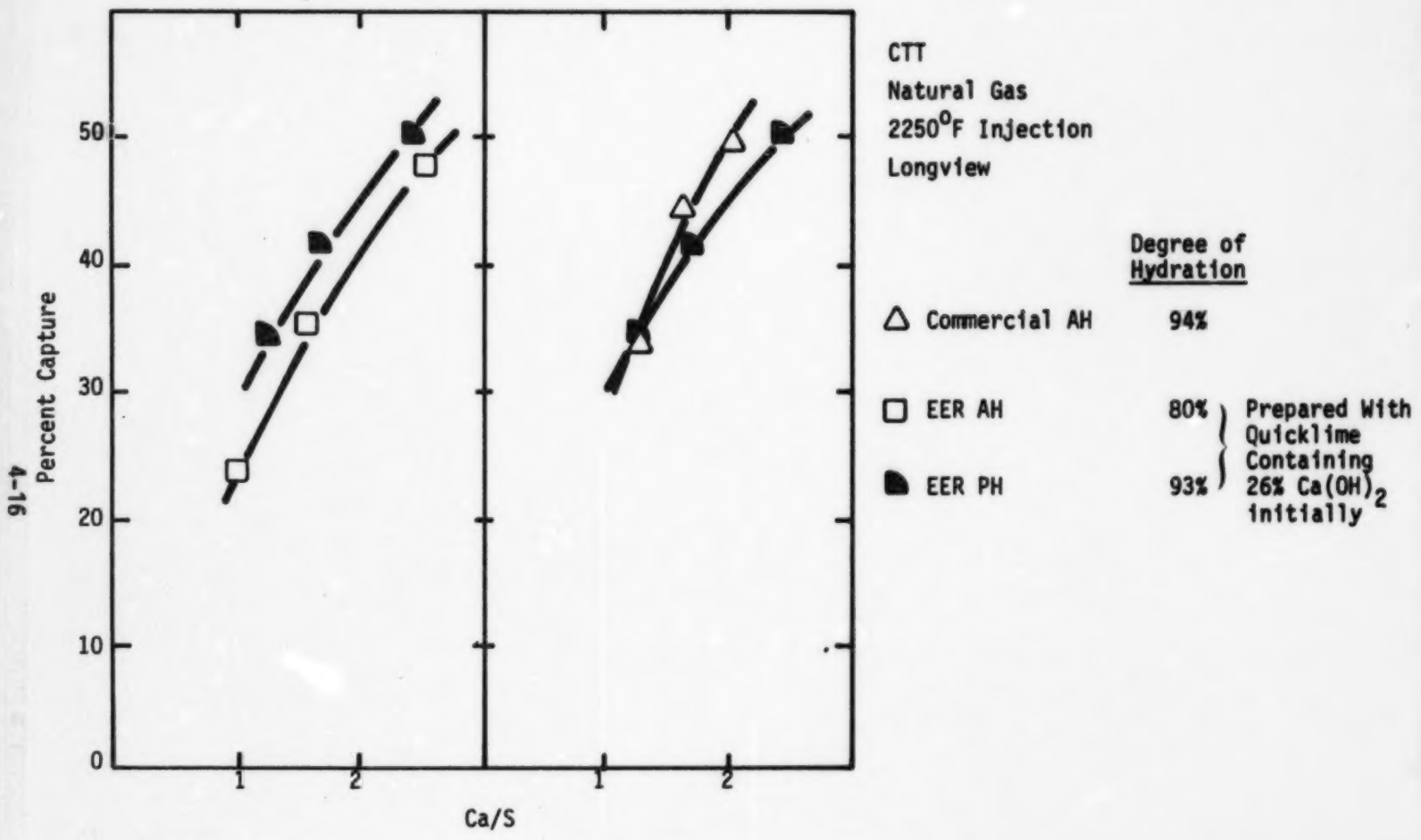

Figure 4-12. Effect of pressurization process on partially hydrated sorbent.

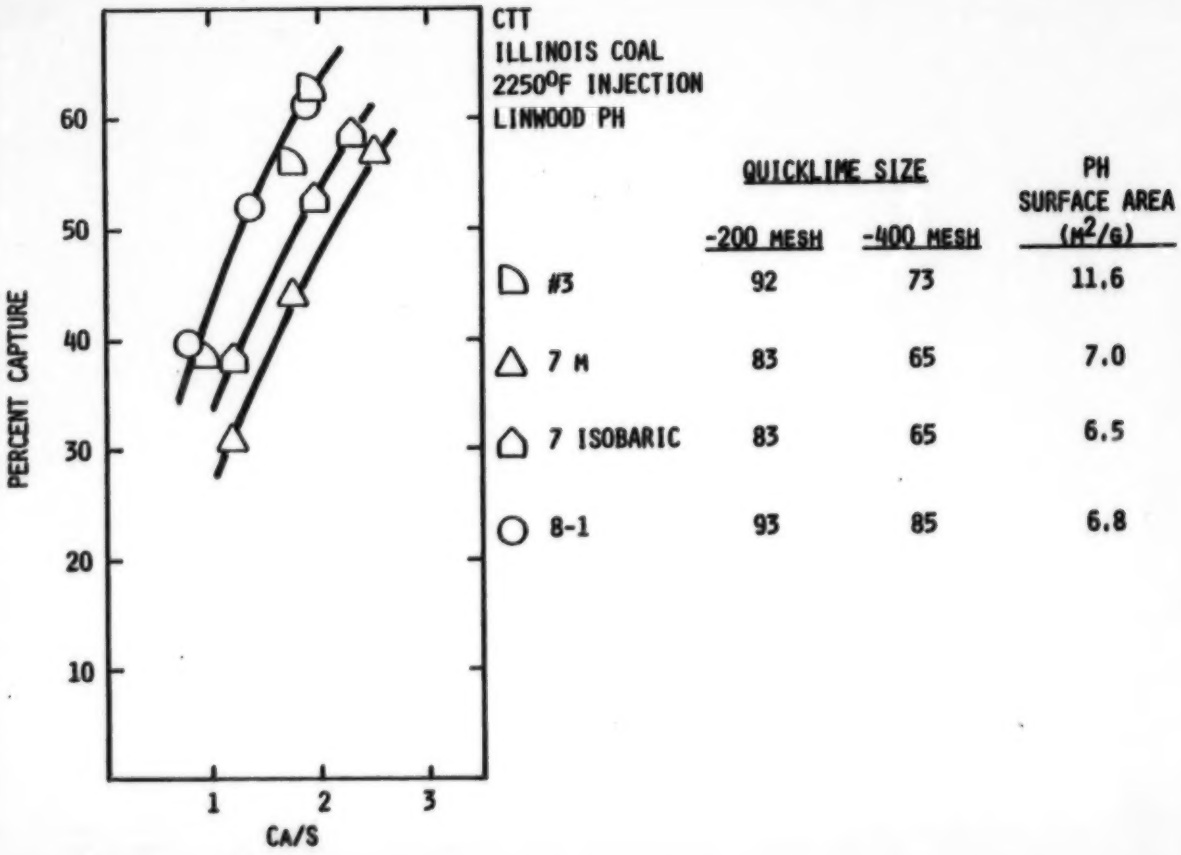

Figure 4-13. Variations in Pressure hydrate generation.

two #7 batches indicates that isobaric discharge yielded more reactive materials than under uncontrolled discharge conditions (both batches #3 and 8-1 were generated with isobaric discharge).

Another process variable examined was the water addition time. Figure 4-14 is a plot of two batches that were nearly identical in terms of all of the process parameters (P, T, SR_{H2O}, discharge, etc.) except one; the rate of water addition. Batch 8-1 was produced with a water addition time of 8 minutes which was approximately the standard for all of the other batches. For batch 8-4, the water addition time was nearly 30 minutes which was caused in part by some difficulty in getting all of the water into the reactor. After all of the water was in the hydrator, the procedure resumed without incident. When both of these batches were tested on the CTT, the 8-1 batch was significantly better than the 8-4 batch even though the surface area was lower. This result led the researchers to believe that reacting all of the quicklime rapidly may help generate a more reactive pressure hydrate rather than intermittently injecting sub-stoichiometric quantities of water over a longer time period.

In a comprehensive investigation, the performance of a highly reactive pressure hydrate produced from Linwood quicklime and the commercial Linwood atmospheric hydrate was compared. Both materials were injected over a broad range of temperatures with natural gas as the fuel in the BSF. The left half of Figure 4-15 illustrates the results and indicates that at a Ca/S ratio of 2.0, the pressure hydrate outperformed the atmospheric hydrate at all injection temperatures. Both curves exhibited an optimum injection temperature at about 2300°F with capture levels tailing off at higher and lower temperatures. At low injection temperatures, there was little time available in the sulfation window for the reaction to occur, and at high temperatures, some dead burning of the sorbent particles probably took place. At the high and low ends of the curves, the capture levels of the two sorbents tended to merge which suggests that in order to take advantage of the difference in reactivity, the injection temperature must fall somewhere between 2500 and 2000°F. The right half of Figure 4-15 shows data taken at approximately the optimum injection temperature with Illinois coal as the

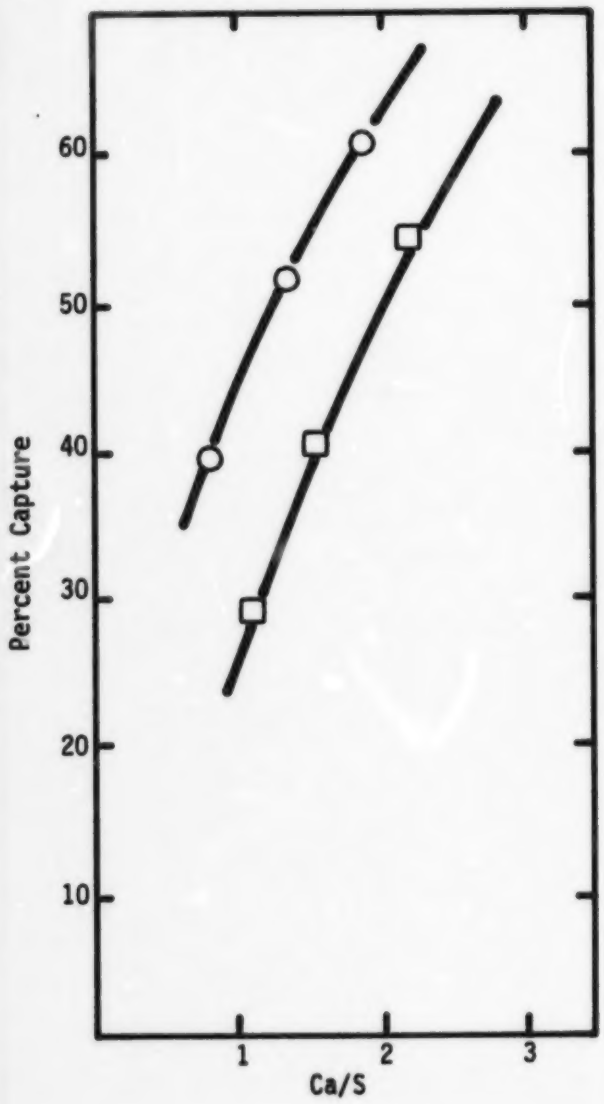

CTT
Illinois Coal
Injection @ 2250°F
Linwood PH

		SA(M^2/G)	Water Addition Time (Min)
○	8-1	6.8	8
□	8-4	8.8	30

Figure 4-14. Effect of H_2O addition time.

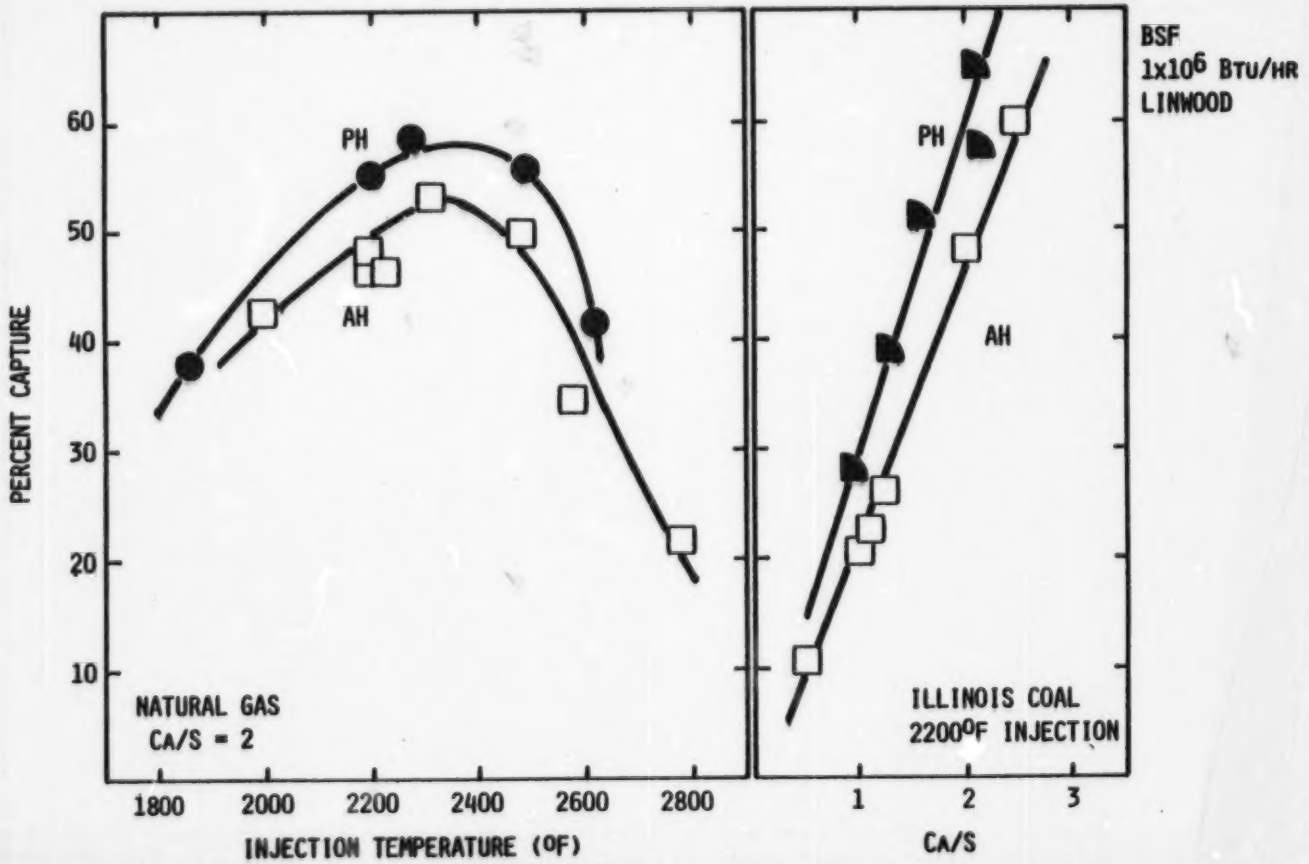

Figure 4-15. Comparison of Linwood AH and PH on BSF.

fuel. As with the gas, an increase in sulfur capture of approximately the same magnitude was observed with the pressure hydrate.

4.3 Comparison of Commercial Hydrates

This subsection describes the test results of the three atmospheric hydrates most widely used in this program; Linwood AH, Longview AH, and Colton AH. Figure 4-16 compares the performance of the hydrates with natural gas and Illinois coal on the CTT at an injection temperature of 2250°F. For both fuels, the Linwood AH was the most reactive with capture of between 55 and 60 percent at a Ca/S ratio of 2.0, followed by the Longview, and finally the Colton. The only apparent fuel effect was that the range of reactivity was compressed slightly with the coal but generally the trends were similar with both fuels. The superiority of Linwood AH was probably due to its finer size distribution (see Table 3-2). The poor performance of Colton AH might have been due to its chemical composition. Analysis showed that the Colton AH contained a high level of silicon which likely led to the formation of calcium silicates, thus reducing the amount of calcium available for reaction with SO_2 (Slaughter, 1986).

The influence of injection temperature was investigated for the three sorbents on the BSF with natural gas as shown in Figure 4-17. These curves again exhibited an optimum injection temperature of about 2300 to 2400°F depending on the sorbent. As injection temperature increased, the curves came together such that at 2600°F, the Linwood and Longview were identical, and at 2800°F, all three sorbents gave the same capture. At the lower injection temperatures, the three sorbents remained separated but below 1800°F, the curves probably would have merged due to the limited sulfation time.

Figure 4-18 shows a comparison of the CTT and BSF data with Illinois coal at approximately the same injection temperature for each of the hydrates. Consistently, the CTT data fell above the BSF data by about 5 percent. Two reasons that the capture on the CTT was higher than on the BSF were that mixing was somewhat faster on the CTT and the gas sampling

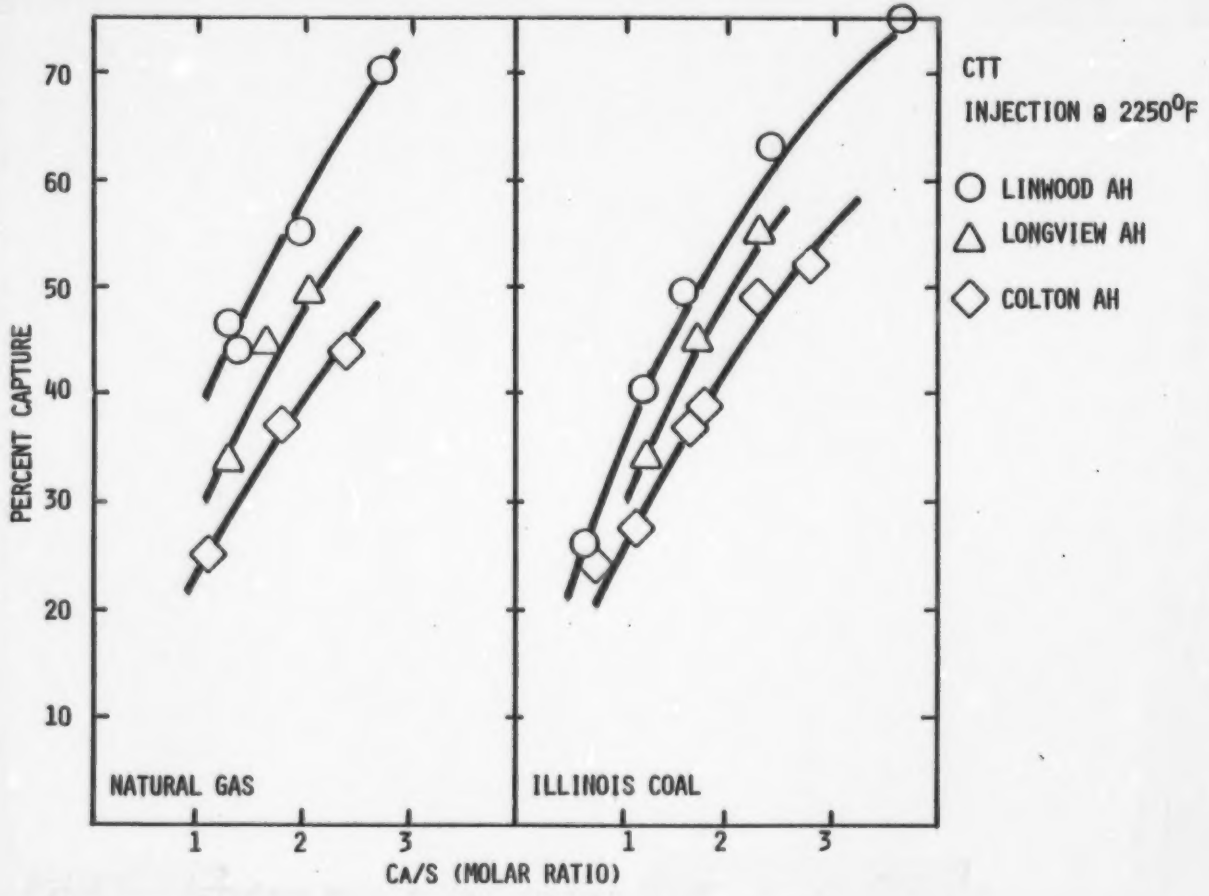

Figure 4-16. Comparison of commercial hydrates on CTT.

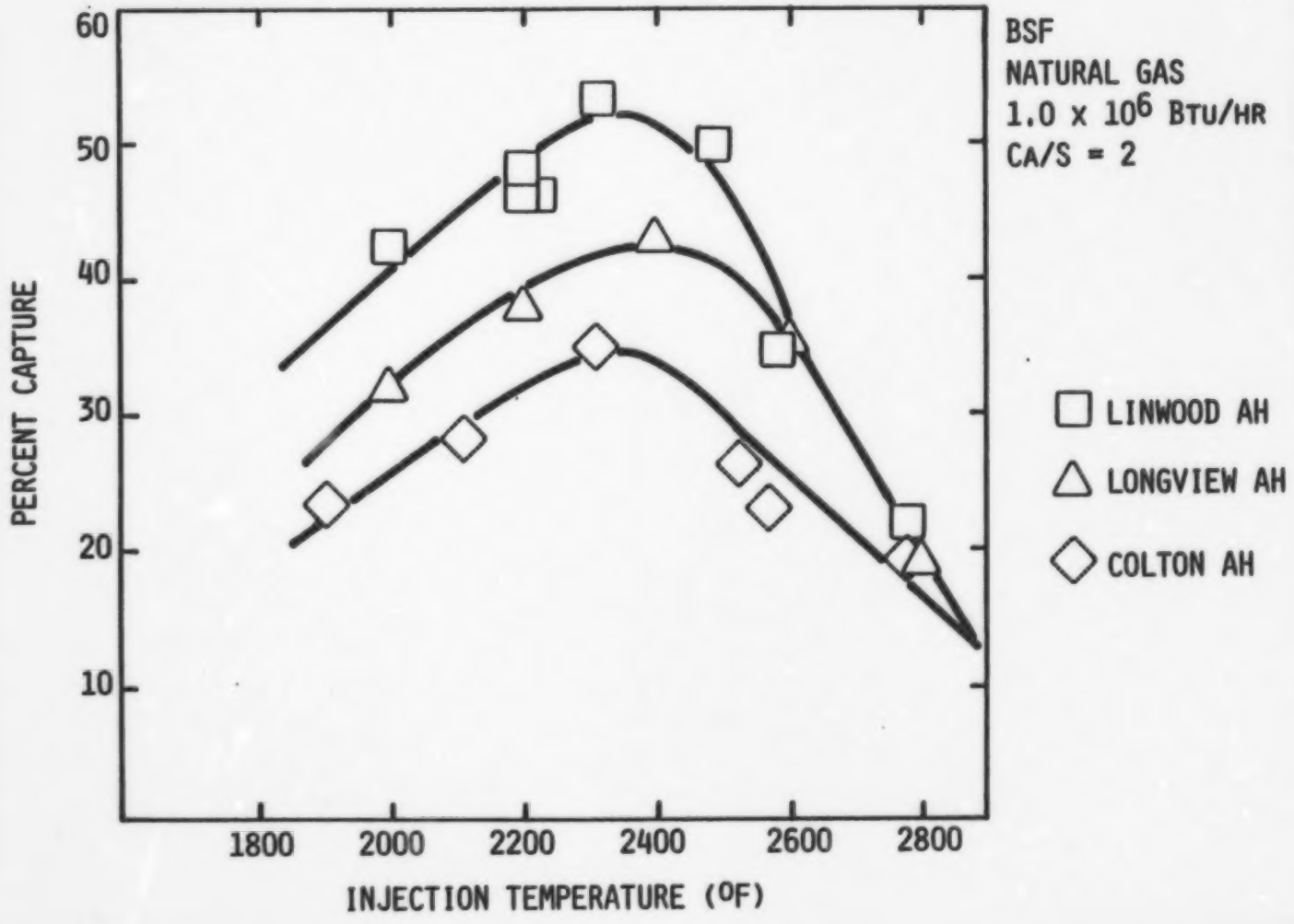

Figure 4-17. Influence of injection temperature.

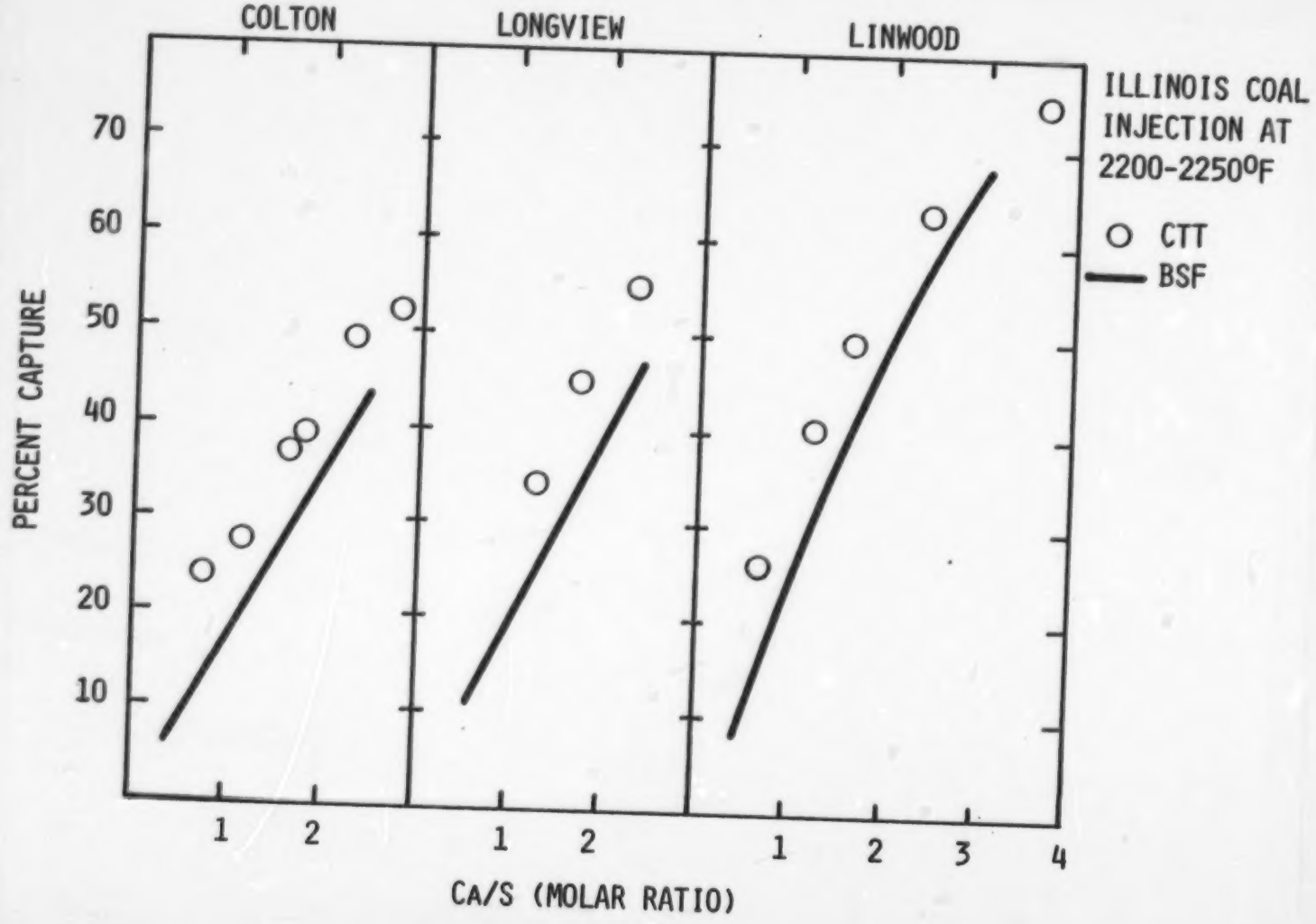

Figure 4-18. Facility comparison.

temperature was slightly lower on the CTT. Both factors would effectively yield a longer residence time and higher capture. Figure 4-19 summarizes the capture levels obtained on both facilities for a Ca/S ratio of 2.0 at near the optimum injection temperature. For both facilities, the Linwood was the best hydrate followed by the Longview and then the Colton. For each sorbent, the capture results were slightly higher on the CTT than on the BSF.

4.4 Performance of Demo Sorbents

In anticipation of the full-scale sorbent injection demonstration in Edgewater, Ohio, six candidate sorbents were identified and tested on the CTT. The demo sorbents were chosen primarily because they were manufactured in the same geographic area as the test facility which would impact transportation costs. Of the six demo sorbents, four were high-calcium atmospheric hydrates, one was a dolomitic atmospheric hydrate, and one was a dolomitic pressure hydrate. A summary of the performance of these sorbents with natural gas and Illinois coal is given in Figure 4-20 for an injection temperature of 2250°F. For some of the sorbents, firing with natural gas was better than coal while for others, the inverse was true. In general, there was little difference between fuels and in terms of overall capture, the two dolomitic sorbents outperformed the high-calcium sorbents. The Mercer AH was the best of the calcium-based sorbents with sulfur capture of about 50 percent at a Ca/S ratio of 2.0 and the Kemikal was the poorest with capture at only slightly above 40 percent. Again, the reactivity differences cannot simply be explained with the differences in particle size (see Table 3-3).

The demonstration coal (Pittsburgh #8) was run with one of the demo sorbents (Marblehead AH) and with the Linwood AH in order to determine if there was any fuel effect. Figure 4-21 indicates that for both of these sorbents, the capture was identical for natural gas, Illinois coal, and the demo coal. It is expected that the other demo sorbents would perform at about the same level with the demo coal as with the Illinois coal shown in Figure 4-20.

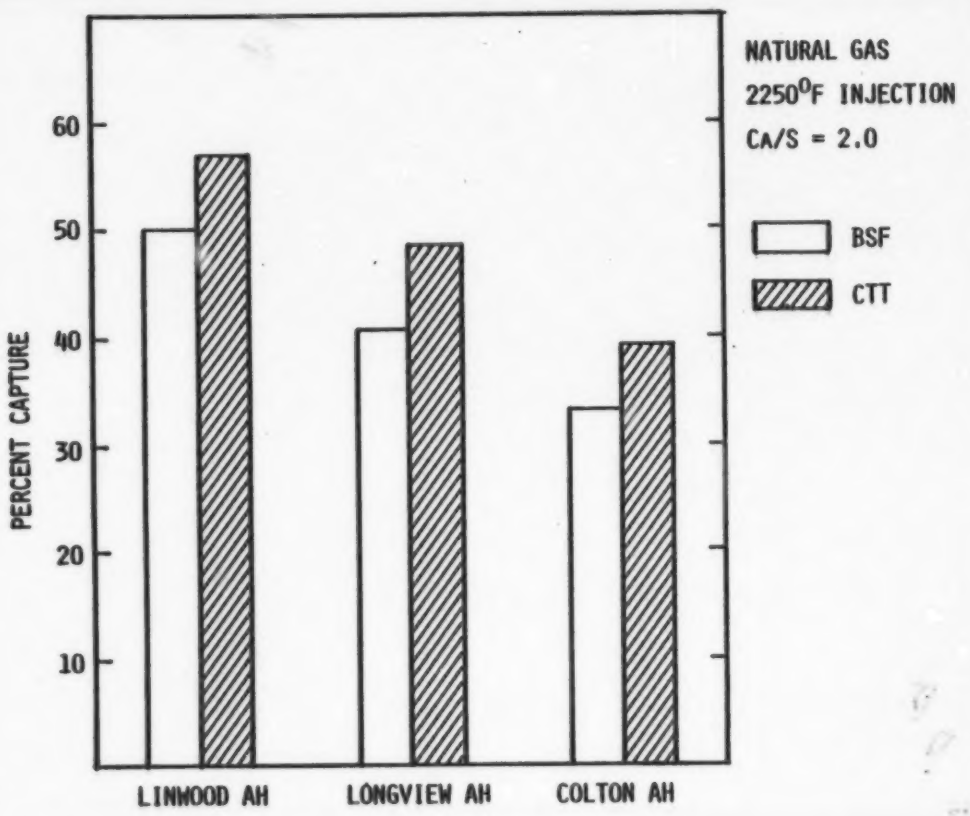

Figure 4-19. Commercial hydrate performance summary.

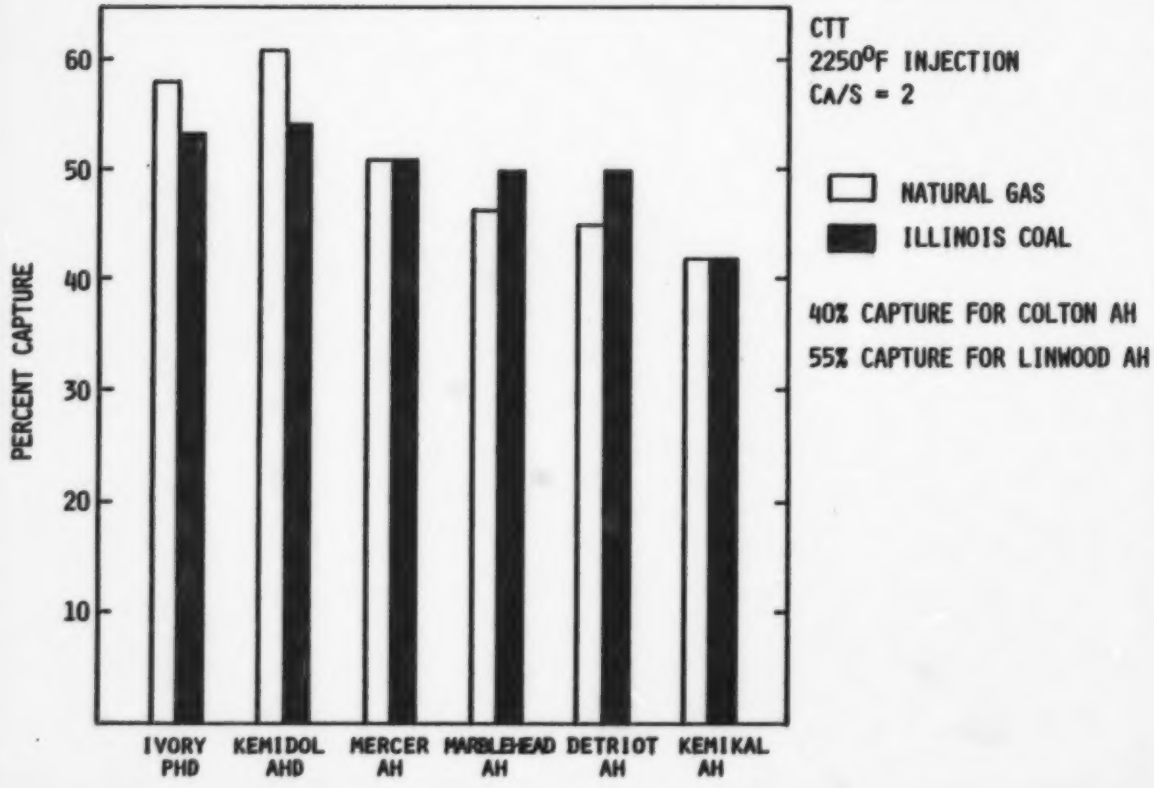

Figure 4-20. Demo sorbent performance summary.

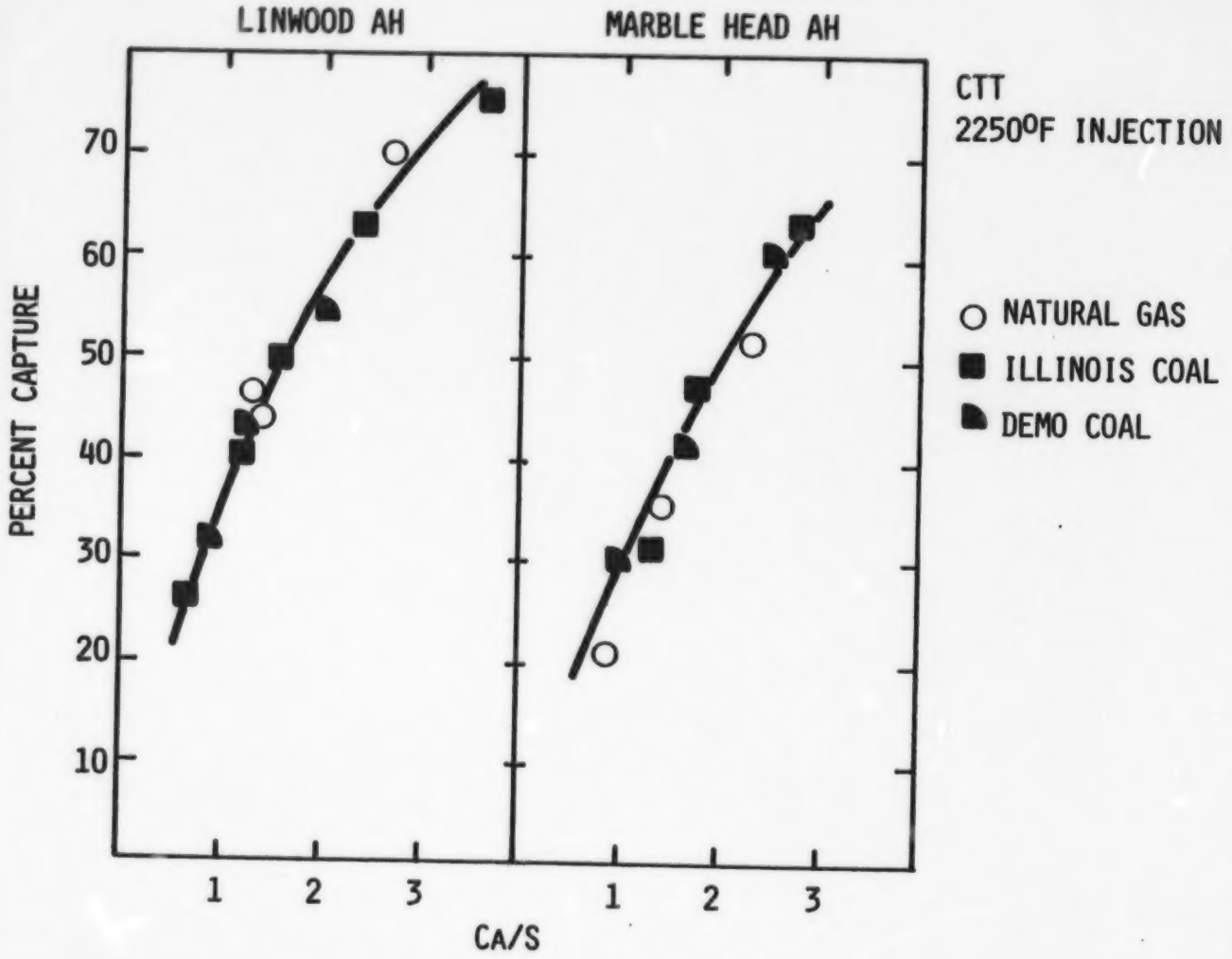

Figure 4-21. Performance with different fuels.

After screening the demo sorbents on the CTT, the best overall sorbent (Kemikal) and the best of the high-calcium sorbents (Mercer) were run on the BSF with the demo coal and injected at the optimum injection temperature as determined in the previous sections. Figure 4-22 shows the capture of these two sorbents compared against the Linwood AH and suggests that with the Mercer, capture of at least 50 percent at a Ca/S ratio of 2.0 is attainable. If the dolomitic sorbent is used in the demonstration, capture of above 60 percent may be achieved.

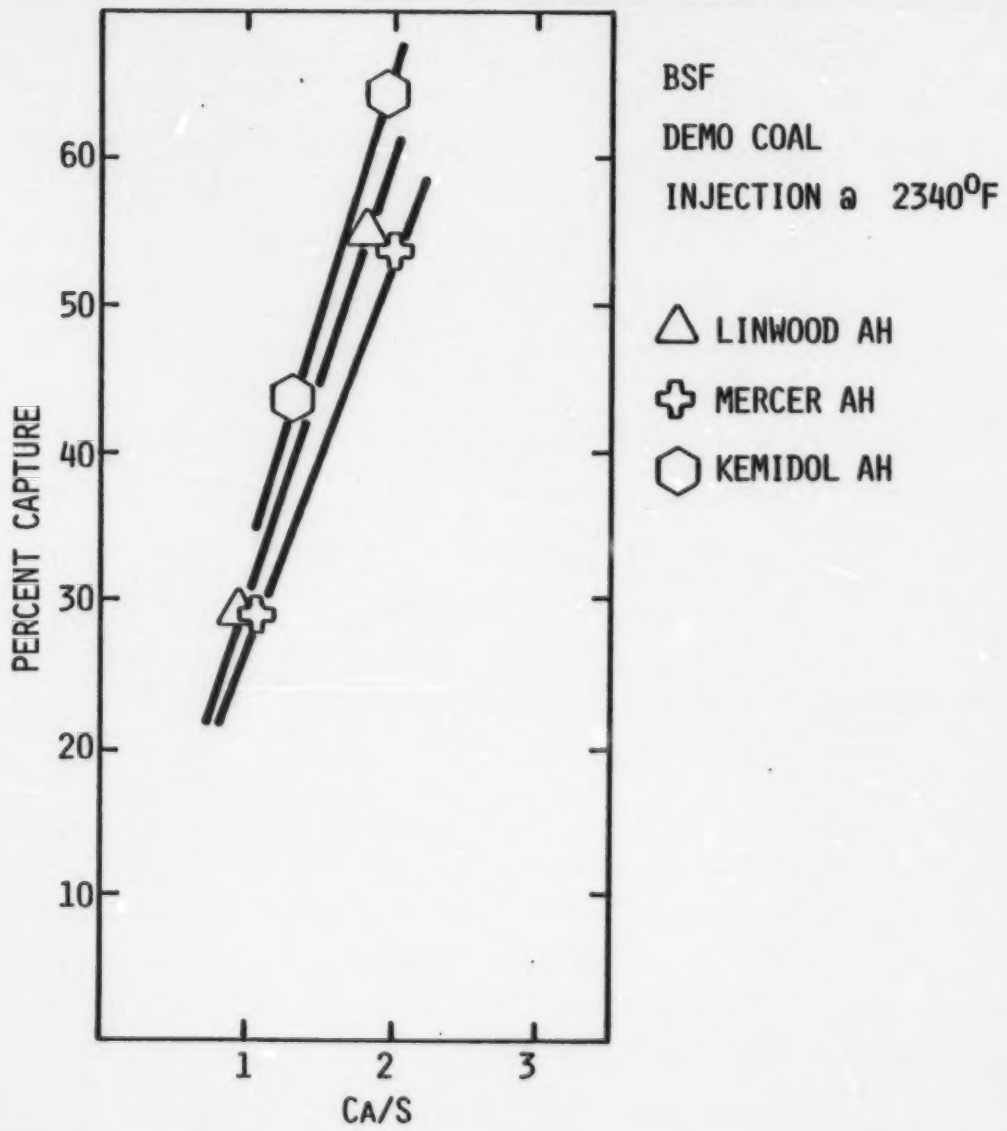

Figure 4-22. Large scale performance - BSF.

5.0 CONCLUSIONS

The results of this study provided information on the reactivity of various calcium based sorbents toward SO_2 in a coal fired furnace and determined factors which influenced the reactivity of calcium hydrates. Initial testing with the Linwood and Longview sorbents indicated that for both series of sorbents, capture with the hydrates was significantly higher than with the limestones. Testing with the Linwood and Longview quicklimes gave some surprising results due to the fact that the materials hydrated very easily under ambient conditions to yield more reactive hydrates. When the relative effects of the quicklime and hydrate were uncoupled, it was shown that the quicklime was less reactive than the limestone. A direct comparison of the Linwood and Longview sorbents indicated that in every category, the Linwood sorbents were as or more reactive than the Longview sorbents with both gas and coal firing.

The overall effect of pressure hydration was an increase in sorbent reactivity compared with atmospheric hydration. Under optimal process conditions, several pressure hydrated batches were produced that yielded higher capture than the commercial atmospheric hydrate. In contrast, several batches of pressure hydrate were produced under different process conditions that gave lower capture than the commercial atmospheric hydrate. The general conclusion drawn from the study of pressure hydration was that many variables can influence the ultimate reactivity of the material. Among these were the size of the quicklime, extent of hydration of the quicklime, the water addition rate, and the manner in which the product was discharged. Experiments with different batches of quicklime suggested that the finer the starting material, the more reactive the final product. Pure CaO was desirable for the starting material since partial hydration may have had several negative effects on sorbent reactivity. The first of these was that the water stoichiometry was altered because less water was actually required to fully hydrate the remaining quicklime. Secondly, it is not known what effect pressure hydration had on the material that was already atmospherically hydrated but the data suggests that reactivity was inhibited. Another variable affecting reactivity appears to be the water addition rate.

Fast addition of the water produced a more reactive batch than one in which the water was added over a longer period of time. Discharge manner also appears to be important in generating a reactive product. One batch that was discharged isobarically with the use of back pressure produced slightly higher capture than the batches that were discharged with the pressure in the reactor oscillating with the opening and closing of the discharge valve. Surface area was one parameter that surprisingly did not seem to influence the sorbent reactivity since some of the lowest surface area batches gave the highest capture.

In terms of the commercially available hydrates, distinct differences in reactivity were noted. The Linwood was the most reactive which was in part due to a finer particle size distribution. The Longview was next in reactivity and was followed by the Colton hydrate. This trend held regardless of the firing conditions or the fuel. Of the demonstration sorbents, the dolomitic hydrates (Ivory Finish Lime and Kemidol) gave the highest capture though they were not significantly better than the high-calcium atmospheric hydrates. The Mercer AH performed the best of the high-calcium sorbents with capture levels in excess of 50 percent at a Ca/S ratio of 2.0 observed. The worst of the high-calcium sorbents was the Kemikal with capture only slightly above 40 percent.

6.0 REFERENCES

1. Borgwardt, R. H., Environ. Sci. Technol., 4, 59 (1970).

2. Beittel, R. et al., "Studies of Sorbent Calcination and SO_2-Sorbent Reactions in a Pilot-Scale Furnace." In: Proceedings: First Joint Symposium on Dry SO_2 and Simulataneous SO_2/NO_x Control Technologies, Volume 1. Fundamental Research and Process Development, EPA-600/9-85-020a (NTIS No. PB85-232353), pp. 16-1 to 16-33, July (1985).

3. Cole, J. A., J. C. Kramlich, G. S. Samuelsen, and W. R. Seeker, "Reactivity of Calcium-Based Sorbents for SO_2 Control." In: Proceedings: First Joint Symposium on Dry SO_2 and Simultaneous SO_2/NO_x Control Technologies, Volume 1. Fundamental Research and Process Development, EPA-600/9-85-020a (NTIS No. PB85-232353), pp. 10-1 to 10-21, July (1985).

4. Greene, S. B., S. L. Chen, W. D. Clark, M. P. Heap, D. W. Pershing and W. R. Seeker, "Bench Scale Process Evaluation of Reburning and Sorbent Injection for In-Furnace NO_x/SO_x Reduction." EPA-600/7-85-012 (NTIS No. PB85-185890), March 1985.

5. Overmoe, B. J., S. L. Chen, Seeker, W. R., Pershing, D. W. and M. P. Heap, "Boiler Simulator Studies on Sorbent Utilization for SO_2 Control." EPA-600/7-86-028, September 1986.

6. Overmoe, B. J., S. L. Chen, L. Ho, W. R. Seeker, M. P. Heap, and D. W. Pershing, "Boiler Simulator Studies on Sorbent Utilization for SO_2 Control." In: Proceedings: First Joint Symposium on Dry SO_2 and Simultaneous SO_2/NO_x Control Technologies, Volume 1. Fundamental Research and Process Development, EPA-600/9-85-020a (NTIS NO. PB85-232353), pp. 15-1 to 15-17, July (1985).

7. Slaughter, D. M., G. D. Silcox, P. M. Lemieux, G. H. Newton, and D. W. Pershing, "Bench Scale Evaluation of Sulfur-Sorbent Reactions." In: Proceedings: First Joint Symposium on Dry SO_2 and Simultaneous SO_2/NO_x Control Technologies, Volume 1. Fundamental Research and Process Development, EPA-600/9-85-020a (NTIS No. PB85-232353), pp. 11-1 to 11-15, July (1985).

8. Slaughter, D. M., S. L. Chen, and W. R. Seeker, "Enhanced Sulfur Capture by Promoted Calcium-Based Sorbents," paper presented at Second Joint Symposium on Dry SO_2 and Simultaneous SO_2/NO_x Control Technologies, Raleigh, NC, June 2-6, 1986.

9. Weber, G. F., M. H. Bobman, and G. L. Schelkoph, "Pilot-Scale Studies of In-Furnace Hydrated Lime Injection for Flue Gas SO_2 Emission Control." In: Proceedings: First Joint Symposium on Dry SO_2 and Simultaneous SO_2/NO_x Control Technologies, Volume 1. Fundamental Research and Process Development, EPA-600/9-85-020a (NTIS No. PB85-232353), pp 19-1 to 19-19, July (1985).

Appendix A. Design of a Bench Scale Pressure Hydrator

A.1 INTRODUCTION AND BACKGROUND

A.1.1 Introduction

In recent years, calcium-based compounds have been investigated as possible sorbents for the removal of sulfur dioxide from flue gas evolved from the combustion of fossil fuels. Calcium hydrates ($Ca(OH)_2$) have shown considerable promise for this application. Due to the aroused interest in calcium hydrates, Energy and Environmental Research Corporation (EER) has been contracted under EPA Work Assignment Number 1/017 to construct a bench scale facility capable of pressure or atmospheric hydration of limes. The laboratory scale hydrator operated by the University of North Dakota Energy Research Center (UNDERC) was the prototype design for this reactor. This report contains background information on hydration, as well as information on the UNDERC hydration process and the development and ultimate make up of the EER facility.

A.1.2 Background

Due to the sulfation reaction that occurs between calcium and sulfate ions, calcium-based compounds received immediate attention when possible sorbents were considered for the dry removal of SO_2 from fossil fuel combustion exhaust. Several common calcium compounds are available due to their widespread use in various commercial applications such as masonry and construction. Tests have been completed at EER with commercial compounds in order to investigate their SO_2 capture potential. These tests show that the calcium in hydrates is utilized more efficiently than that in limestone ($CaCO_3$) or lime (CaO) for SO_2 removal and hydrates formed at high pressure appear to perform better than those hydrated at atmospheric pressure. It is not known whether the increased reactivity exhibited by the hydrates is due to a physical alteration which occurs upon hydration, or due to the decreased particle size and accompanying increase in surface area which occurs upon hydration.

When hydrate is processed at high pressure in an excess of water, the formation of small particles with large surface areas are promoted by controlled, explosive discharge of the hydrate. The discharge of hydrate from high pressure (usually in excess of 80 psig) to atmospheric pressure results in flash vaporization of water within the pores of the particles. This rapid expansion effectively explodes the particle into smaller particles with a large surface area. The process of hydration at high pressure was originally developed for masonry applications, in order to promote complete hydration of "hard-burned" or dolomitic ($CaO \cdot MgO$) limes, which do not hydrate completely at atmospheric pressure.

A.2 LITERATURE REVIEW

The design of the EER pressure hydrator was to be a large scale version of the UNDERC laboratory scale hydrator. However, since construction and operation of the hydrator were to be performed by EER, it was necessary for EER personnel to have a working knowledge of the hydration process as employed in the production of atmospheric- and pressure-lime hydrates. For this reason, a review of the literature available on hydration was undertaken.

Initially, familiarity with the nomenclature, reactions, and hydration methods common for limestone were gained by perusal of the text authored by Boynton (1). The design and operation of the UNDERC facility was examined by review of UNDERC technical papers (2-4) and consultation with Greg Weber, the project supervisor for the UNDERC SO_X/NO_X control program. To gain further insight into the hydration process and for comparison with UNDERC, the design and operation of prototype pressure hydrators (5-9) as well as current commercial processes (10) were investigated. A list of possible design/operational parameters was formed from information obtained from this review. From this list of parameters, those deemed as critical for the hydration process were chosen and quantified. These variables, and a comparison of their common values with those employed by UNDERC are presented in Table A-1. Parameters not presented in the table are the characteristics of the parent lime. These vary for each manufacturer, and can also vary from one batch to another.

Based on the literature, and a critique of the UNDERC design as outlined by Cole (11), several comments can be made of the UNDERC design:

- Carbon steel construction of the reactor may result in contamination of the product. Past results have shown that hydrates with non-calcium metallic ions in their crystalline structure can exhibit significantly different reactivity with SO_2 than hydrates not "contaminated."

TABLE A-1. CRITICAL OPERATING PARAMETERS FOR HYDRATION PROCESS.

Parameter	UNDER C	Corson	Genstar	Corson (prototype)	Garvin	Huntzicker	Warner	Volk
Pressure (psig)	150	~100	100 - 200	to 600	80 - 140	150 - 200	10 - 50	150 - 300
Temperature (°F)	380 - 420	300 - 400	300 - 400	400 - 450	to 365	~350	to 300	300 - 420
Residence Time (min)	20	10 - 30	-	5 - 10	15 - 20	-	~60	10 - 15
Water/Lime Mixing Rate	Slow	Premixed (fast)	-	Premixed	Fast	Fast	-	Premixed
$(H_2O/lime)_{molar}$	1.4	~2	1.9 - 2.0	2.0	1.3	>1.0	2.0	>1.0
Discharge Method	Explosive	Explosive	Explosive	Explosive	Explosive	Explosive	-	Explosive
Mode	Batch	Continuous	Batch	Batch	Batch	Batch	Continuous	Batch
Scale	Laboratory	Full Scale Production	Bench	-	-	-	-	-

- The initial mixing rate of water and lime is quite slow. This can result in a nonuniform product due to variations in local residence times.

- The control of the system temperature and pressure is limited at best.

A.3 DESIGN CRITERIA/FEATURES

Based on specifications outlined in Work Plan Number 1/017 and scaling of the UNDERC hydrator design, criteria for the design of the bench scale facility included:

- A production capacity of 20 lbs of hydrate per batch. A batch of this size will supply a sufficient amount of sorbent for testing on the 1 MMBtu/hr boiler simulator furnace.

- A pressure and temperature capability of 200 psig and 450°F, respectively. These are within the range of values commonly employed for the pressure hydration process.

- A controlled and explosive discharge. This causes the fragmentation of the product particles, promoting the formation of small particles with a large surface area.

- The ability to electrically heat the reactor. Since significant heat losses occur from the reactor due to the large surface area to volume ratio which is characteristic of small systems, it is necessary to have an external heat source.

The UNDERC hydrator has a volume approximately five times the volume of the reacting slurry. Current industrial reactors are typically twice the volume of the slurry. The slurry volume for twenty pounds of product with a water to lime ratio of two is less than 0.3 ft^3. Thus, a reactor with a volume of about one cubic foot was deemed appropriate for the desired application. Since heat losses are dependent on surface area, the surface area to volume ratio was minimized. The resulting dimensions chosen for the reactor were ten inches in diameter by two feet in length. Since the volume of the reactor as based on UNDERC criteria is essentially oversized, the batch size can be increased if desired. Figure A-1 shows the approximate depth of the initial reaction slurry in the hydration vessel as a function of batch size. Although the surface area was minimized for the reactor, roughly

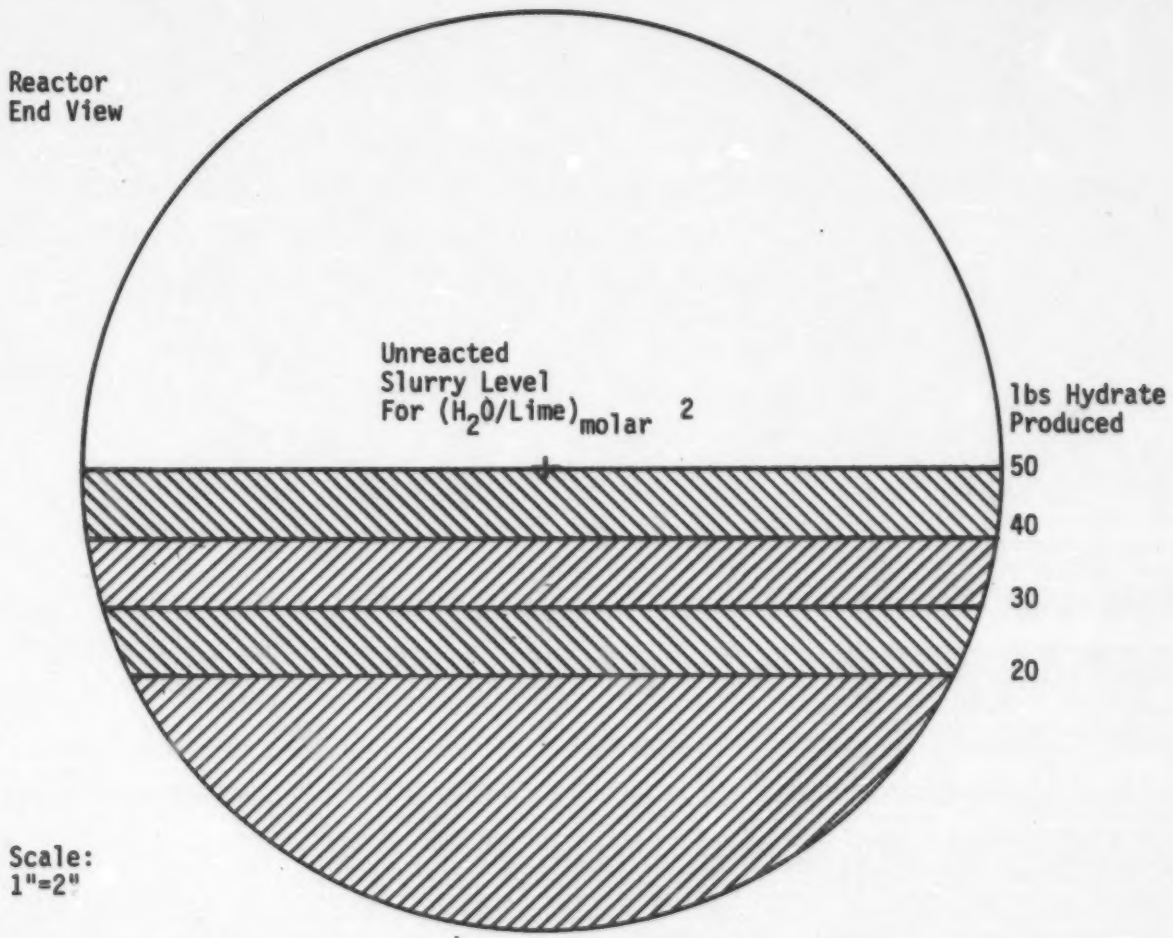

Figure A-1. Level of unreacted slurry in the reactor for various batch sizes.

ten to 15 percent of the heat evolved from hydration will still be lost from the reactor, so external heating capabilities are necessary in order to maintain the high reaction temperature and pressure desired.

The review of the literature, and consultation with members of the UNDERC staff enlightened EER to a number of other features not inherent to the UNDERC system which could be incorporated into the design. Addition of these design features to the EER hydrator would enhance the operation of the hydrator and limit possible problem areas for the process. Features considered include:

- Stainless steel construction to avoid ionic contamination of the reaction slurry.

- Automatic pressure relief and hydrator compression. The UNDERC hydrator has no decompression abilities, with the exception of opening the product discharge valve or splitting a safety rupture disc. This limits the rate of water addition to the lime, since no relief of a possible rapid pressure escalation is available. The automatic system solves this problem and also allows operation of the system at approximately isobaric conditions.

- Monitoring of the hydrator space gas, plus the slurry temperature at several axial locations. UNDERC only monitors the reactor wall temperature. The slurry temperature should be approximately constant throughout if mixing between the lime and water is thorough. Temperature gradients (i.e., poor mixing) within the slurry may result in a nonuniform product.

- Logging of the temperature and pressure progression of the process with a chart recorder. An accurate, hard-copy of two critical operation parameters is thus obtained.

- Variable speed operation of the slurry mixing shaft (to 12 rpm). UNDERC mixes at a constant rate of 2 rpm, which may not be fast

enough for promotion of a uniform slurry when water is initially added.

- Flange the reactor at both ends. The UNDERC reactor is flanged at one end only. The ability to completely dismantle the reaction vessel allows thorough cleaning in order to diminish the chances of contamination which could result when altering conditions (i.e. different lime, addition of promoters) between successive batches.

The major impact that these features have on the process are in the area of slurry mixing and purity.

Although UNDERC claims that a slow water addition rate (about ten minutes) and agitator speed (2 rpm) don't affect the uniformity of their product, investigation of mixing and its possible impact on the hydrate have not been undertaken. The suggested design changes add abilities for quick water addition, faster agitator revolution, and monitoring of slurry uniformity via temperature measurements. Insight into the mixing process would be gained from the temperature measurements, and the faster mixing rates available would be in agreement with both past and current methods generally employed in the hydration process (see Table A-1).

Recent information indicates that impurities in the reaction slurry can become impregnated in the crystalline structure of the hydrate, altering the reactivity of the sorbent and often promoting the capture potential of the sorbent. For this reason, it is desirable to have a reaction slurry as free from contaminants as possible. UNDERC suggested a flange at both ends of the reactor so that the reactor can be more thoroughly cleaned to avoid contaminations from previous batches. The use of stainless steel limits the possibilities of ionic contamination from the reactor walls and water feed system. Since the thermal conductivity of stainless steel is only one third that of carbon steel, heat losses from the reactor will also be diminished due to stainless steel construction.

A.4 UNDERC HYDRATION PROCESS

A.4.1 Pressure Hydration

After insight into the hydration process was obtained, a trip was taken to UNDERC to view the hydrator design and witness operation of the facility. The physical design of the hydrator, as applied to the bench scale facility at EER, will be described in detail in the following section. The only differences between the two facilities are those outlined in the previous section. The operational procedure for the facility was observed so that a similar process can be applied to the EER hydrator with the intention of developing a hydrated product which resembles the UNDERC hydrate both physically and chemically.

UNDERC generally follows the same procedure whenever the facility is operated. To initiate the process, the reactor was charged with 2700 grams (48.1 moles) of Linwood high-calcium lime. The lime was received in a pebble form by UNDERC, where it was ground with a ball mill and pulverized. Surface area, pore size distribution, and particle size distribution analyses are currently being performed on a sample of lime in order to characterize the physical nature of the hydrate precursor. The reactor was then sealed and heated to 380°F. A water tank was filled with 1200 ml (66.5 moles) of water and pressurized with nitrogen to 150 psig. Since pressure within the reactor will increase as water is added to the lime, it is necessary to pressurize the water tank to the reaction pressure to avoid back flow of the slurry into the water tank. The molar ratio of water to lime was 1.38. The heating system was turned off as addition of water began. The water was added in short bursts to avoid a rapid escalation in the system pressure, and the temperature and pressure of the system were allowed to equilibrate between successive water injections. Complete injection of the water took approximately ten minutes with the system attaining a peak temperature and pressure of 434°F and 170 psig respectively. The slurry was then allowed to react for about twenty minutes with the system temperature and pressure remaining fairly stable at 420°F to 434°F and 150 psig for the duration of

the reaction time. Temperature and pressure readings were manually recorded at five minute intervals.

The twenty minutes of reaction time were followed by discharge of the product and collection in a cotton cloth filter bag. A ball valve was opened slightly and the reactor pressure quickly dropped to 105 psig. This pressure was maintained throughout the remainder of the discharge process by back pressurization of the reactor with nitrogen. The pressure drop across the valve was maintained at two to four inches of water, which corresponds to a flowrate in the range of 10 SCFM. Slight adjustments to the amount the ball valve was opened were necessary during discharge to maintain this flow rate. Since the ball valve opening was the discharge orifice size, a variation in the orifice size occurred during discharge. Total discharge time was ten minutes, and electrical backheating was once again employed to maintain a reactor wall temperature above 370°F. The temperature and pressure progression with time for the complete process are shown in Figures A-2 and A-3 respectively.

Upon discharge, a small amount of product escaped through the wall of the filter bag before a film of hydrate covered the wall and hindered further loss of product particles, but still allowed steam to escape. An additional, more significant amount of product remained in the reactor after discharge was complete. This included hydrate stuck to the reactor walls and agitator, and several agglomerated masses of hydrate. Due to these losses of product, the yield for the process witnessed was about seventy percent of that which would result for total recovery of the hydrated lime. A yield in this range was common for the UNDERC process.

The length of the discharge time for the process was quite long relative to the residence time. The reason this discharge rate was employed is twofold: the discharge flow rate was similar to those used by industry for continuous production of hydrate; the filter bag was capable of handling the pressure which resulted from this flow rate. Due to the long discharge and water addition times, the residence time for any particular volume of hydrate could range from twenty to forty minutes. The patent literature (5-9)

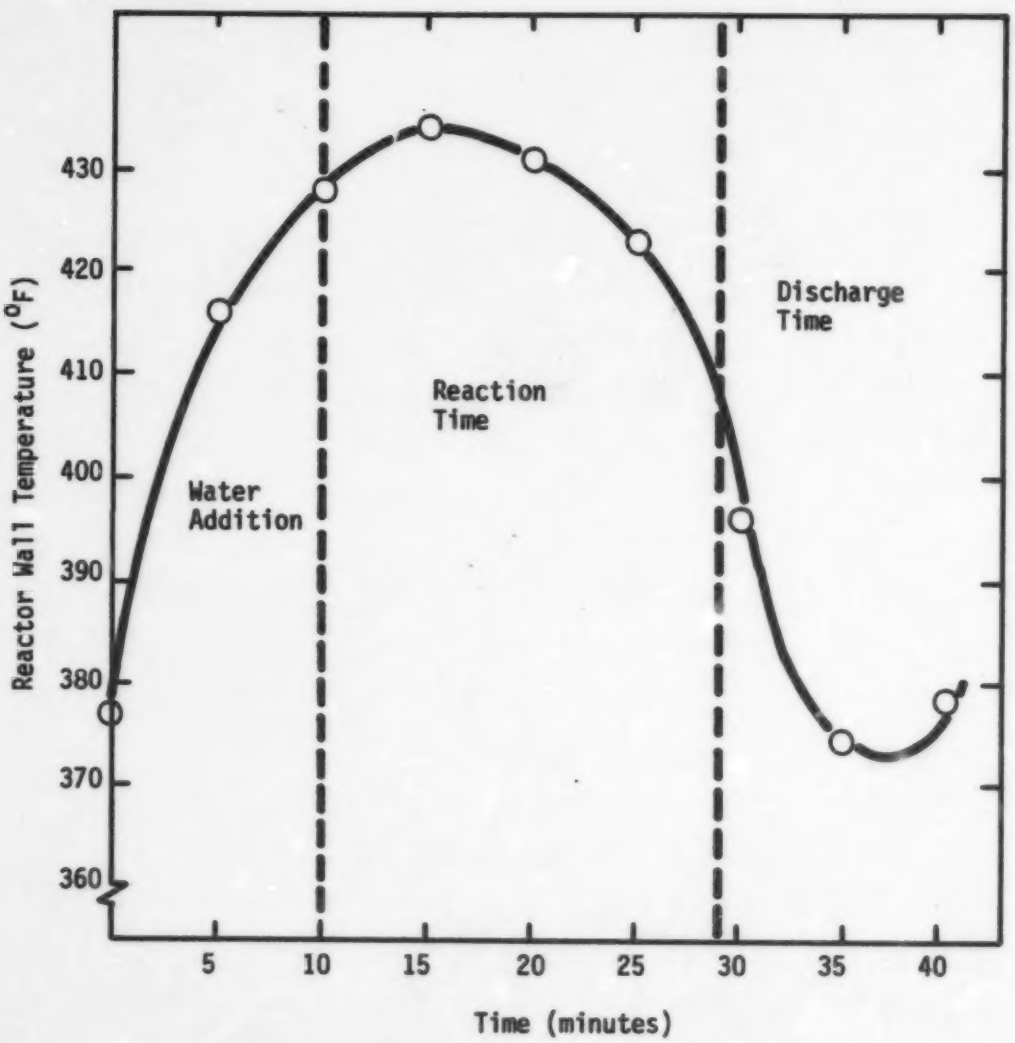

Figure A-2. Reactor wall temperature vs. time for UNDERC hydration process.

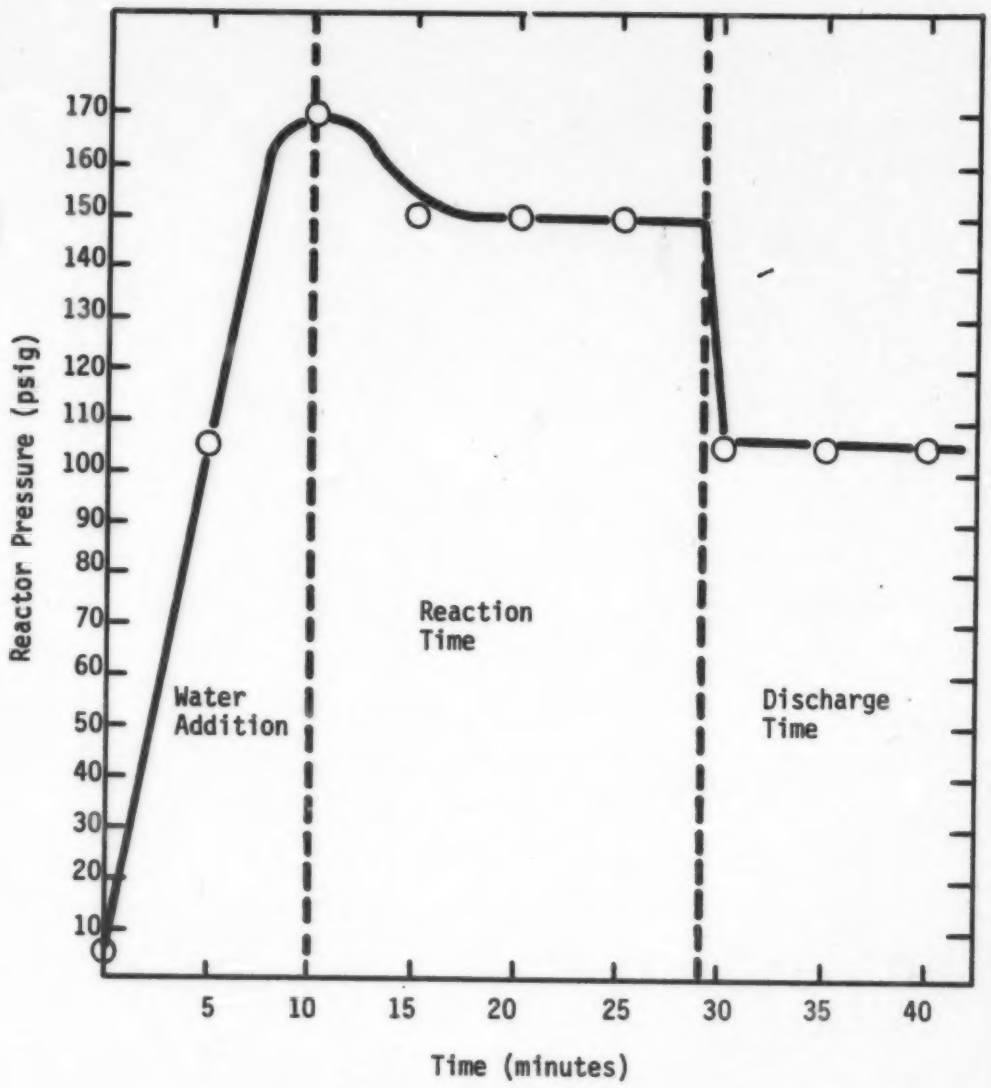

Figure A-3. Reactor pressure vs. time for UNDERC hydration process.

indicates that excessive residence time can be detrimental to the product in that it may result in the growth of larger crystals, thus affecting product uniformity. UNDERC reported no problems in this area, but care will have to be taken to minimize deviations in local residence times.

The final product was allowed to cool, then placed in a plastic bag. The hydrate was now available for utilization as a sorbent or storage for future use. A BET surface area analysis of this hydrate yielded a surface area of 9.2 m^2/g. Pore and particle size distribution analyses are forthcoming.

A.4.2 Atmospheric Hydration

Although not witnessed while at UNDERC, the operational procedure for atmospheric hydration of lime was outlined by the UNDERC staff. The process is similar to that used for pressure hydration. For atmospheric hydration, the wall of the charged reactor is heated to 380°F, with the charge hatch left open. A similar water to lime ratio is employed and water addition occurs at a faster rate since excess pressure is vented to the environment. After twenty minutes of reaction time, the wet product is removed from the hydrator and air dried. The product must then be milled and pulverized before utilization as a sorbent.

A.4.3 Addition of Promoters

In the past, UNDERC has often added promoters to the reaction slurry. The presence of additives such as sodium, copper, iron or manganese in the hydrate appears to enhance the sorbent SO_2 capture potential under certain conditions. Initial test plans at EER do not include investigation of additive effects, but the procedure for addition of promoters to the hydrate was delineated by UNDERC. For addition of promoters, an ionic compound which contains the desired additive is dissolved in the reaction water prior to injection of the water into the reactor. The remainder of the operational procedure is unchanged. UNDERC has found that upon reaction, approximately

seventy percent of the additive is generally incorporated into the hydrate crystalline structure.

A.5 EER HYDRATOR DESIGN

The design of the EER hydrator is a scaled up version of the UNDERC system, with improvements made as suggested in section 3.0 of this report. The EER facility is illustrated in Figure A-4, with a list of the majority of materials and parts necessary for construction of the facility presented in Table A-2. In Table A-3, the principle design and operation parameters of the EER and UNDERC hydrators are compared. Any set of experimental conditions which are possible with the UNDERC facility will also be feasible for the EER hydrator.

A.5.1 Reactor Shell

The reactor shell, which was sized to minimize the surface area to volume ratio for the vessel, consists of a schedule 40, 304 Grade stainless steel pipe ten inches in diameter by twenty-four inches long flanged at both ends. The design drawing for the reactor is presented in Figure A-5. The flanges are standard 10IPS, stainless steel blind and slip-on flanges designed for a working pressure of 150 psig. A four inch charge hatch is located on the top and center of the hydrator. It is constructed of 4IPS, schedule 40, 304 Grade stainless steel and sealed with a standard 4IPS pipe flange, as shown in Figure A-6. The reactor ends, which are the aforementioned blind flanges, are designed to accommodate the mixing shaft, pressure gauge, thermocouple ports, and discharge orifice. The end caps are illustrated in Figure A-7.

A.5.2 Water Delivery System/Mixing Configuration

When hydrating, pressure may develop as soon as water is mixed with lime. Since water injection may occur over an extended period of time, water will be delivered to the reactor by a pressurized tank via fingers that extend from the mixing shaft. The water jets are illustrated in Figure A-8, and are positioned on the shaft as shown in Figures A-9 and A-10. Jets at six axial locations spray water into the reaction chamber by the five outlets on each jet. This configuration promotes dispersion of water in the reaction

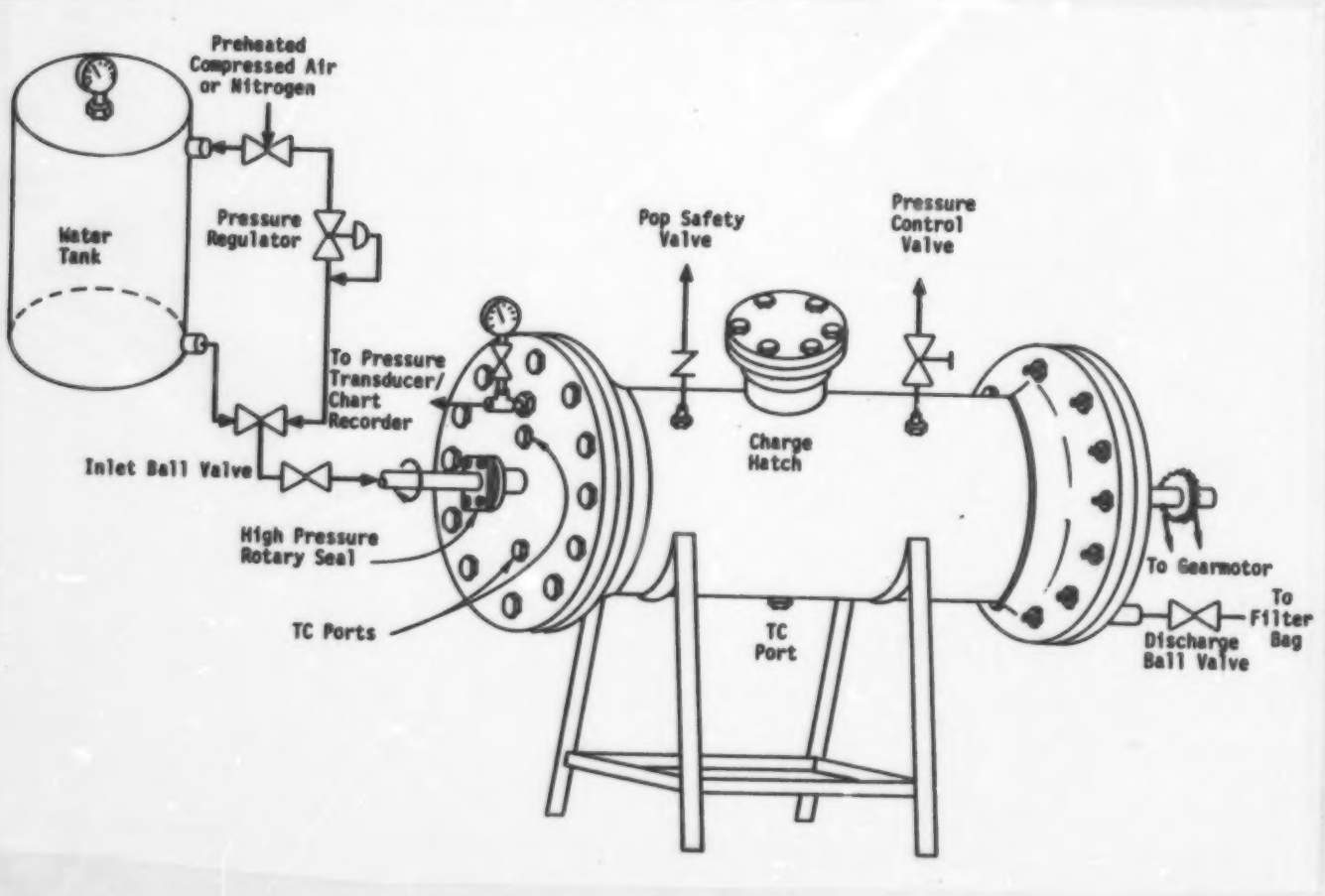

Figure A-4. Pressure hydrator.

TABLE A-2. MATERIALS FOR CONSTRUCTION OF A PRESSURE HYDRATOR FACILITY

Item	Function
10IPS x 2', Schedule 40, 304 Grade SS Pipe	Reactor Shell
10IPS, 150 psig, SS Blind Flange (2)	Reactor Shell
10IPS, 150 psig, SS Slipon Flange (2)	Reactor Shell
4IPS x 3", Schedule 40, 304 Grade SS Pipe	Reactor Shell
4IPS, 150 psig, SS Blind Flange	Reactor Shell
4IPS, 150 psig, SS Slip on Flange	Reactor Shell
1" SS Ball Valve	Discharge Valve
3/8" SS Ball Valve	Water/Air Inlet Valve
1/4" SS Ball Valve	Shut-off for P-gauge Failure
3/8" SS 3-Way Valve	Water/Air Inlet
3/8" Brass 3-Way Valve	Air Splitter (Water Tank or Reactor)
Pressure Gauges (2)	
Heating Belts (4)	Reactor Backheating
Variable Autotransformer	Heating Belt Control
Water Tank	
Manometer	Monitor Discharge Pressure Drop
2-Pen Chart Record + Pre Amps	Record System, T,P Progression
Pressure Transducer + Power Supply	Convert P to Signal for Recording
Bearing (2)	Mixing Shaft Rotation
Gearmotor/Chain/Sprockets	Mixing Shaft Drive
Speed Control	Vary Gearmotor rpm

TABLE A-2. MATERIALS FOR CONSTRUCTION OF A PRESSURE HYDRATOR FACILITY (continued)

Item	Function
Digital Pyrometer	Digital Temperature Output
Pop Valve	Safety, Pressure Relief
Cotton Filter Bags	Product Collection
Rotating Union	Water/Air to Mixing Shaft Connector
Pressure Regulator and Pressure Control Valve	Automatic Pressure Control

TABLE A-3. PRESSURE HYDRATOR COMPARISON

	EER	Under C
Mode of Operation	Batch	Batch
Capacity (lb/run)	20	5
Reactor Size	10"D x 24"	8"D x 12"
Pressure (psig)	to 200	to 150
Temperature (^{o}F)	300-400	380 - 420
Residence Time (min)	10 - 30	20
$(H_2O/CaO)_{molar}$	1.3 ~ 2.0	1.4
Explosive Discharge Method	Pressure Controlled	Approximately Isobaric @ 100 psig
Material of Construction	Stainless Steel	Carbon Steel

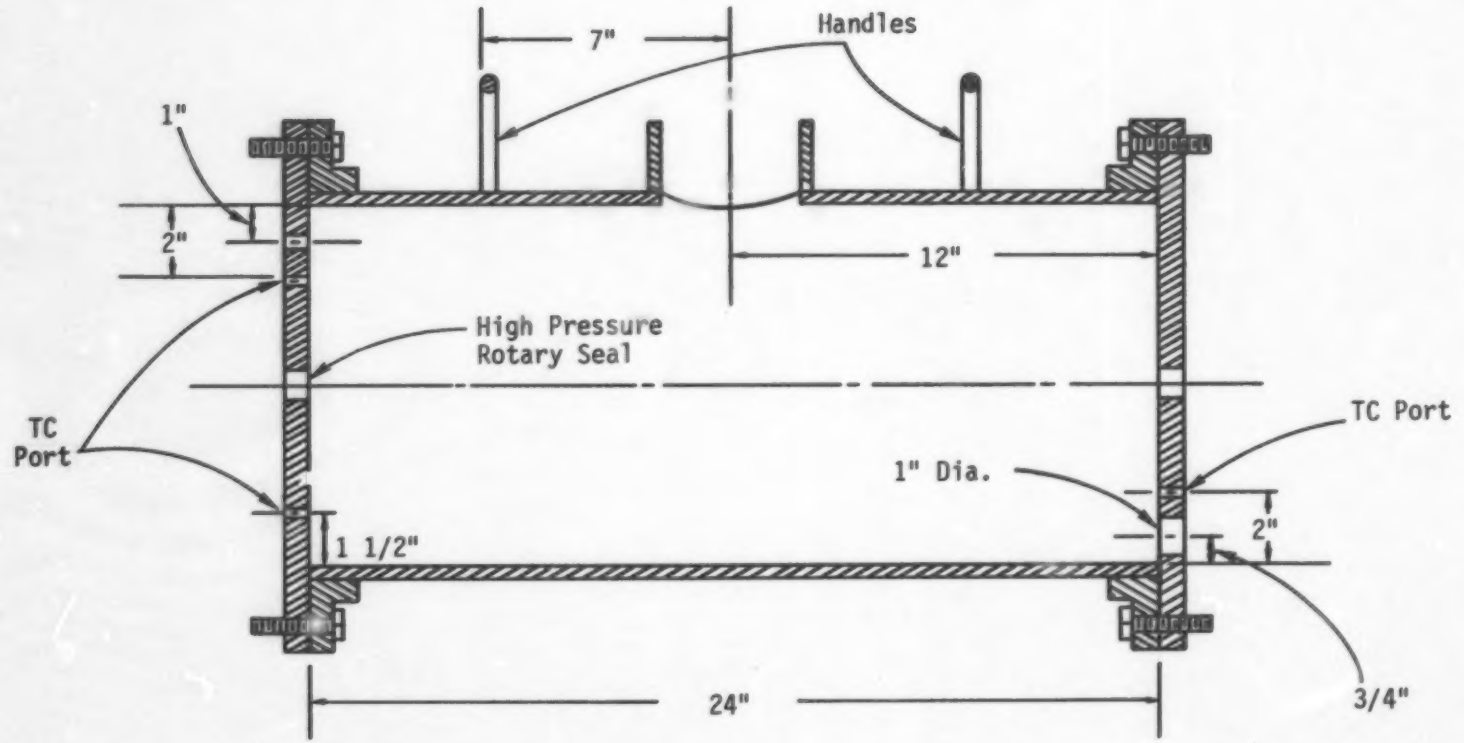

Figure A-5. Cross-sectional, side view of the reactor shelf.

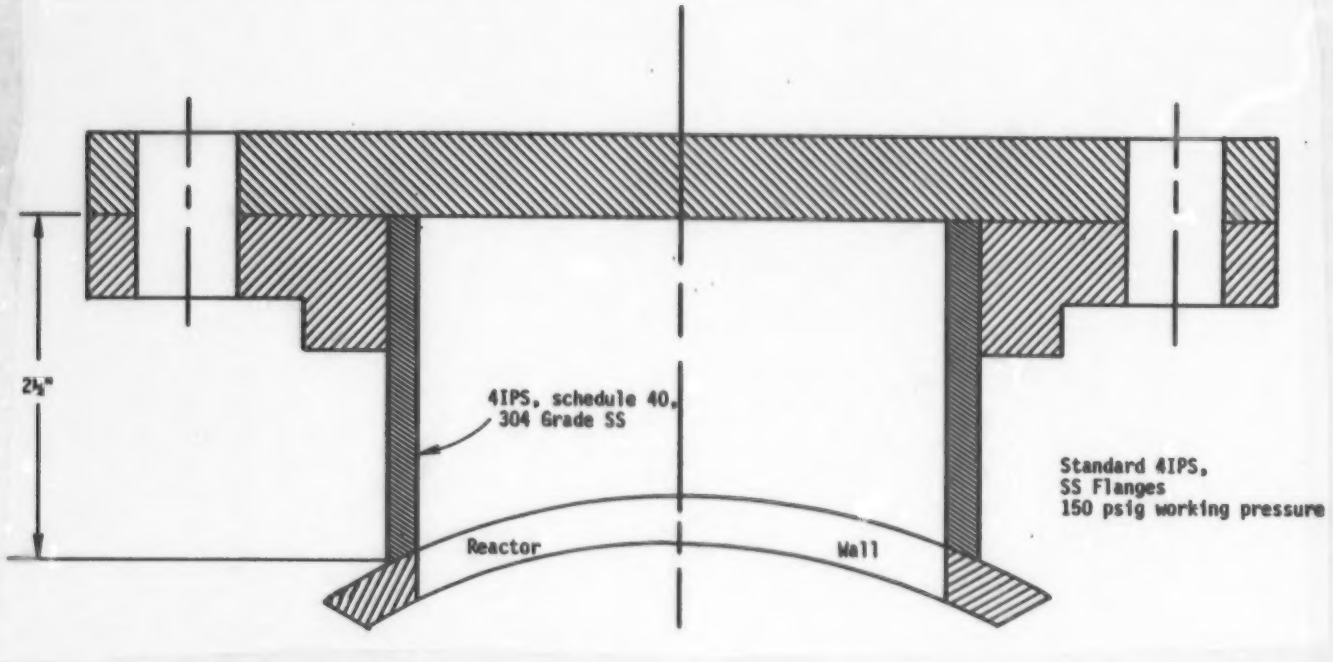

Figure A-6. Cross-sectional, end view of charge hatch.

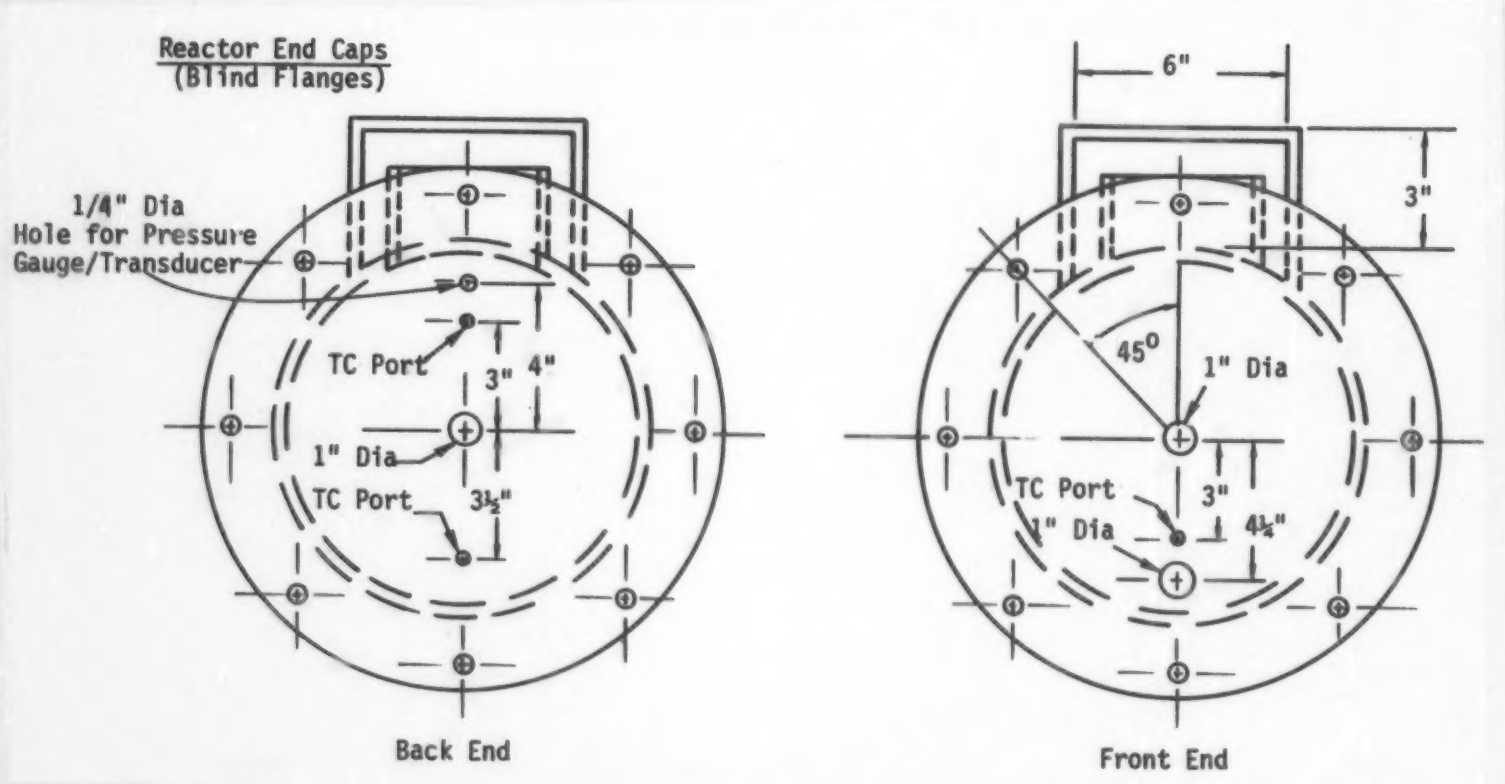

Figure A-7. Reactor ends.

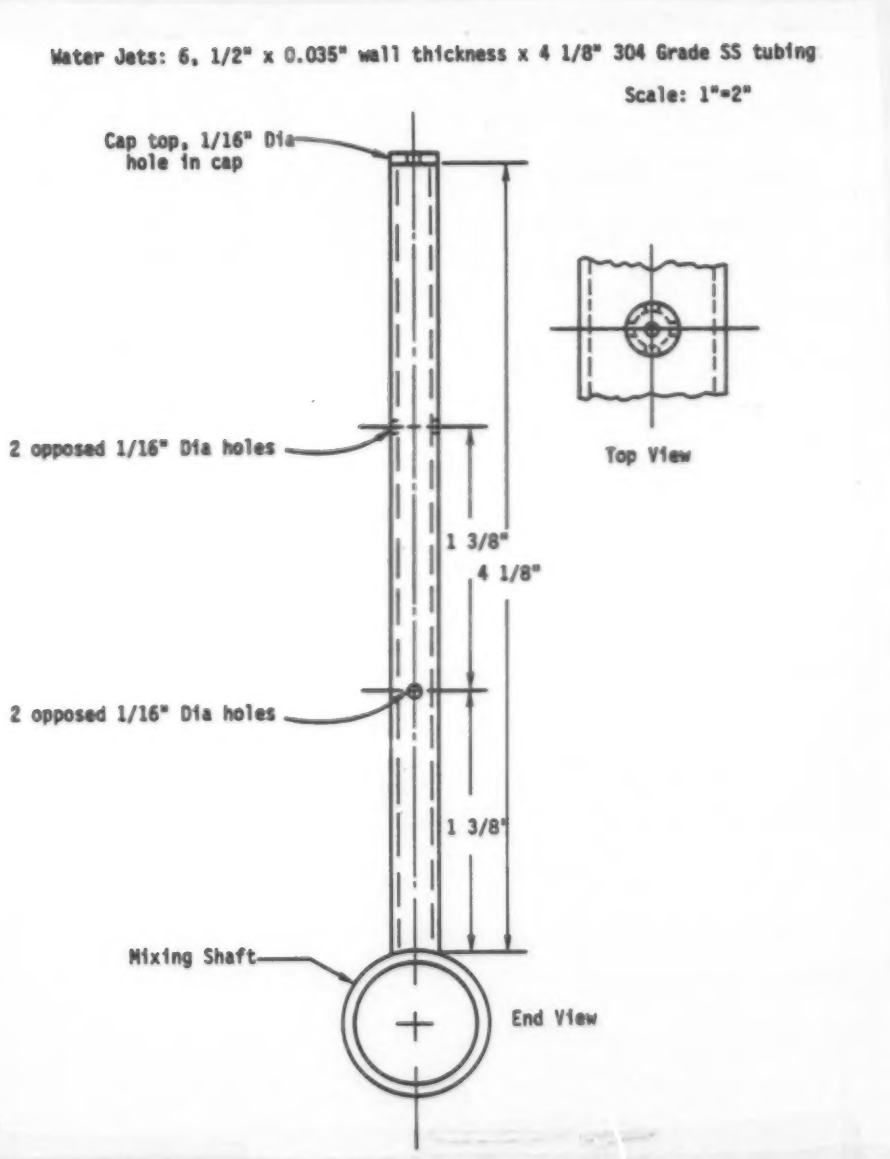
Water Jets: 6, 1/2" x 0.035" wall thickness x 4 1/8" 304 Grade SS tubing
Scale: 1"=2"
Cap top, 1/16" Dia hole in cap
2 opposed 1/16" Dia holes
2 opposed 1/16" Dia holes
Mixing Shaft
1 3/8"
4 1/8"
1 3/8"
Top View
End View

Figure A-8. Water jet.

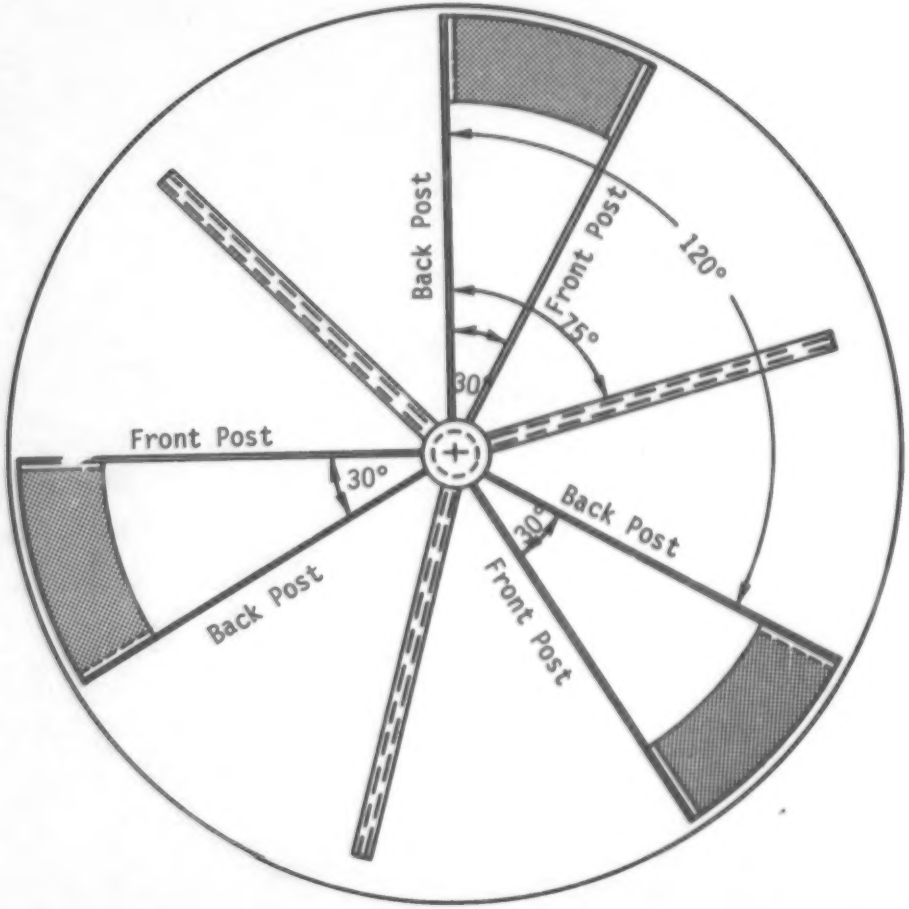

Figure A-9. Agitator configuration; front view.

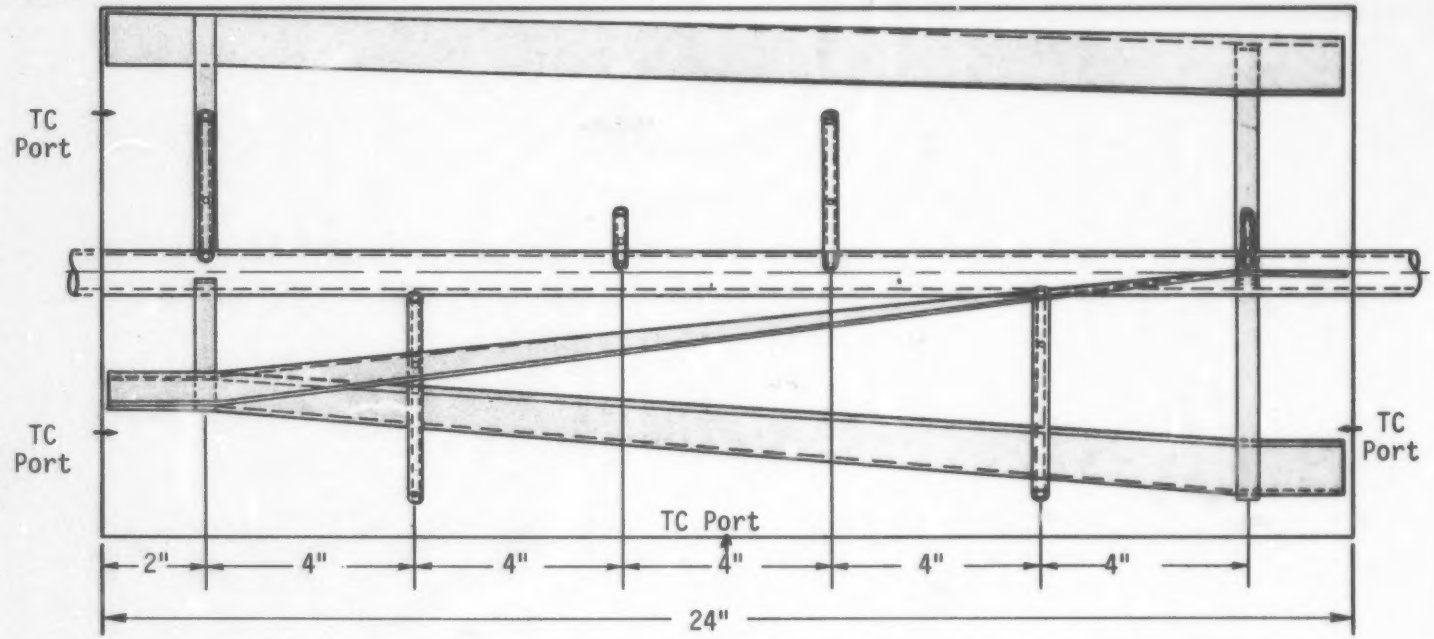

A-26

Figure A-10. Mixing configuration and thermocouple port location; side view.

chamber. Figures A-9 and A-10 also present the configuration of the paddle wheel mixing blades. The one inch blades are pitched at an angle of thirty degrees from front to back, so that the larger hydrate aggregates which inevitably form are forced away from the discharge orifice to prevent blockage.

The mixing shaft, which is constructed of three quarter inch stainless steel tubing, has high pressure rotary seals, illustrated in Figure A-11. Sealed bearings are attached to a flange that is extended three inches from the end flange. Placement of the bearing away from the reactor wall permits bearing operation at a cooler, less destructive temperature. An O-Ring held in a notch in the flange increases the seal strength. The shaft is driven by a variable speed gearmotor via a chain.

A.5.3 Pressure Control and Heating Systems

The system pressure is controlled with a Research Control Valve and pressure regulator. The 98H model control valve, manufactured by Badger Meter, Inc., automatically decompresses the reactor to its set point value whenever pressure exceeds this value. The set point can range from approximately 60 to 160 psig. If a considerable pressure decrease occurs, compression of the system results via a Fisher model 95H pressure regulator connected to a compressed air supply. A safety pop valve will serve as a backup, in case of control valve failure. Location of the pressure relief valves and heating belts are presented in Figure A-12. Four, 3-inch belts controlled by a Staco variable autotransformer supply the required heat to the insulated system.

A.5.4 Product Discharge and Collection

The product is discharged from the reactor via a one inch stainless steel ball valve. The amount that the ball valve is opened controls the discharge orifice size, with a maximum possible orifice diameter of one inch. A manometer will display the pressure drop across the valve, thus discharge flow rates can be calculated. The product is collected in a cotton cloth

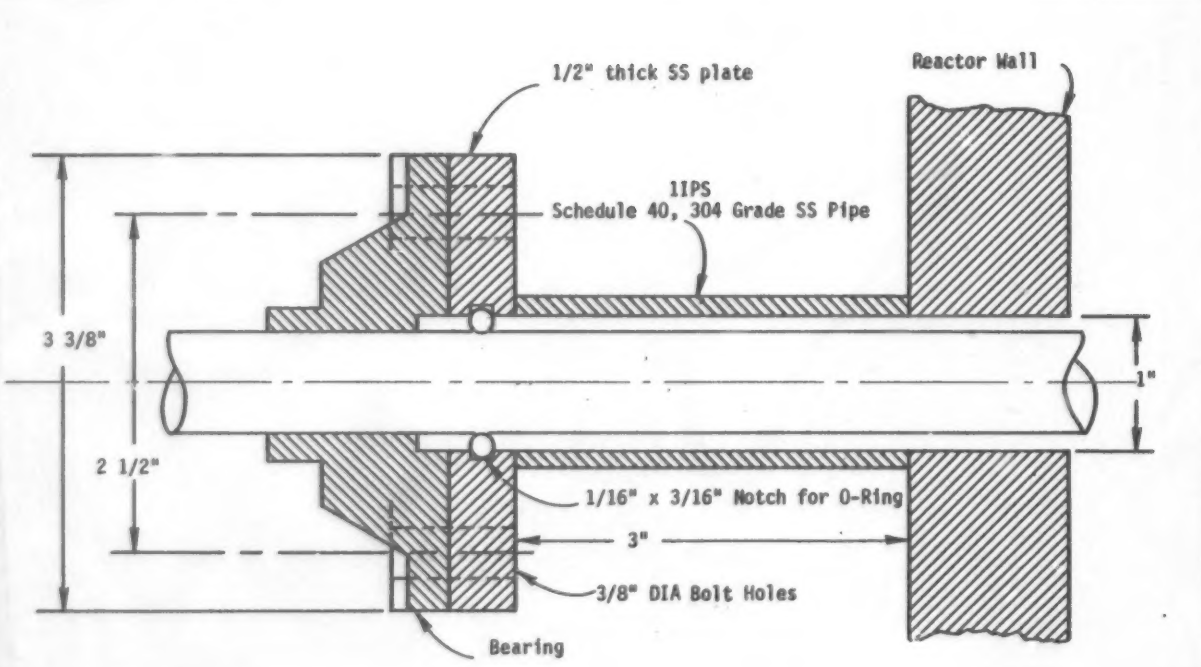

Figure A-11. Mixing shaft seal; cross-section.

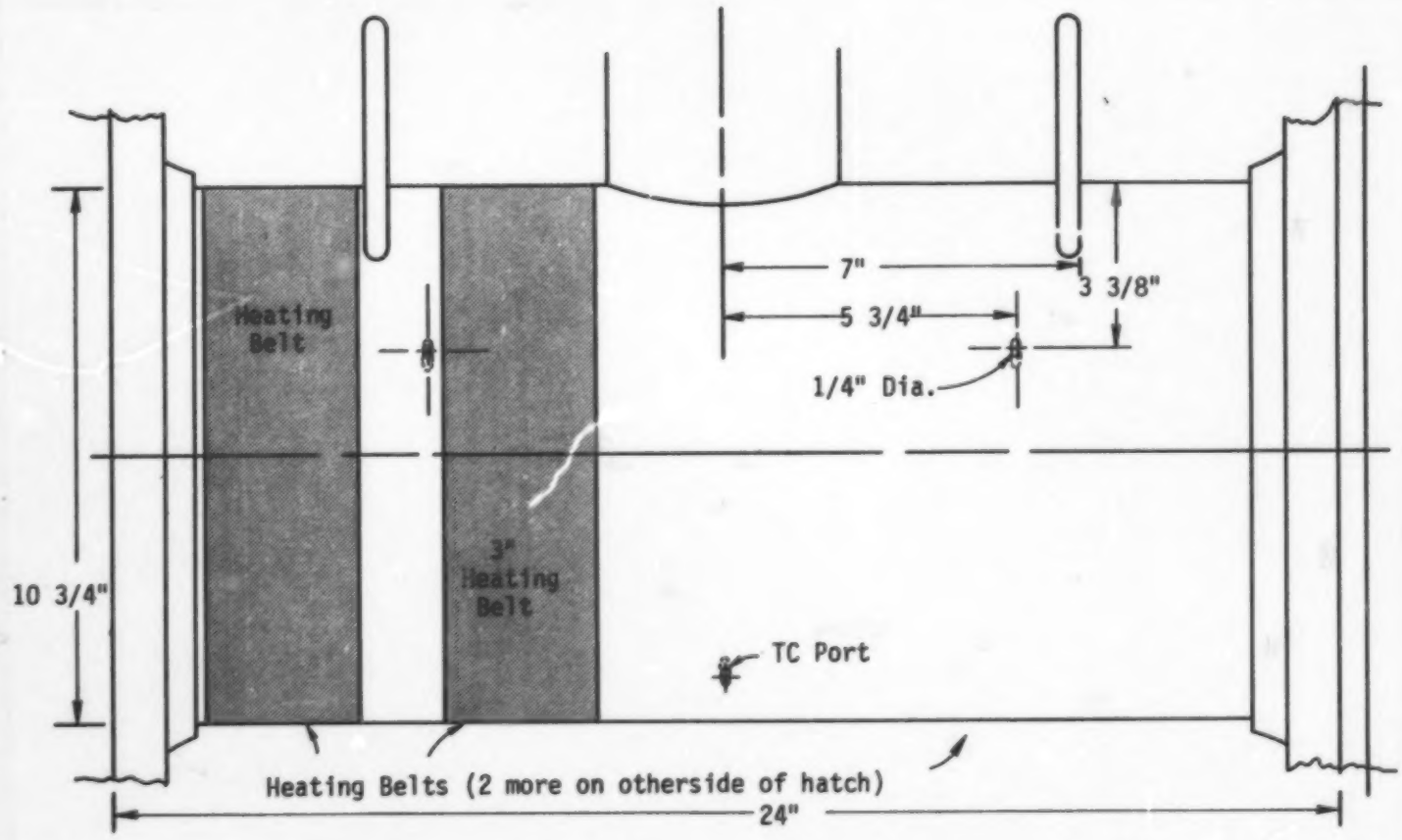

Figure A-12. Placement of pressure relief valves

filter bag which permits steam to escape so that a dry product is obtained. After cooling, the product is ready for utilization as a sorbent.

A.5.5 Temperature and Pressure Monitoring System

Thermocouple port locations are shown in Figures A-7, A-10 and A-12. Digital readout of the space gas temperature can be monitored, as well as the slurry temperature at three axial locations. The progression of temperature, and pressure, by use of a transducer, are recorded on a Servocorder strip-chart recorder. Pressure can also be monitored via a pressure gauge.

A.6 OPERATION PROCEDURES AND CHARACTERISTICS

A.6.1 Hydration Process Set Up

Prior to a run on the hydrator certain preparations must be completed. These include peripheral equipment hook up, leak checks, pressure and temperature calibration, reactor preheat, and reactant addition. Each run should start with a clean and dry hydrator.

The initial preparation for pressure hydration is connection of peripheral devices. First of all, heating belts are attached to the reactor and plugged into a variable auto-transformer which controls the voltage supply to the belts. The reactor is then wrapped with insulation to diminish heat losses. Leads from the reactor pressure transducer and thermocouple are connected to a DC power supply and digital temperature readout, respectively, and are then connected to the chart recorder. Power to these devices is then turned on, with the auto-transformer at the maximum setting, to begin reactor heat up and allow pressure and temperature calibration.

As the reactor is heating, instrument calibration can be completed. Temperature calibration uses an ice bath and boiling water for zero and span. With the chart recorder on at 30 cm/hr, the TC lead is connected to a thermocouple which is placed in an ice bath. Temperature is verified on the digital readout and the bias control on the recorder is adjusted so that the pen records 32°F. The TC is then placed in boiling water, temperature verified, and the pen adjusted to 212°F via the amplitude adjustment control. The TC is returned to the ice bath to check the zero and any necessary adjustment is made. The TC lead can then be connected to the reactor space gas TC to monitor the reactor preheat temperature.

With the outlet orifice open, the bias switch for pressure should be adjusted until the pressure pen records zero. The outlet valve is closed and the hydrator compressed to 150 psig with nitrogen. Any leaks present should be sealed, and the pressure pen adjusted to 150 psig on the strip chart. The

outlet valve is opened to bleed the reactor and check the zero, and then closed again.

After calibration, if the space gas temperature has reached 160°F, the reactor can be loaded with quicklime. The charge hatch is opened, 15 lbs of quicklime (plus any desired additives) are added, the hatch is sealed, and the mixing shaft turned on at a low rpm to establish a uniform temperature in the reactor. It is important at this time to ensure proper position of the valves: the reactor inlet and outlet valves should be closed; the 3-way valves on the inlet lines should allow nitrogen flow to the water tank and water flow from the tank. The desired amount of water or aqueous additive solution is then added to the water tank and the tank is sealed. The nitrogen preheater should then be turned on and a filter bag attached to the reactor outlet. When the preheat temperature reaches 200°F, the hydration process can begin.

A.6.2 Hydration Process

After the space gas temperature reaches 200°F, the water tank should be pressurized to 150 psig (or desired pressure) with nitrogen, and the mixing shaft turned to its maximum speed. The reactor inlet valve is then opened for one to two seconds to allow a surge of water to enter the reactor. A temperature and pressure response will occur, and upon equilibration or maximization of the two, another spurt of water can be added. As water is added, an extremely thick slurry is formed which can cause the mixing blades to freeze. If this occurs, the mixing shaft should be turned off and then slowly increased to its maximum speed. This should free the blades and allow proper operation. The surges of water are added at a reasonable rate until water addition is complete. The direction of the 3-way valves is then reversed to bypass the water tank. To optimize hydrate reactivity, the total water addition time should never exceed ten minutes.

After the water is added, another ten minutes of reaction time should be allowed before discharge begins. The outlet valve is then opened and reactor pressure dropped to 100 psig (or desired pressure). The valve is then

adjusted such that the effluent flowrate is equal to the nitrogen flowrate so that an isobaric discharge is maintained. Discharge should be continued until solids are no longer present or hydrator temperature drops below 200°F. A typical pressure and temperature history for the process is shown in Figure A-13. The hydrate can then be placed in a plastic bag, sealed, labeled, and weighed to determine the yield. Pressure and temperature calibration should be checked to determine drift, and the peripheral devices dismantled and stored.

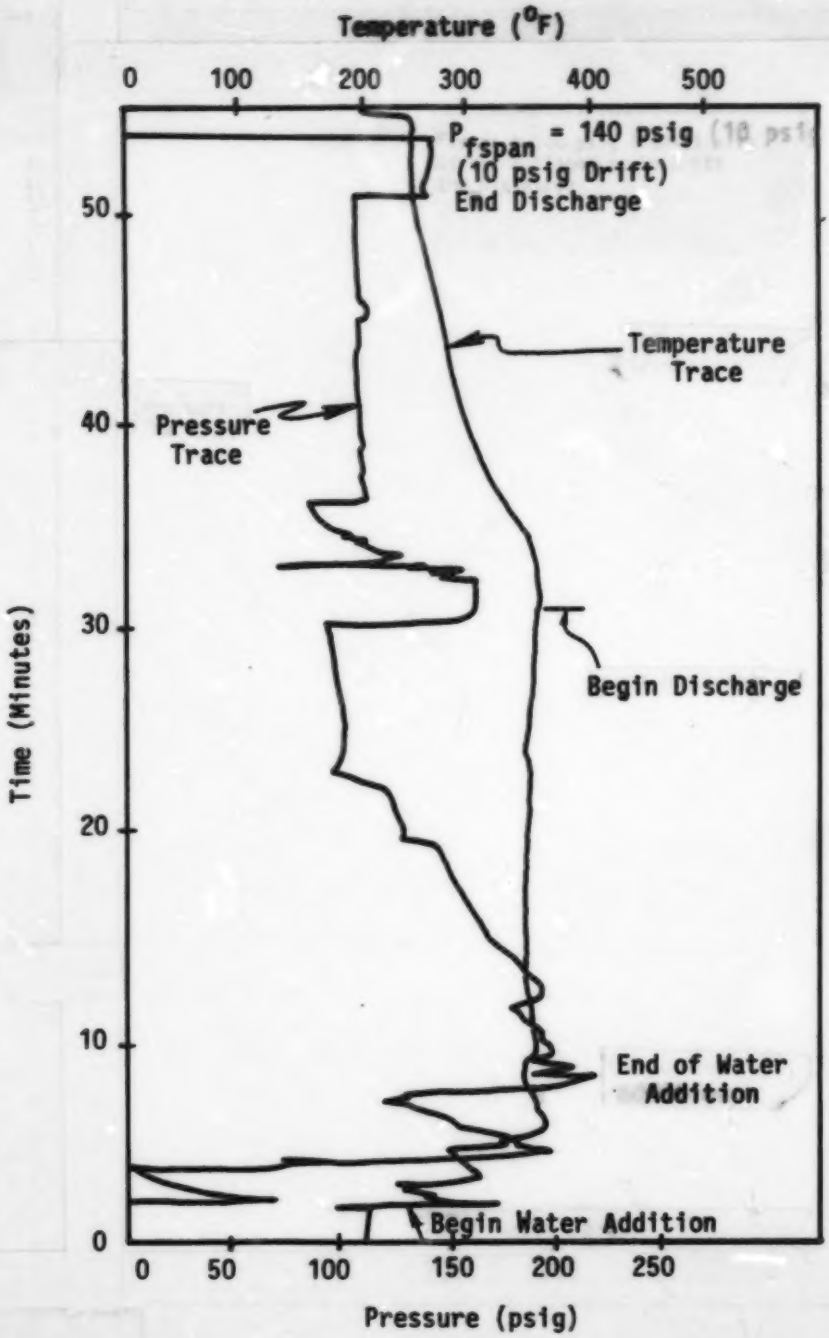

Figure A-13. Typical temperature and pressure trace for hydration run.

A.7 LITERATURE CITED

1. Boynton, R. S., "Chemistry and Technology of Lime and Limestone," 2nd edition, John Wiley and Sons, Inc., NY (1980).

2. Weber, G. F., M. H. Bobman, and G. L. Schelkopf, "Pilot Scale Studies of In-Furnace Hydrated Lime Injection for Flue Gas SO_2 Emission Control." In: Proceedings: First Joint Symposium on Dry SO_2 and Simultaneous SO_2/NO_x Control Technologies, Volume 1. Fundamental Research and Process Development, EPA-600/9-85-020a (NTIS No. PB85-232353), pp 11-1 to 11-15, July (1985).

3. Wiltsee, G. A., Director, Quarterly Technical Progress Report for the Period January-March, 1984, UNDERC, Grand Forks, ND, DOE/FE/60181-1574.

4. Wiltsee, G. A., Director, Quarterly Technical Progress Report for the Period April-June, 1984, UNDERC, Grand Forks, ND, DOE/FE/60181-1642.

5. Corson, B. L., Dry Lime Hydrate and Process for Producing Same, U.S. Patent 2,309,168, January 26, 1943.

6. Garvin, W. C., Method of Hydrating Dolomitic Limes, U.S. Patent 2,356,760; August 29, 1944.

7. Warner, I., Method of Hydrating Dolomitic or Other Relatively Slow-Slaking Limes, U.S. Patent 2,365,736; December 26, 1944.

8. Huntzeker, H. N., Process of Making a Plastic Hydrated Lime, U.S. Patent 2,439,033; November 22, 1949.

9. Volk, J., Pressure Hydrated Lime, U.S. Patent 2,902,346; September 1, 1959.

10. Corson, G., and W. H., Inc., Plymouth Meeting, Pa, 19462, Product Literature.

11. Cole, J. A., "Development of a Laboratory-Scale Pressurized Hydrator," EER, January, 1985.

APPENDIX B

QUALITY ASSURANCE

B.0 QUALITY ASSURANCE

The collection and analysis of quality data has been the primary objective of this program. In order to ensure that the reported data is accurate, many quality assurance measures have been taken in all phases of the program. Most of the procedures and measurements used for data acquisition have been standardized by EPA or ASTM and those which have not are described in detail in this appendix.

Three facilities at EER were involved in procuring the data presented in this report; the CTT, BSF, and the Pressure Hydrator. All of the quality assurance information presented in this appendix applies to these three facilities.

B.1 GAS SPECIES MEASUREMENTS

Exhaust gas-phase species composition was measured using the BSF and CTT laboratory sampling systems. These systems were constructed in strict conformance with EPA performance specifications and their use helped ensure data quality. The species that were measured included: NO, NO_2, SO_2, CO, O_2, and CO_2, all of which were measured by continuous gas analyzers.

Table B-1 lists the specific instruments and full-scale ranges. The instrument ranges have been selected to exceed the maximum expected concentrations by a small margin.

Figure B-1 shows a schematic diagram of the continuous monitoring system for NO, NO_x, CO, CO_2, and O_2. The system was nearly identical for both the BSF and CTT. All components in contact with the sample were stainless steel or Teflon to ensure sample integrity and corrosion resistance. The gas sample was provided to the instruments by a sample conditioning system consisting of a pump, moisture condenser and particulate filters.

Gas phase measurements were made routinely at Port 10B in the BSF and at the exhaust in the CTT. Phase discrimination probes (see Figure B-2 were used at both locations. The probes supplied two gas streams simultaneously. The main, particle-laden stream, which was used for continuous monitoring of O_2, CO, CO_2, NO_x, and the side, nearly particle-free stream, which was used for SO_2 measurement.

Figure B-3 shows a diagram of the continuous monitoring system for exhaust SO_2 measurements. The SO_2 gas sample in the nearly particulate-free stream was transported in a heated Teflon line maintained above 115°C under vacuum to a heated filter followed by a permeation tube drier. The permeation tube drier selectively removed water vapor from the gas sample. Dry air was used as the dry gas medium in the permeation drier. The sample was then pressurized and delivered to the analyzer. SO_2 concentration was measured using a non-dispersive ultraviolet instrument manufactured by DuPont.

TABLE B-1. BSF AND CTT INSTRUMENTATION

Gas Measured	Type of Instrument	Manufacturer	Model No.	Range	Reference
NO, NO_x	Chemiluminescent	Thermo Electron Corp. (TECO)	10 AR	1000 RPM	Teco Model 10 Operating Manual
CO	Nondispersive Infrared (NDIR)	Anarad, Inc.	(BSF) AR500R (CTT) AR600R	500 ppm 10 percent	Anarad AR 500 Operating Manual Anarad AR 600 Operating Manual
CO_2	Nondispersive Infrared (NDIR)	Anarad, Inc.	(BSF) AR500R (CTT) AR600R	25 percent 40 percent	Anarad AR 500 Operating Manual Anarad AR 600 Operating Manual
O_2	Paramagnetic	Beckman Taylor Servumex	(BSF) 755 (CTT) OA250	10 percent 100 percent	Beckman 755 Operating Manual Taylor OA250 Operating Manual
SO_2	UV Absorption	DuPont	400	5000 ppm	DuPont 400 Operating Manual

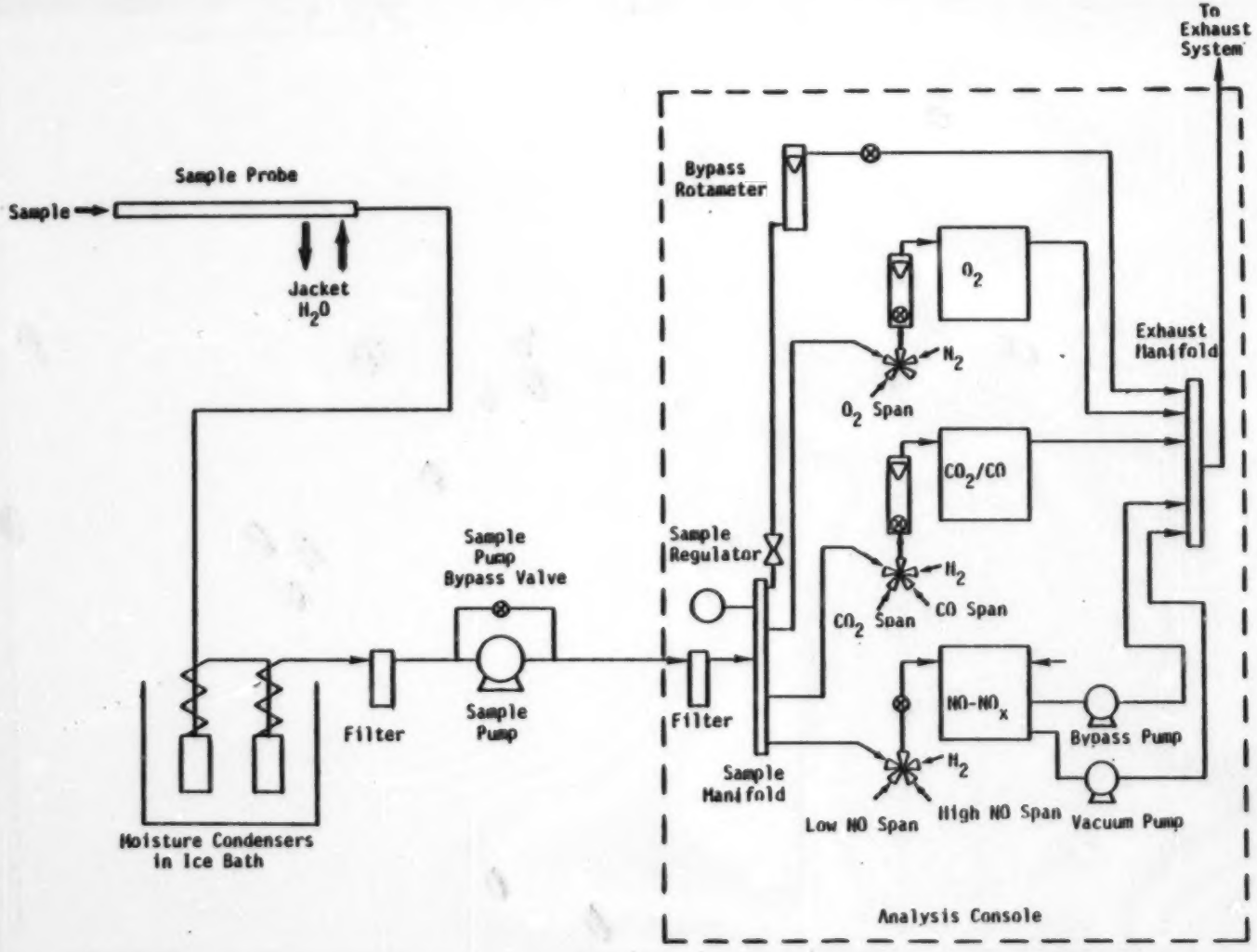

Figure B-1. Continuous monitoring sampling system.

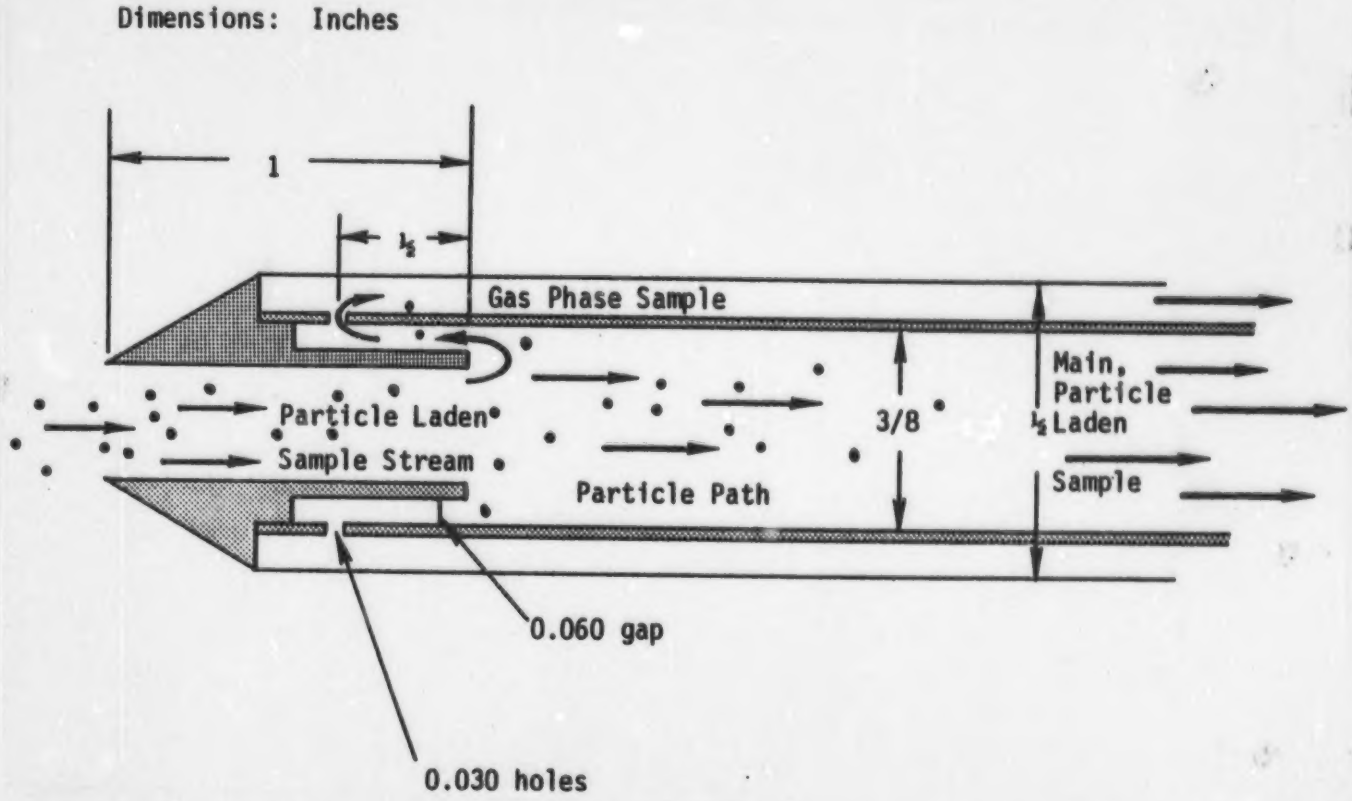

Figure B-2. Phase discrimination probe.

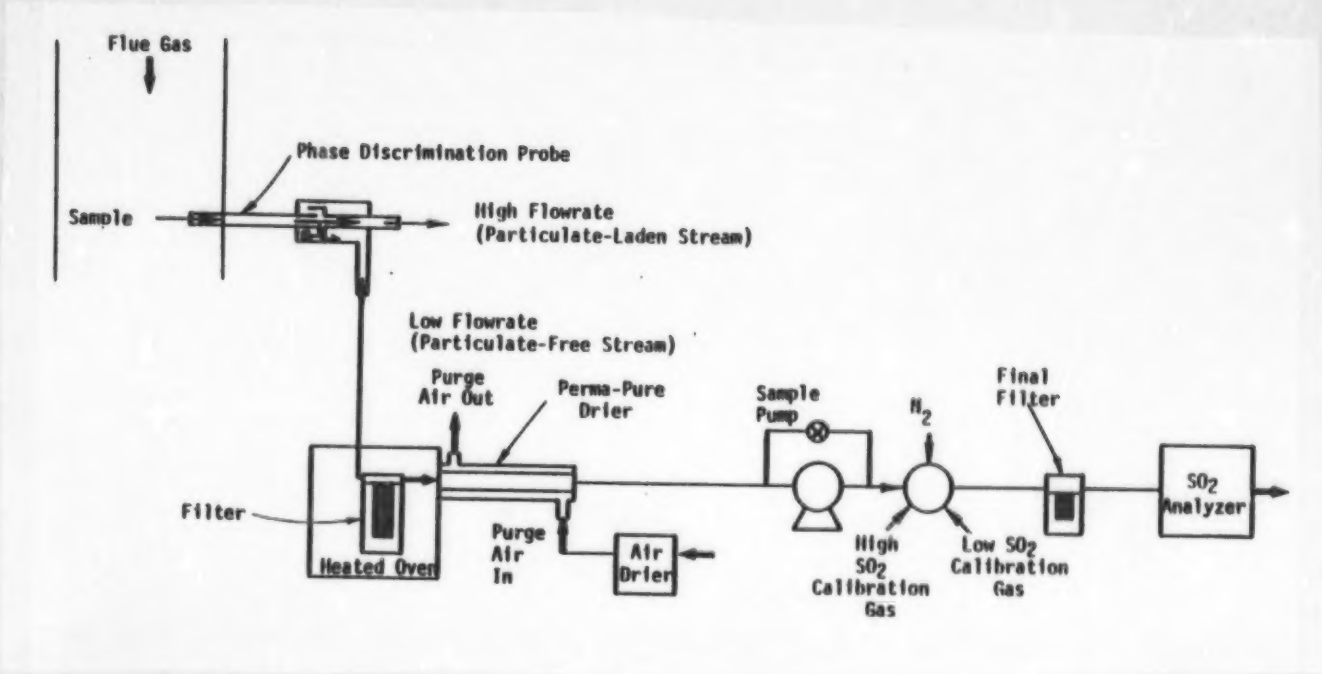

Figure B-3. SO_2 continuous monitoring system.

Table B-2 gives the precision, accuracy, and completeness data for both sets of instruments used on the BSF and CTT. In every case, the program goals for precision and accuracy were met.

TABLE B-2. PRECISION, ACCURACY AND COMPLETENESS DATA FOR GAS SPECIES INSTRUMENTS

Gas Measured	Precision (%)			Accuracy (%)			Completeness (%)		
	Goal	Actual BSF	Actual CTT	Goal	Actual BSF	Actual CTT	Goal	Actual BSF	Actual CTT
NO_x (Chemiluminescent)	2	1.4	0.3	20	14.2	12.3	90	100	100
CO (NDIR)	2	0.4	0.5	20	No Std.	No Std.	90	100	100
CO_2 (NDIR)	2	0.8	0.1	20	6.7	2.5	90	100	100
O_2 (Paramagnetic)	2	0.5	0.2	20	11.2	13.1	90	100	100
SO_2 (UV Absorption)	2	0.2	0.3	20	8.1	10.2	90	100	100

B.2 SOLID SAMPLES

B.2.1 Grab Samples

Grab samples are used to obtain materials for specific surface area and particle size analysis. Suitably sized samples are removed at random from bulk containers of the material to be tested. Since the total quantity of each of the bulk materials involved in this study is quite small (a few kg at most) minimal effort, beyond stirring, needs to be taken in order to ensure the representativeness of the sample.

B.2.2 Solids Analysis

The composition of solid samples was generally determined by EER's Analytical lab though some samples were sent to an independent laboratory. Carbon, Hydrogen and Nitrogen were analyzed on a Perkin-Elmer 240B and solid sulfur species were determined from a Leco SC32 Analyzer. Table B-3 gives the precision and accuracy data for these instruments. Calcium analysis was done with a Chelometric titration method which is covered under ASTM D 2795.

TABLE B-3. SOLID ANALYSES PRECISION AND ACCURACY DATA.

MEASUREMENT		PRECISION (%)		ACCURACY (%)	
		ACTUAL	GOAL	ACTUAL	GOAL
Carbon	Perkin-Elmer 240 B	.24	2	0.8	2
Hydrogen		1.38	5	0.6	5
Nitrogen		2.13	10	1.9	10
Ash		0.33	10	1.42	10
Moisture		2.55	10	8.71	10
Sulfur - Leco SC32		2.36	10	0.55	10

B.3 TEMPERATURE MEASUREMENTS

High-temperature gas measurements within furnaces are subject to large inaccuracies due to the effects of thermal couple radiation loss. Therefore, in-furnace gas temperatures were measured using a suction pyrometer system as shown in Figure B-4. The suction pyrometer consisted of a high-temperature thermocouple (B type) in a porous ceramic radiation shield. The pyrometer was placed in the gas stream with the opening in the alumina sheath pointing downstream. A high flow rate of furnace gas was withdrawn through the sheath and over the thermocouple to increase convective heat transfer to the thermocouple and reduce radiation loss. As the gas flow rate was increased, the gas temperature increased to a constant value, indicting no additional reduction in radiation loss. Figure B-5 shows the results of the motive side pressure (a measure of suction flow rate) calibration for the CTT. A suction pressure of 40 psig was adopted for all the temperature measurements for the CTT system.

The BSF system used a pressure of 30 psig for all temperature measurements (see Figure B-6).

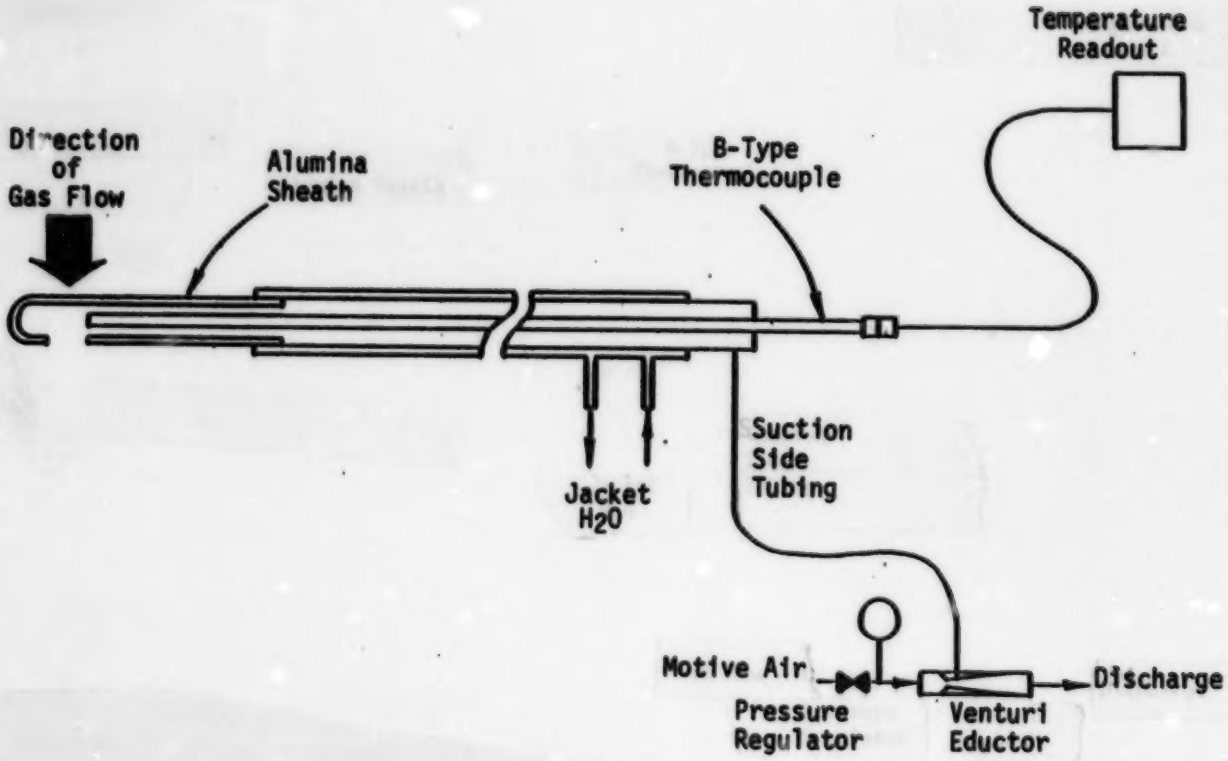

Figure B-4. Gas temperature measurement system.

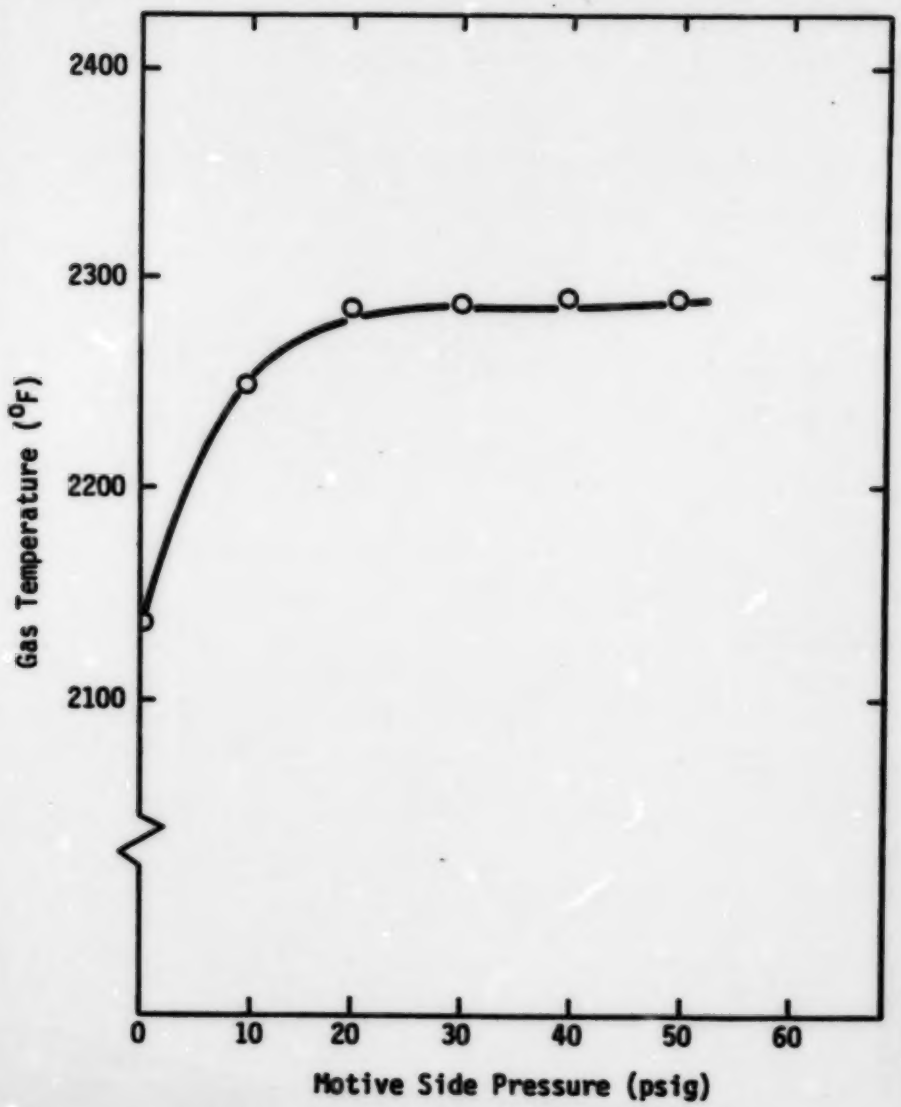

Figure B-5. Suction pyrometer aspirator pressure calibration for CTT.

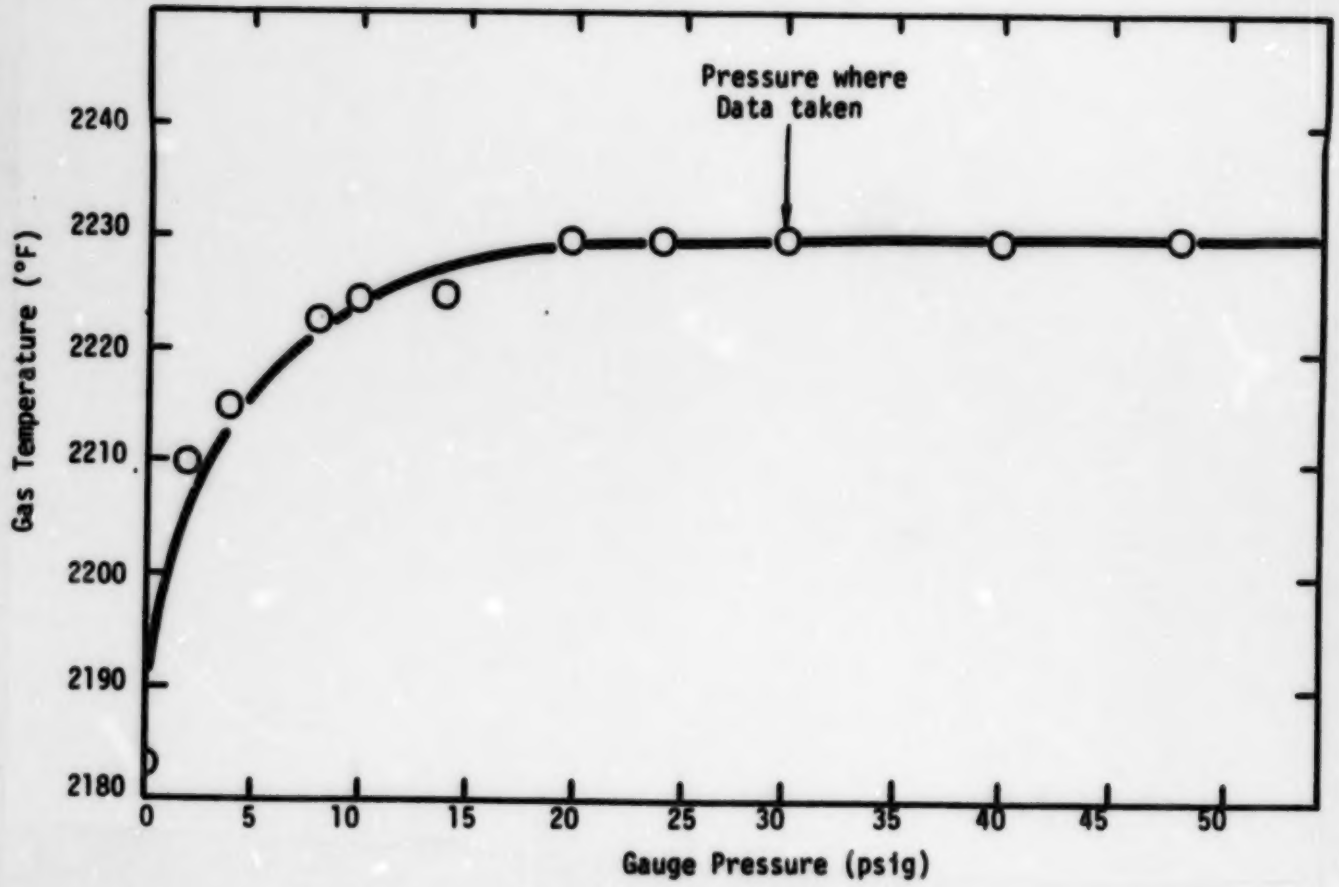

Figure B-6. Suction pyrometer aspirator pressure calibration for BSF.

B.4 CALIBRATION PROCEDURES

Calibration procedures and frequency for each measurement system are listed in Table B-4. As shown in the table, standard calibration procedures were used for each system. Each system was calibrated at the frequency shown in the table to ensure the accuracy of the measurement were traceable to the calibration standards.

Each of the continuous monitoring instruments was calibrated with three gases: a zero gas and two span gases. Table B-5 lists the span gases used to calibrate instruments for the CTT sample system.

TABLE B-4. CALIBRATION PROCEDURES

MEASUREMENT PARAMETER	CALIBRATION PROCEDURE	CALIBRATION FREQUENCY	CALIBRATION STANDARD	REFERENCE
Fuel Composition:				
Carbon	Standard Samples	Daily	Known quantity of 100% acetanilide	Perkin Elmer 240 B Operating Manual
Hydrogen				
Nitrogen				
Ash				
Moisture				
Sulfur	Standard Sample	Daily	Certified sulfur standards	Leco SC 32 Operating Manual
Exhaust Gas Composition				
NO, NO_2	Compare to standard compressed gas	Daily	EPA Protocol 1 Gases or custom gas blends. See Section 10.0	EPA EMSL Protocol No. 1, June 1, 1978
O_2				
CO				
CO_2				
SO_2				
Hydrocarbons				
Sorbent Surface Area		Daily	Known quantity of N_2	Quantasorb Surface Area Analyzer Operating Manual
Sorbent Flowrate	Weigh feed over measured time with independent balance		Standard weights	

TABLE B-5. CALIBRATION GASES

Gas	Concentration	Percent of Full-Scale	Balance Gas	Grade
NO	836 ppm	84	Nitrogen	Certified Standard
NO	166 ppm	16	Nitrogen	Certified Standard
SO_2	2915 ppm	73	Nitrogen	Certified Standard
SO_2	437 ppm	11	Nitrogen	Certified Standard
CO	1227 ppm	82	Nitrogen	Certified Standard
CO_2	12.3%	31	Nitrogen	Certified Standard
CO_2	5%	13	Nitrogen	Certified Standard
O_2	10%	10	Nitrogen	Certified Standard
O_2	4%	4	Nitrogen	Certified Standard
CO	10%	100	Nitrogen	Certified Standard
CO	2%	20	Nitrogen	Certified Standard

B.5 DATA REDUCTION

Equations used to calculate results for each of the measurements are discussed below. Many of the results are obtained directly from the measurements and thus do not require calculations.

B.5.1 SO_2 Capture

The gas compositions are measured as chart divisions on a strip chart recorder. The measured divisions are converted to concentration (ppm or percent) based on calibrations with certified gases.

SO_2 capture with sorbent injection is defined as:

$$\text{Percent Capture} = \frac{(SO_2)_1 - (SO_2)_2}{(SO_2)_1} \times 100\%$$

where: $(SO_2)_1$ = SO_2 concentration without sorbent, ppm

$(SO_2)_2$ = SO_2 concentration with sorbent injection, ppm

B.5.2 Percent Calcination

Percent calcination is the percentage of the calcium in a sample of initially $CaCO_3$ or $Ca(OH)_2$ which has been converted to CaO due to heating. Percent calcination is calculated directly from results of the 240B (wt% C) and the calcium titration (wt% Ca).

$$\text{Percent Calcination} = \left(1 - \frac{10}{3} \times \frac{\text{wt\% C}}{\text{wt\% Ca}}\right) \times 100\%$$

An alternate check on the percent calcination is obtained by a mass balance involving the results from the 240B (wt% C, wt% H, wt% ash) and the SC32 (wt% S). Tests have shown that during 240B analysis, $CaSO_4$ is retained in the ash, while $Ca(OH)_2$ and $CaCO_3$ are completely devolatilized. Percent calcination is calculated as follows:

$$\text{Percent Calcination} = \left(1 - \frac{14}{3}\left(\frac{\text{wt\% C}}{\text{wt\% Ash} - 2.5 \times \text{wt\% S}}\right)\right) \times 100\%$$

B.5.3 Particle Size Distribution

Particle size distribution is provided directly as a plot of cumulative mass-percent finer versus equivalent spherical diameter. An example particle size distribution plot is shown in Figure B-7.

B.5.4 Specific Surface Area

Specific surface area is measured by a Quantasorb Analyzer by the BET method. This analyzer measures the quantity of nitrogen adsorbed on a sample surface as a function of the relative (to saturation) partial pressure of nitrogen. Two equations are used to determine the specific surface area:

$$\frac{1}{X(Po/P-1} = \frac{C-1}{X_mC}\frac{P}{P_o} + \frac{1}{X_mC}$$

where:

X = weight of N_2 adsorbed at P/Po

P = partial pressure of N_2

P_o = saturation pressure of N_2

X_m = weight of N_2 adsorbed for monolayer coverage

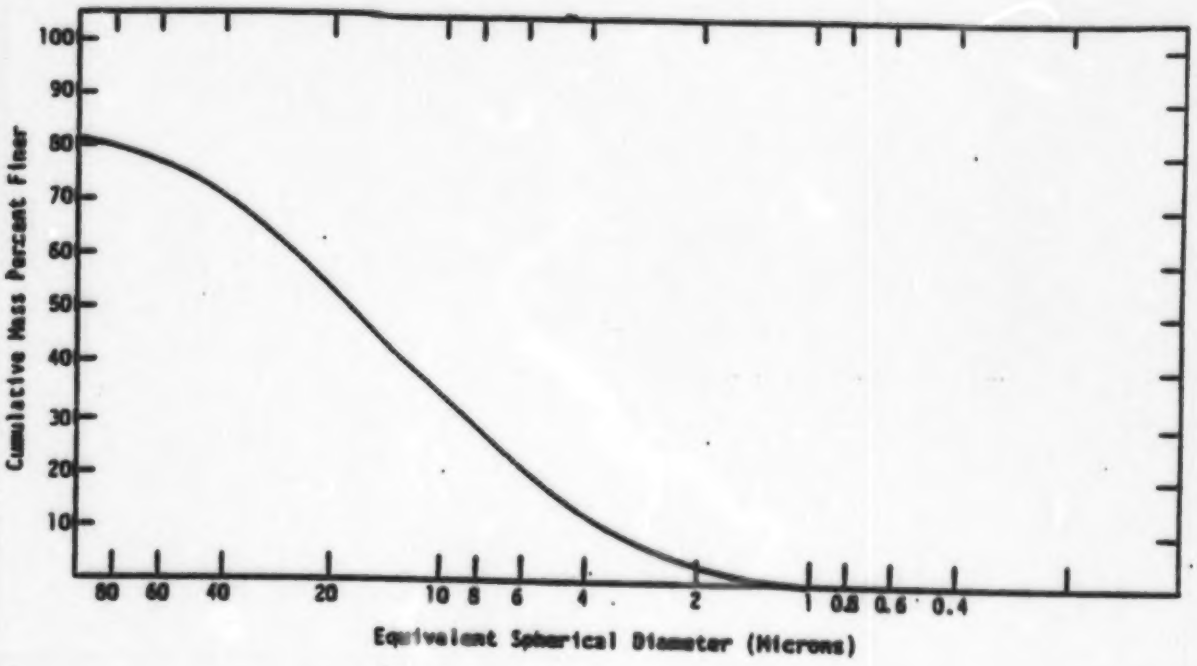

Figure B-7. Example of sorbent particle size distribution.

C = a constant which is a function of the heat adsorption and the heat of condensation of N_2

By measuring X for two or more values of P/Po the slope, $c-1/x_m c$, and intercept, $1/x_m c$, are obtained. After solving for X_m the specific surface area, S, is obtained from:

$$S = \frac{X_m N A}{M_a M_s}$$

where:

N = Avograro's number

A = cross-sectional area of an adsorbed N_2 molecule

M_a = mass of N_2 molecule

M_s = mass of sample

B.5.5 Combustion Air Flowrate/Distribution

Combustion air flowrate is read directly from rotameters or is calculated from pressure drop measured across laminar flow elements based on the equation:

$$Q = K \left(\frac{\Delta P}{T} \right)^{1/2}$$

B.5.6 Combustion Air, Furnace Gas, and Exhaust Gas Temperatures

Temperatures are measured by thermocouples and provide results in units of degrees centigrade which can then be converted to other temperature scales, as required.

B.5.7 Residence Time

Residence times are calculated by assuming a one-dimensional flow in the furnace. Based on the measured temperatures, the bulk mean residence time of the reburning zone (τ_2) was calculated by using the following equation:

$$2 = \frac{V}{\dot{V}} \left(\frac{T_o}{T_m} \right)$$

where:

V = volume of reburning zone, ft^3

$\dot{V}$ = volumetric flow rate of gas, SCF-S

T_o = 530^oR

T_m = bulk mean gas temperature

= $1/2\ (T_1 + T_2)$

T_1 and T_2 are center line temperatures measured at the exit of the primary and reburning zones, respectively.